UNIVERSITY OF NAPLES FEDERICO II

DEPARTMENT OF CHEMICAL, MATERIALS AND PRODUCTION ENGINEERING

PhD
in
INDUSTRIAL PRODUCT AND PROCESS ENGINEERING
XXIX Cycle

Synthesis and Characterization of Expandable Graphite using different Oxidizing Agents

MARCELLA SALVATORE

TUTOR
Prof. Veronica Ambrogi

PhD COORDINATOR
Prof. Giuseppe Mensitieri

CO-TUTOR
Dr. Gianfranco Carotenuto

Academic Year 2016-2017

Abstract

Graphite intercalation compounds (GIC), i.e., graphite flakes embedding small molecules or ions, have been described in the literature since 1851 by Schafheutl. These extraordinary materials can be exploited for a number of technological applications, in different industrial fields (for example, they have been used for the industrial preparation of *expanded graphite*, novel superconductors, catalysts, anode materials, etc.). Some GICs (e.g., graphite nitrate and graphite bisulfate) are able to expand remarkably by thermal heating, and the achieved expanded graphite can be used to prepare graphite nanoplatelets (GNP), Few Layer Graphene (FLG), and graphene monolayer. Here an expandable graphite (graphite bisulfate) is prepared by intercalation of graphite with sulfuric acid, in presence of an oxidizing agent. In this study, different chemical formulations for the synthesis of highly intercalated graphite bisulfate have been tested. In particular, nitric acid, potassium nitrate, potassium dichromate, potassium permanganate, sodium periodate, sodium chlorate, and hydrogen peroxide have been used in this synthesis scheme as the auxiliary reagent (oxidizing agent). The intercalation reaction was performed in a glass-flask reactor (placed in a thermostatic bath), using air bubbling as homogenizing approach. The reaction time always was 1h and the H_2SO_4: oxidizing agent ratio was $9 : 1$ by volume for all reactive mixtures. Graphite flakes were placed in the glass reactor and then the oxidizing compound, dissolved in absolute H_2SO_4, was added. The reactions were stopped by adding deionized water to the systems. In order to evaluate the presence of delamination, and pre-expansion phenomena, and the achieved intercalation degree in the prepared samples, the obtained graphite intercalation compounds have been characterized by scanning electron microscopy (SEM), transmission electron microscopy (TEM), X-ray powder diffraction (XRD), infrared spectroscopy (FT-IR), micro-Raman spectroscopy ($\mu-$RS) and thermal analysis (TGA). Delamination and pre-expansion phenomena were observed only for nitric acid, potassium dichromate and hydrogen peroxide, while the presence of strong oxidizers ($KMnO_4$, $NaIO_4$) led to stable graphite intercalation compounds. The largest content of intercalated bisulfate is achieved in the GICs obtained from $NaIO_4$ and $NaClO_3$.

Table of Contents

Introduction

Carbon and its Allotropic Forms

Carbon is the only element able to make a wide variety of chemical compounds in arrangement with Hydrogen, Oxygen, Nitrogen and other heteroatoms. It also has the unique ability to form long chains whose central core consists of carbon atoms exclusively. It exists in two classical allotropic forms, namely diamond and graphite and another one, discovered in 1985, namely fullerenes [1]. The main difference between diamond and graphite is that the carbon
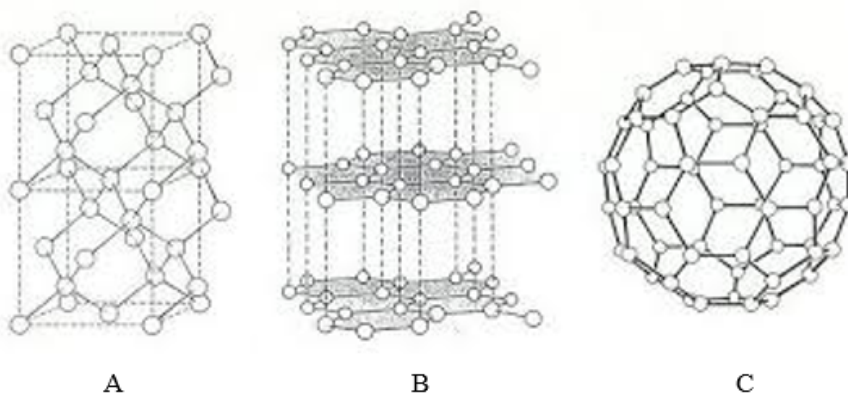
Figure 1: Carbon allotrops, A: Diamond, B: Graphite, C: Fullerene [2]

bonding involves sp^3 (tetrahedral) hybridization in diamond and sp^2 (trigonal) hybridization in graphite (see Figure 1). As a result, diamond has a three-dimensional crystal structure (covalent network solid), whereas graphite consists of carbon layers (with covalent and metallic bonding within each layer) which are stacked in an AB sequence and are linked by a weak van der Walls interaction produced by a delocalized π-orbital. The carbon layers in graphite are known as graphene layers [3].

Graphite Structure and Layered Materials

Since ancient times, people have exploited the properties of layered materials. This gradually developed into scientific research, leading to the elucidation of the laminar structure of layered materials, detailed understanding of their properties, and eventually experiments to exfoliate or delaminate them into individual, atomically thin nanosheets. This culminated in the discovery of graphene, resulting in a new explosion of interest in two-dimensional materials. Layered materials consist of two-dimensional platelets weakly stacked to form three-dimensional structures. The archetypal example is graphite, which consists of stacked graphene monolayers. However, there are many others: from MoS_2 and layered clays to more exotic examples such as MoO_3, $GaTe$, and Bi_2Se_3. These materials display a wide range of electronic, optical, mechanical, and electrochemical properties. Over the past decade, a number of methods have been developed to exfoliate layered materials in order to produce monolayer nanosheets. Such exfoliation creates extremely high-aspect-ratio nanosheets with enormous surface area, which are ideal for applications that require surface activity. More importantly, however, the two-dimensional confinement of electrons upon exfoliation leads to unprecedented optical and electrical properties [4]. Graphite has a layer structure, within each layer, the carbon atom is bound to three others, forming a series of continuous hexagons in what can be considered as an essentially infinite two-dimensional molecule. The bond is covalent (σ-type) and has a short length (0.141nm) and high strength (524^{kJ}/$_{mole}$). Its atoms are arranged in a hexagonal pattern within each layer and, the layers, are stacked in the AB sequence in the z direction (see Figure 2) [5]. This results in a hexagonal unit cell with dimensions $c = 6.71$Å and $a = 2.46$Å [6]. The hybridized fourth valence electron is paired with another delocalized electron of the adjacent plane by a much weaker van der Waals bond (a secondary bond arising from structural polarization) of only 7^{kJ}/$_{mol}$ (π bond). Carbon is the only element to have this particular layered hexagonal structure. The spacing between the layer planes is relatively large, 3.35Å, or more than twice the spacing between atoms within the basal plane and approximately twice the van der Waals radius of carbon [7]. There are 4 atoms per unit cell, as labeled by A, A', B and B' in Figure 2. The structure possesses a center of inversion symmetry at the point halfway between the atoms A and A'. The peculiar crystal structure of graphite results in a considerable anisotropy, that is the properties of the material may vary considerably when measured along the xy directions (within the plane) or the z direction (perpendicular to the planes). Such anisotropy, in particular in electrical and thermal properties, can often be of good use. Due to the anisotropy, the carbon layers can slide to each other quite easily, making graphite a good lubricant and pencil material [3, 8]. An other consequence of the anisotropy, is the ability of the graphite to undergo chemical reactions by allowing the reactant (called the intercalate) to reside between the graphene layers, forming compounds called *Graphite Intercalation Compounds* (GICs) [9, 10]. Some GICs have the ability to expand under thermal heating (i.e. graphite bisulfate and graphite nitrate) and are also named *Expandable Graphite* (EG). From the GICs
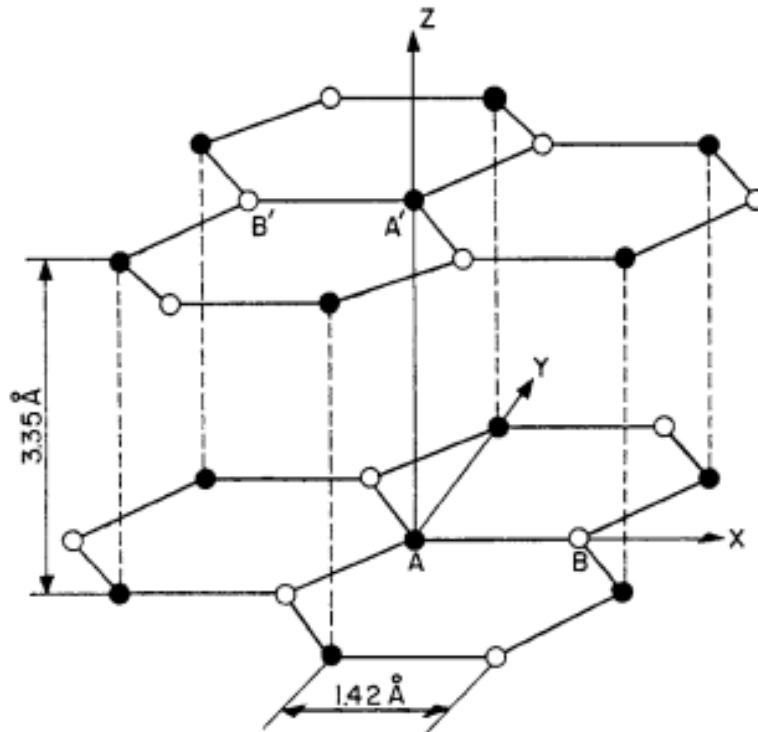
Figure 2: Graphite structure [3]

it is possible to obtain the single layer of the graphite lattice: the *graphene.*

Graphene and 2D-Materials

Graphene is a single sheet of graphite. It has been discovered in 2004 by Novoselov and Geim [11] and has received world-wide attention due to its exceptional charge transport, thermal, optical, and mechanical properties. Unlike 3D matter, whose bulk is hidden from direct observation and influence, graphene "bulk", its 2D surface, is always exposed, and its structure may be inspected or modified more easily. Graphene is often categorized by the number of stacked layers: single layer, few-layer (2–10 layers), and multi-layer which is also known as thin graphite or graphite-nanoplatelets. The properties of graphene, such as high surface area, high thermal conductivity, fast charged carrier mobility and strong Young's modulus, have been well documented and reported in Table 1 [12]. It is the thinnest known material in the universe and the strongest ever measured. Its charge carriers exhibit giant intrinsic mobility, have zero effective

Table 1: Graphene properties

Property	Value	Unit
Surface Area	2630	$\mathrm{m^2/g}$
Young's modulus	~ 1	TPa
Thermal Conductivity	~ 5000	$\mathrm{W/m \cdot K}$
Electrical Conductivity	~ 106	$\mathrm{S/cm}$
Tensile strength	130	GPa

mass, and can travel for micrometers without scattering at room temperature. Graphene can sustain current densities six orders of magnitude higher than that of copper, shows record thermal conductivity and stiffness, is impermeable to gases, and reconciles such conflicting qualities as brittleness and ductility [13]. For these reasons, the development of various methods to produce graphene has stimulated the research in recent years. There are many techniques for the preparation of graphene sheets, these techniques can be divided into two main groups: *bottom-up* and *top-down* techniques. The common bottom-up techniques are the Chemical Vapor Deposition (CVD), the reduction of GO, the extraction by the carbon nanotubes. With these methods it is possible to produce small quantities of large graphene sheets without defects, however, these techniques are more suitable for production on a laboratory scale or for electronics applications. In the top-down manufacturing techniques the graphene sheets are produced by separation or exfoliation of graphite or its derivatives (such as GICs). These techniques can be easily scaled to industrial size, in fact graphite is commercially available in less than $1000\,\mathrm{\$/ton}$. Through the micro-mechanical method of engraving it is possible to produce graphene sheets of large size and of good quality. Recently it has been developed a direct exfoliation process of the graphite in single or multiple sheets of graphene by sonication in the presence of poly (vinyl pyrolidone) or of N-Methylpyrrolidone. The direct sonication process potentially can be reported on an industrial scale to produce large amounts of graphene for the production of composite materials [14, 15, 16, 17]. Graphene layered structure has opened new prospects for the exploration of properties of other monolayer-thick two-dimensional (2D) layered crystals. The emergence of these inorganic 2D atomic crystals beyond graphene promises a diverse spectrum of properties. For example, hexagonal-boron nitride ($h-BN$), a layered material closest in structure to graphene is an insulator, while niobium selenide ($NbSe_2$), a transition metal dichalcogenide, is metallic, and monolayers of other transition metal dichalcogenides such as molybdenum disulfide (MoS_2) and tungsten disulfide (WS_2) are direct band gap semiconductors. The rich spectrum of properties exhibited by these 2D layered material systems can potentially be engineered on-demand and creates exciting prospects for using such systems in device applications ranging from electronics, photonics, energy harvesting, flexible electronics, transparent electrodes, and sensors [18].

Graphite Intercalation Compounds (GIC)

Intercalation compounds of graphite are formed when foreign species such as atoms, ions, or molecules are inserted between the layers of the graphite lattice (graphene sheets) [3, 19, 20, 21, 22]. Stacking order, bond distances, and bond direction may be altered, but the characteristic lamellar identity of the host must be preserved [23]. These compounds can be divided into two general classes with clearly different characteristics: (a) the covalent compounds, and (b) the intercalation compounds. Intercalation compounds have a large spread of composition as the percentage of intercalated material changes by regular steps. Numerous methods for GIC synthesis have been developed. They
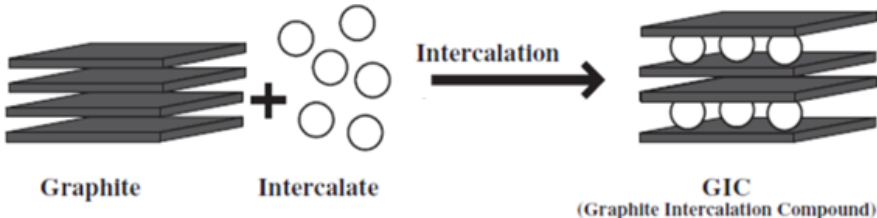

Figure 3: Graphite intercalation compound

are commonly subdivided into chemical (including vapor- or gas-phase synthesis and liquid-phase intercalation) and electrochemical, including galvanostatic or potentiostatic oxidation [24]. Graphite intercalation compounds (GICs) are technologically useful functional materials. Such materials have been intensively studied because of the 'Staging phenomenon' [25] and the manifold anomalous physicochemical behaviors [26, 27, 28, 29, 30, 31]. In addition, GICs are very important in graphite manufacturing [32] and potentially useful in other industrial fields like that of superconductors [33, 34], heterogeneous catalysts [35], anode materials [36], pyrophoric reactants stabilization [36], etc. Currently, GICs are used as expanded graphite which is an important material for the industrial production of flexible graphite sheets, sealing, packing and thermal insulator [37], it has attracted attention because of its very high adsorption capacity of spilled heavy oils and their easy recovery [38]. GICs are used in the preparation of Graphite Nanoplatelets (GNP), Few Layer Graphene (FLG) and single-layer graphene [1, 40, 41, 42]. Graphite nitrate and graphite bisulfate have the ability to significantly expand by thermal heating, they are also named Expandable Graphite. Owing to the intercalation/expansion processes, the π-π interactions, acting along the graphite z-crystallographic direction, are significantly weakened. Therefore, graphite fragmentation in separated nanocrystals takes place by simply applying some sono-acustic energy. The resulting graphite nanocrystals thickness depends on the GICs intercalation degree, usually classified in terms 'staging' index m, i.e. the number of graphite layers between two intercalant layers [3] and consequently the highest 'staging index' is required in the
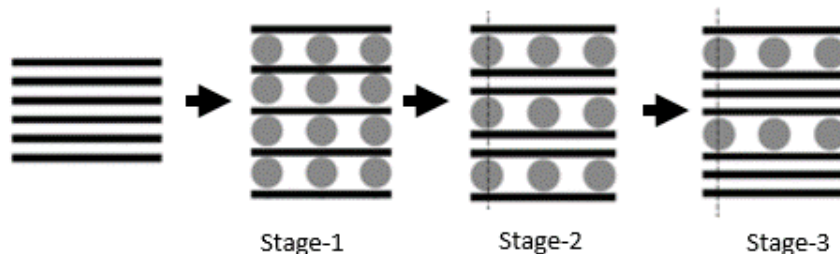
Figure 4: Staging Rudorff model

graphene preparation. Depending on the nature of the intercalating agent, the type of oxidant, and the experimental conditions, it is possible to obtain GICs as 'Stage-I', 'Stage-II', 'Stage-III', etc. [33]. In particular (see Figure 4) in a Stage-I compound, a single layer of graphene is alternated regularly with intercalated species. In a second-stage (third-stage, etc.) compounds two (three, etc.) graphene layers are separated by layers of intercalating [43]. According to the literature [24, 44], expandable graphite can be prepared by using various type of GICs hosting Brønsted acids (e.g., sulfuric acid, nitric acid, acetic acid, etc.), metal chlorides ($FeCl_3$, $CuCl_3$, $ZnCl_2$) [45], gold [46], metals (Na) and alkali metals (Li, Cs, K) in tetrahydrofuran (THF) [47].

Aim of the work

The stage and kinetics of bisulfate formation depend on the sulfuric acid concentration and on the type of oxidizing agent involved in the reactive system [24, 48]. Very limited structural information are given in the literature concerning these systems, since X-ray diffraction was one of the few available characterization approaches. Here, graphite bisulfate has been prepared by classical liquid-phase synthesis techniques, and some new reaction scheme based on never investigated oxidizing agents. The achieved materials have been fully characterized regarding their morphology and structure by means of scanning electron microscopy (SEM), energy dispersive X-ray spectroscopy (EDS), transmission electron microscopy (TEM), X-ray powder diffraction (XRD), infrared spectroscopy (FT-IR), micro-Raman spectroscopy (µ-RS) and thermogravimetric analysis (TGA). In this work two classes of Graphite Intercalation Compounds have been prepared and characterized, in particular graphite bisulfates by using seven different types of oxidizing agents and graphite iron-chloride. The first one is the main activity of this work. Seven different oxidizing agent (in a mixture with concentrated sulfuric acid) have been used to obtain the best expandable graphite with the highest intercalation degree. The second-one has
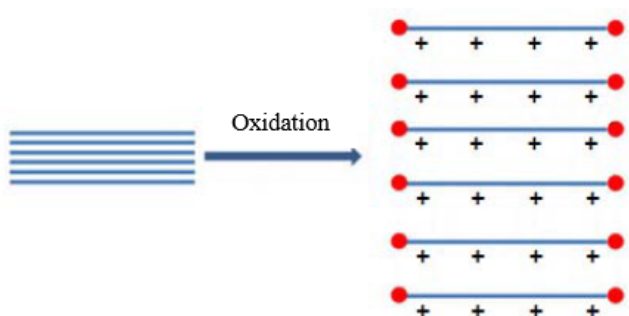
Figure 5: Oxidation Graphite scheme

been prepared to obtain an expendable graphite with magnetic property. The literature shows that a magnetic GIC is obtained from the chemical reduction of the intercalation compound $FeCl_3$ - GIC, using a potassium-naphthalene complex in tetrahydrofuran [49].

Graphite Bisulfates

Intercalation - Step 1

To obtain an intercalated structure, where intercalating molecules are placed between the graphite layers, it is necessary to oxidize or reduce the starting graphite sheets. Using this method, the charges created (positive or negative depending on the method chosen) cause a repulsion between the graphite layers that increase their relative distance (see the scheme in Figure 5), in this way the intercalating agent can enter in the graphite gaps. Graphite-bisulfate is classically made by dipping natural graphite in concentrated sulfuric acid with sufficient nitric acid [50]. Firstly C. Schafheutl [51] in 1840 described the graphite bisulfate synthesis based on the following reaction scheme [24, 52]:

$$24nC + Ox^z + mH_2SO_4 \rightarrow C + 24 \cdot HSO_4^- \cdot (m-1) H_2SO_4 + HO^{(z-1)} \ (1)$$
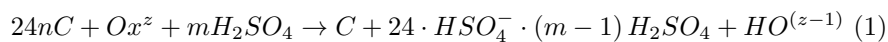
Where Ox is the oxidizing agent and C are the carbon atoms in the graphite. Therefore, graphite bisulfate compounds consist of graphite layers intercalated by HSO_4^- and H_2SO_4 molecules [24, 54].

Expansion\Exfoliation - Step 2\3

Graphite bisulfates have the ability to expand under thermal heating (*Expandable Graphite*). Camino et al. [55] have proposed that the expansion is a consequence of the formation of carbon dioxide (CO_2), sulfur dioxide (SO_2), and water vapor (H_2O) produced by the reaction (2) that occurs between the intercalating agent and graphite [56].

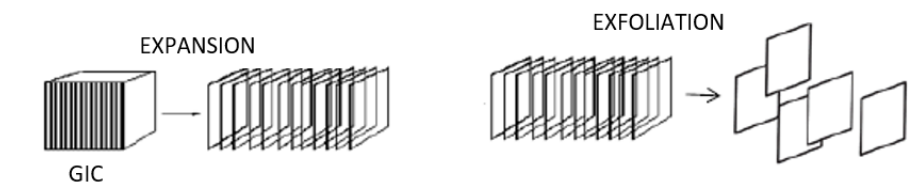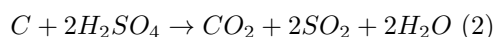Figure 6: Expansion-Exfoliation

$$C + 2H_2SO_4 \rightarrow CO_2 + 2SO_2 + 2H_2O \ (2)$$

During expansion process, the distance between graphite layers increases, in this way the van der Waals forces, present in z-direction, decrease. This phenomenon results in a great simplicity to divide layers and exfoliate graphite by an easy high energy treatment (see Figure 6). In this way it is possible to obtain some different nanostructures: GNP, FLG or graphene monolayer.

Iron(III) Chloride - Graphite

$FeCl_3$ - graphite compound (see Figure 7), is one of the many well-known GICs. Cowley & Ibers [57] found that reaction of excess $FeCl_3$ with graphite at 300 ℃ yielded both graphite and a first stage compound $C_{6.69}FeCl_3$.
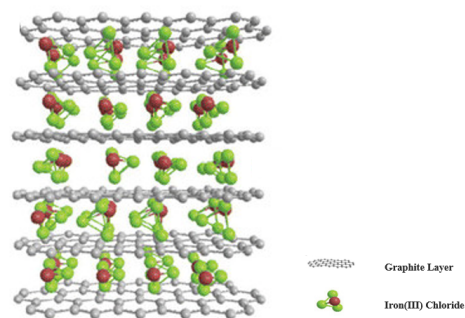
Figure 7: Schematic illustration for FeCl$_3$ intercalated graphite [58]

Nowadays it is of interest because from this compound it is possible to obtain a magnetic-expanded graphite by means of a chemical reduction [49]. In this work, it is presented a new method for obtaining a magnetic-expanded graphite heating a solid-mixture of iron(III)-chloride and natural graphite by means of microwaves.

Thesis Outlines

The present dissertation is divided into two parts. **Part I** is mainly focused on the synthesis and the characterization of Graphite Bisulfate using seven different types of oxidizing agents. Materials and reagents used for synthesizing graphite bisulfate, chemical synthesis and expansion methods, and techniques used to characterize the achieved graphite intercalation compounds (GICs), are extensively described in *Chapter 1*. *Chapter 2* of the thesis provides a preliminary study of the influence of time and temperatures on the chemical reactions and it has been performed using the most common system used in the literature to obtain graphite bisulfate: H_2SO_4/HNO_3. The basic purpose of this study was to determine the optimal reaction conditions. Results of the characterizations performed on the prepared compounds, and the related discussions, are presented and described in *Chapters 3* and *4*. In particular the morphology and crystallographic structure are discussed in *Chapter 3* and chemical structure of the prepared GICs in *Chapter 4*. *Chapter 5* is devoted to the expansion phenomenon and the thermal behavior of the GICs. There are reported experimental results related to the expansion reaction and a description of the morphological changes due to samples under heating. *Part I Conclusions* summarizes the main findings obtained and is also reported for sake of clarity in the final conclusions of the thesis. **Part II** describes the study of an Expandable Graphite with magnetic properties. This GIC is prepared by intercalation of Iron(III) Chloride in natural graphite. In *Chapter 6* are given some information about the preparation of a magnetic-GIC, results of preliminary characterization and some suggestion on future work. Finally, the *Conclusions* section is dedicated to a brief summing up of the activities, aiming to highlight the main findings of the performed research. Additional study, based on micromechanical technique for the synthesis of graphene supported by polymeric film, has been provided separately in the *Appendix* at the end of dissertation, to preserve the fluency when presenting and discussing the main results of the work.

References

[1] H.W. Kroto, J.R. Heath, S.C.O' Brien, Curl & R.E. Smalley, C_{60}: *Buckminsterfullerene*, Nature 318, 162-163, **(1985)**

[2] J. Hare, *Fullerenes, Nanotubes and Nobel Prizes: 25 years of C60,* Ethical Record, Vol. 115, No.8, **(2010)**

[3] D.D.L. Chung, *Review Graphite*, J. Mater. Sci. 37, 1475, **(2002)**

[4] V. Nicolosi1, M. Chhowalla, M.G. Kanatzidis, M.S. Strano, J.N. Coleman, *Review Liquid Exfoliation of Layered Materials*, Science, 340, 6139, **(2013)**

[5] J.D. Bernal, *The Structure of graphite*, Proceedings of the Royal Society of London 106, 740, 749-773, **(1924)**

[6] R.W.G. Wyckoff, *The elements and compounds RX and RX_2*, Crystal Structures 1, **(1965)**

[7] H.O. Pierson, *Handbook of carbon, graphite, diamond, and fullerenes : properties, processing, and applications,* NP Noyes Publications, 43-44. **(1993)**

[8] H.O. Pierson, *Handbook of carbon, graphite, diamond, and fullerenes : properties, processing, and applications,* NP Noyes Publications, 50-51. **(1993)**

[9] M. Inagaki, *Graphite intercalation compounds-synthesis, structure and application*, Journal-japan Institute Of Energy, **(1998)**

[10] M.S. Dresselhaus, G. Dresselhaus, *7th International Symposium on Intercalation Compounds*, Molecular Crystals & Liquid Crystals Science & Technology, Section A, 244, 1, **(1994)**

[11] K.S. Novoselov, A.K.Geim, et al., *Electric field effect in atomically thin carbon films*, Science, 306, (5696):666–669, **(2004)**

[12] A. Geim, *Graphene: Status and Prospects*, Science 324, 1530, **(2009)**

[13] M.S. Khot, A.S. Gadekar, M.J. Kahane, V.V. Potnis, D.B. Baghwan, S.P. Dhamane, A.S. Kulkarni *Graphene – A Review*, International Journal of Pharma. and Phytoph. Research 3, 337-342, **(2014)**

[14] Y. Hernandez, V. Nicolosi, M. Lotya, F.M. Blighe, Z. Sun, S. De, I.T. McGovern, B. Holland, M. Byrne, Y.K. Gun'Ko, J.J Boland, P. Niraj, G. Duesberg, S. Krishnamurthy, R. Goodhue, J. Hutchison, V. Scardaci, A.C. Ferrari, J.N. Coleman, *High-yield production of graphene by liquid-phase exfoliation of graphite,* Nature Nanotechnology 3, 563–568, **(2008)**

[15] S. Park, R.S. Ruoff, *Chemical methods for the production of graphenes*, Nature Nanotechnology 4, 217-224, **(2009)**

[16] V. Singh, D. Joung, L. Zhai, S. Das, S.I. Khondaker, S. Seal, *Graphene based materials: Past, present and future,* Progress in Materilas Science, 1178-1271, **(2011)**

[17] C. Soldani, A. Mahmood, E. Dujardin, *Production, properties and potential of graphene*, Carbon 48, 2127-2150, **(2011)**

[18] A.B. Kaul, *Two-dimensional layered materials: Structure, properties, and prospects for device applications*, Journal of Materials Research, 29(3), 348–361, **(2014)**

[19] M.S. Dresselhaus, G. Dresselhaus, *New Directions in Intercalation Research*, Mol. Crystals & Liquid Crystals Scie. and Tech. Section A 244, **(1994)**

[20] W. Zhao, P.H. Tan, J. Liu, A.C. Ferrari, *Intercalation of few-layer graphite flakes with $FeCl_3$: Raman determination of Fermi level, layer by layer decoupling, and stability*, J. Am. Chem. Soc. 133, 5941–5946, **(2011)**

[21] H. Zhang, Y. Wu, W. Sirisaksoontorn, V.T. Remcho, M.M. Lerner, *Preparation, characterization, and structure trends for graphite intercalation compounds containing pyrrolidinium cations*, Chem. Mater. 28, 969-974, **(2016)**

[22] S. Tian, L. Qi, H. Wang, *Difluoro(oxalate)borate anion intercalation into graphite electrode from ethylene carbonate*, Solid State Ionics 291, 42-46, **(2016)**

[23] L.B. Ebert, *Intercalation compounds of graphite*, Annual Review of Materials Science, 6.1, 181-211, **(1976)**

[24] A.V. Yakovlev, A.I. Finaenov, S.L. Zabud'kov, E.V. Yakovleva, *Thermally Expanded Graphite: Synthesis, Properties and Prospects for Use*, Russian J. App. Chemistry 79, 1741-1751, **(2006)**

[25] A.M. Dimiev, G. Ceriotti, N. Behabtu, D. Zakhidov, M. Pasquali, R. Saito et al., *Direct real- time monitoring of stage transition in graphite intercalation compounds*, ACSNano 7, 2773-2780, **(2013)**

[26] T. Enoki, M. Suzuki, M. Endo, *Graphite Intercalation Compounds and Applications*, Oxford University Press, London **(2003)**

[27] N. Caswell, S.A. Solin, *Vibrational excitations of pure FeCl$_3$ and graphite intercalated with ferric chloride*, Solid State Commun. 27, 961-967, **(1978)**

[28] C. Underhill, S.Y. Leung, G. Dresselhaus, M.S. Dresselhaus, *Infrared and Raman spectroscopy of graphite-ferric chloride*, Solid State Commun. 29**,** 769-774, **(1979)**

[29] H.S. Cheng, X.W. Sha, L. Chen, A.C. Cooper, M.L. Foo, G.C. Lau et al., *An enhanced Hydrogen adsorption enthalpy for fluoride intercalated graphite compounds*, J. Am. Chem. Soc. 131, 17732-17733, **(2009)**

[30] A. Gruneis, C. Attaccalite, A. Rubio, D.V. Vyalikh, S.L. Molodtsov, J. Fink et al., *Electronic structure and electron-phonon coupling of doped graphene layers in KC8*, Phys. Rev. B 79, **(2009)**

[31] A. Gruneis, C. Attaccalite, A. Rubio, D.V. Vyalikh, S.L. Molodtsov, J. Fink J et al., *Angle-resolved photoemission study of the graphite intercalation compound KC8: A key to graphene*, Phys. Rev. B 80, **(2009)**

[32] D.D.L. Chung, *Review exfoliation of graphite*, J. of Materials Sci. 22, 4190-4198, **(1987)**

[33] R. Matsumoto, Y. Hoshina, N. Azukawa, *Thermoelectric Properties and Electrical Transpor tof Graphite Intercalation Compounds*, Materials Transaction 50, 1607-1611, **(2009)**

[34] Y. Takada, *Theory of Superconductivity in Graphite Intercalation Compounds*, arXiv:1601.02753, **(2016)**

[35] R. Setton, *Intercalation compounds of graphite and their reactions, in Preparative chemistry using support reagent*, P. Laslzo Ed., Academic Press, Inc, San Diego, 255-280, **(1987)**

[36] L. Wang, Y. Zhu, C. Guo, X. Zhu, J. Liang, Y. Qian, *Ferric chloride-Graphite Intercalation Compounds as anode materials for Li-ion batteries*, Chem. Sus. Chem.7**,** 87-91, **(2014)**

[37] B. J. Lee, *Characteristics of Exfoliated Graphite Prepared by Intercalation of Gaseous SO$_3$ into Graphite*, Bulletin-korean Chemical Society, 23(12), 1801-1805, **(2002)**

[38] M. Toyoda, & M. Inagaki, *Heavy oil sorption using exfoliated graphite: New application of exfoliated graphite to protect heavy oil pollution*, Carbon, 38(2), 199-210, **(2000)**

[39] G. Carotenuto, S. De Nicola, M. Palomba, D. Pullini, A. Horsewell, T.W. Hansen et al., *Mechanical properties of low-density polyethylene filled by graphite nanoplatelets*, Nanotechnology 23, 485705. 17, **(2012)**

[40] G. Carotenuto, A. Longo, S. De Nicola, C. Camerlingo, L. Nicolais, *A simple mechanical technique to obtain carbon nanoscrolls from graphite nanoplatelets*, Nanoscale Res. Lett.8 403, **(2013)**

[41] A. Melezhyk, E. Galunin, N. Memetov, *Obtaining graphene nanoplatelets from various graphite intercalation compounds*, IOP Conf. Series: Mat. Sci. Eng. 98, 012041, **(2015)**

[42] G. Carotenuto, A. Longo, L. Nicolais, S. De Nicola, E. Pugliese, M. Ciofini M et al., *Laser-Induced Thermal Expansion of H2SO4 -Intercaleted Graphite Lattice*, J. Phys. Chem. C 119, 15942-15947, **(2015)**

[43] H.P. Boehm, R. Setton, E. Stumpp, *Nomenclature and Terminology of Graphite Intercalation Compounds*, Pure and Appl. Chem. 66, 1893-1901, **(1994)**

[44] A. Herold, *Crystallo – chemistryof carbon intercalation compounds*, in Intercalated layered materials. F. Levy Ed., Spronger Publ., Dordrecht, 323-421, **(1979)**

[45] R. Matsumoto, T. Okabe, *Electrical conductivity and air stability of FeCl$_3$. CuCl$_2$, MoCl$_5$ and SbCl$_5$ graphite intercalation compounds prepared from flexible graphite sheets*, Synth. Met. 212, 62-68, **(2015)**

[46] M. Fauchard, S. Cahen, P. Lagrange, J.F. Marech, C. Hérold, *Gold nanosheets intercalated between graphene planes*, Carbon 65, 236-242, **(2013)**

[47] J. Assouik, L. Hajji, A. Boukir, M. Chaouqi, P. Lagrange, *Heavy alkali metal-arsenic alloy-based graphite intercalation compounds: Investigation of their physical properties*, C.R. Chimie, 1-9, **(2016)**

[48] J.M. Benoit, J.P. Buisson, O. Chauvet, C. Godon, S. Lefrant, *Low-frequency Raman studies of multiwalled carbon nanotubes: Experiments and theory* Phys. Rev. B 66, 073417, **(2002)**

[49] A. Messaoudi, M. Inagaki, F. Beguin, *Chemical reduction of FeCl 3–graphite intercalation compounds with potassium–naphthalene complex in tetrahydrofuran*, Journal of Materials Chemistry, 1(5), 735-738, **(1991)**

[50] M. Inagaki, *On the formation and decomposition of graphite-bisulfate*, Carbon, 4.1, 137-141, **(1966)**

[51] C. Schafheutl , *Ueber die Verbindungen des Kohlenstoffes mit Silicium, Eisen und anderen Metallen, welche die verschiedenen Gallungen von Roheisen, Stahl und Schmiedeeisen bilden*, J. Prakt. Chem. 21, 129-157, **(1840)**

[52] G. U. Sumanasekera, J. L. Allen, S. L. Fang, A. L. Loper, A. M. Rao, and P. C. Eklund, *Electrochemical Oxidation of Single Wall Carbon Nanotube Bundles in Sulfuric Acid*, J. Phys. Chem. B, 103, 4292-4297, **(1999)**

[53] D. Roy, E. Angeles-Tactay, R.J.C. Brown, S.J.Spencer, Fry T, Dunton T A, et al., *Synthesis and Raman spectroscopic characterisation of carbon nanoscrolls*, Chem. Phys. Lett. 465, 254-257, **(2008)**

[54] A. Bayat, S. F. Aghamiri, A. Moheb, *Oil Sorption by Synthesized Exfoliated Graphite (EG),* Iranian Journal of Chemical Engineering, 5 1 , **(2008)**

[55] G. Camino, S. Duquesne, R. Delobel, B. Eling, C. Lindsay & T. Roels, *Mechanism of expandable graphite fire retardant action in polyurethanes*, ISO 690, **(2000)**

[56] S. Duquesne, M. Le Bras, S. Bourbigot, R. Delobel, G. Camino, B. Eling & T. Roels, *Thermal degradation of polyurethane and polyurethane/expandable graphite coatings. Polymer degradation and stability*, 74(3), 493-499, **(2001)**

[57] J.M. Cowley, J.A. Ibers, Acta Crystal/ogr, 9, 421-3, **(1956)**

[58] Y. Li, & N. Chopra, *Progress in large-scale production of graphene. Part 1: chemical methods*, Jom, 67(1), 34-43, **(2015)**

Part I

Graphite Bisulfates

Chapter 1

Materials and Methods

In this chapter, the materials and reagents used to prepare different Graphite Intercalation Compounds are listed. It is explained the method by which they are prepared and it is described the characterization techniques used on the analyzed samples.

1.1 Materials and Reagents

The materials and the reagents used to obtain different graphite bisulfates are:

1. Natural graphite flakes;

2. Intercalating agent: Sulfuric Acid (H_2SO_4);

3. Oxidizing agents:

   - Nitric Acid (HNO_3);
   - Potassium Nitrate (KNO_3);
   - Hydrogen Peroxide (H_2O_2);
   - Potassium Permanganate ($KMnO_4$);
   - Potassium Dichromate ($K_2Cr_2O_7$);
   - Sodium Periodate ($NaIO_4$);
   - Sodium Chlorate ($NaClO_3$).

1.1.1 Natural Graphite

The Natural Graphite is a non-metallic mineral commercially available in different forms (vein, flakes, amorphous), inexpensive and easy to find. In this study starting natural graphite used is in form of flakes (Figure 1.1), a commercial product supplied by Sigma-Aldrich. The characteristics of the material are reported in Table 1.1.

Figure 1.1: Natural Graphite flakes

Table 1.1: Graphite flakes properties

Material	Graphite
Producer	Sigma-Aldrich
Form	flakes
Particle size	+100 mesh ($\geq 75\,\%$ min)
MP	$3652 - 3697\,°$C(lit.)

1.1.2   Intercalating Agent - H_2SO_4

The Sulfuric Acid is an inorganic strong acid. It has been used as intercalating agent in this work. It may be prepared by catalytic oxidation of sulfur dioxide. The H_2SO_4 properties are shown in Table 1.2.

Table 1.2: Sulfuric acid properties

Reagent	Sulfuric Acid H_2SO_4
Producer	J.T. Baker
Vapor Pressure	$1\,$mmHg(at $146\,°$C)
Description	Nominally $95 - 97\,\%$ H_2SO_4
Assay	$95 - 97\,\%$
BP	˜$290\,°$C(lit.)

1.1.3 Oxidizing Agents

Nitric Acid - HNO_3 The Nitric Acid is the first oxidizing agent used in this work. It is a strong acid and it is the most common auxiliary agent found in the literature to prepare the GICs, expandable graphite and so on [1, 2]. Its properties are reported in Table 1.3.

Table 1.3: Nitric acid properties

Reagent	Nitric Acid HNO_3
Producer	SIGMA-ALDRICH
Grade	ACS reagent
Vapor Density	1 (vs air)
Vapor Pressure	$8\,\mathrm{mmHg}(20\,°\mathrm{C})$
Assay	$68.0 - 70.0\,\%$ (ACS specification)
BP	$120.5\,°\mathrm{C}$(lit.)

Potassium Nitrate - KNO_3 Potassium nitrate is a water-soluble inorganic salt. It was used as oxidizing agent in this work. The properties of KNO_3 are shown in Table 1.4.

Table 1.4: Potassium nitrate properties

Reagent	Potassium Nitrate KNO_3
Producer	ACROS ORGANICS BVBA
Grade	reagent grade
Assay	$\geq 99.0\,\%$
Mp	$334°\,\mathrm{C}$(lit.)
Solubility	H_2O: soluble $20/150\,\mathrm{g/mL}$

Hydrogen Peroxide - H_2O_2 Hydrogen Peroxide is the simplest peroxide. It is used as an oxidizer, bleaching agent and disinfectant. It is an unstable and slowly decomposes. The properties of H_2O_2 are reported in Table 1.5.

Table 1.5: Hydrogen peroxide properties

Reagent	Hydrogen Peroxide H_2O_2
Producer	PANREAC
Density	$1.10\,\mathrm{kg/L}$
Assay	$30\,\%\,\mathrm{w/v}(100\,\mathrm{vol.})$
BP	$107\,°\mathrm{C}$

Potassium Permanganate - $KMnO_4$ Potassium permanganate is suitable for heterogeneous oxidations. It is one of the oxidizers used in the famous *Hummer*'s method [3] where it is used in addition to a mixture of sodium nitrate (another oxidizer) and sulfuric acid. Its characteristics are reported in Table 1.6.

Table 1.6: Potassium permanganate properties

Reagent	Potassium Permanganate $KMnO_4$
Producer	Sigma-Aldrich
Grade	ACS reagent
Assay	$\geq 99.0\,\%$
Solubility	water: soluble

Potassium Dichromate - $K_2Cr_2O_7$ Potassium dichromate is a strong oxidizing agent. In this work it has been used in comparison with other oxidizers. Table 1.7 summarizes its properties.

Table 1.7: Potassium dichromate properties

Reagent	Potassium Dichromate $K_2Cr_2O_7$
Producer	Chem-Lab NV
Grade	ACS reagent
Assay	$\geq 99.8\,\%$
MP	398 °C(lit.)

Sodium Periodate - $NaIO_4$ Sodium periodate is an oxidizing agent used to generate quinones via glycol cleavage and oxidation of hydroquinones. Usually, it is used in mixtures with permanganate to oxidize the olefins [4] and, recently, it been used to oxidize graphite too [5]. In this work it has been used for the first time to oxidize graphite flakes without the catalytic action of the permanganate. $NaIO_4$ properties are reported in Table 1.8.

Table 1.8: Sodium periodate properties

Reagent	Sodium Periodate $NaIO_4$
Producer	Sigma-Aldrich
Grade	ACS reagent
Assay	$\geq 99.8\,\%$
MP	300 °C(dec.)(lit.)

Sodium Chlorate - $NaClO_3$ Sodium chlorate is a hygroscopic non-chiral ionic compound. Its commercial production is by anodic oxidation of $NaCl$. $NaClO_3$ is a very strong oxidizer, it is used in the fabrication of chlorate-based

explosives. In this work, it has been used to oxidize graphite in a novel way with respect to the well-known *Brodie's* and *Staudenmaier's* methods [6, 7]. Its properties are shown in Table 1.9.

Table 1.9: Sodium chlorate properties

Reagent	Sodium Chlorate $NaClO_3$
Producer	CHEM-LAB NV
Grade	ACS reagent
Assay	$\geq 99.0\%$
MP	$248 - 261$ °C(lit.)
Solubility	water: soluble

1.2 Synthesis and Preparation Methods

In this section it is discussed:

1. synthesis method used to obtain the GICs;

2. GICs expansion method.

1.2.1 Graphite Intercalation Compounds Synthesis

The different Graphite Intercalation Compounds have been chemically synthesized by treating graphite flakes with an oxidizing agent/sulfuric acid mixture. In particular, a glass-flask placed in a thermostatic bath has been used as reactor as shown in Figure 1.2. Slow air-bubbling was applied in order to homogenize the system during the reaction. A ratio of 9:1 by volume H_2SO_4/oxidizing agent has been selected for all compositions [8]. This volumetric ratio has been chosen because many works in the literature report a very small amount of oxidizing agent is enough to induce intercalation [9]. Constant quantities of graphite flakes (2 g, Aldrich, > 100 mesh), mixture volume (40 mL), and oxidizing agent molar amounts have been used. Cold deionized water has been added to reactive mixture to end the reaction. At first, a preliminary study was made on the only system H_2SO_4/HNO_3, that is the most common system to produce GICs. The aim of this preliminary study was to find the best reaction conditions for obtaining the intercalation phenomenon. Once the conditions have been chosen, the others oxidizing agents have been used with the intercalating agent to obtain the different GICs. .

1.2.1.1 Synthesis of GICs for study of the Time - Temperature Conditions

The first study was a GIC obtained from a reaction between graphite flakes and H_2SO_4/HNO_3 mixture. A 36 mL volume of H_2SO_4 and 4 mL volume of HNO_3 have been used to maintain a 9 : 1 volumetric ratio in a 40 mL
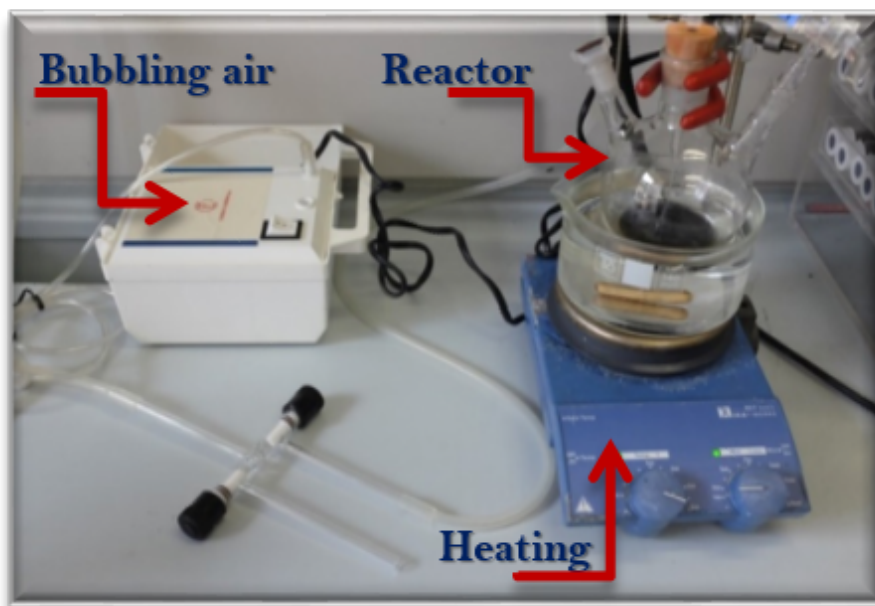
Figure 1.2: Reaction system

volume of solution. In order to find the best conditions for the reaction of GICs preparation, different reaction times and temperatures have been explored. In particular four different times and three different temperature have been set. In Table 1.10 there is a summary of all samples prepared for this part of the study. The results of this preliminary study, as it will be further discussed in the next

Table 1.10: Sample codes of GICs for the *Time-Temperature* study

TEMP. (°C)→	25°	40°	60°
TIME (h)↓			
1	*AI_25_1h*	*AI_40_1h*	*AI_60_1h*
2	*AI_25_2h*	*AI_40_2h*	*AI_60_2h*
3	*AI_25_3h*	*AI_40_3h*	*AI_60_3h*
4	*AI_25_4h*	*AI_40_4h*	*AI_60_4h*

chapters, show that the time of one hour and room temperature are enough to obtain a GIC with a good intercalation degree and, therefore, good expansion properties.

1.2.1.2 Synthesis of GICs from Different Oxidizing Agents

Synthesis of the GICs obtained by others oxidizing agents were the same as described in the previous section. Although the previous study has shown that

the room temperature is enough for the GICs synthesis, slightly higher temperatures were chosen in order to have a real control of the reaction temperature. Therefore, time of 1 hour and temperatures of 30 ℃ or 40 ℃ (depending on the oxidizers reactivity) were selected for the reactions. Table 1.11 summarizes the oxidizers used with the respective temperatures. The used reagents amounts were calculated to preserve the $9:1$ volumetric ratio (H_2SO_4/oxidizing agent) in a mixture of 40 mL.

Table 1.11: Oxidizing agents used in the reactive mixtures with H_2SO_4 and experimental conditions

Oxidizer	HNO_3	KNO_3	H_2O_2	$KMnO_4$
Reaction Temperature (℃)	40	30	40	30

Oxidizer	$K_2Cr_2O_7$	$NaIO_4$	$NaClO_3$	
Reaction Temperature (℃)	30	40	30	

1.2.2 GICs Expansion Method

As explained in the Introduction, some GICs (as graphite bisulfates) have the ability to expand when heating is applied to them. The thermal shock causes a violent reaction between Carbon of the graphite and sulfuric acid molecules and HSO_4^- ions present in the graphite inter-layers. This reaction occurs with gas release, which in turn determines a strong inter-layer distancing. The product of this reaction is named *expanded graphite*. The resulting morphology is very different from that of the GICs flakes, that results in a substantial volumetric expansion. The resultant materials have a worm-like shape [5, 10]. Traditionally the expansion was made in a tube furnace preheated at 1000 ℃ for some seconds [12], or on the flame, or with resistance and induction heating [13]. In this study, the expanded graphite is obtained by heating the GICs by means of a microwave oven (see Figure 1.3). This technique permits to obtain the expansion very quickly, just a few seconds, and very easily [14]. During this process the graphite crystals are converted to very porous filaments by an uniaxial expansion mechanism involving the graphite crystal lattice. Such expansion is due to a mixture of gases (as described in the Introduction section) which are produced in the crystal lattice by the reaction of carbon with H_2SO_4 [9].

1.3 Technical Analysis

The obtained compounds were studied and characterized using the following techniques:

Morphological analysis

- USB microscopy

Figure 1.3: Microwave oven

- Scanning electron microscopy (SEM)

- Energy Dispersive X-ray Spectroscopy (EDS)

- Transmission Electron Microscopy (TEM)

Structural analysis

- Wide Angle X-ray Diffraction (WAXD)

- Micro-Raman Spectroscopy (μ-RS)

- Fourier transform infrared spectroscopy (FT-IR)

Thermal analysis

- Thermogravimetric Analysis (TGA)

1.3.1   Morphological Analysis

1.3.1.1   USB Microscopy

A USB microscope (PCE-MM200 Microscope; PCE Group) has been used to
observe the morphology of obtained GICs, immediately after each reaction.

1.3.1.2 Scanning Electron Microscopy (SEM)

The structure and the morphology of the graphite flakes and obtained GICs were determined by means of a Fei Quanta 200 scanning electron microscope (SEM) Feg. The scanning electron microscope is an instrument characterized by a high resolving power, of the order of $200 - 300 \,\text{Å}$, and provides three-dimensional images of the surfaces observed. At first the samples were fixed on a support. This survey was carried out on the samples to see what treatment may have led to changes in the surface and to have an immediate idea of the effect of the intercalation for each GIC.

Energy Dispersive X-ray Spectroscopy (EDS)   The Energy Dispersive X-ray Spectroscopy is an analytical technique used for the elemental analysis of a sample. This analysis can be made with the Scanning Electron Microscope. The model used was a Inca Oxford 250. Interaction of the e-beam with atoms in the sample causes shell transitions which result in the emission of an X-ray. The emitted X-ray has an energy characteristic of the parent element. Detection and measurement of the energy permits elemental analysis. EDS can provide rapid qualitative, or quantitative analysis of elemental composition.

1.3.1.3 Transmission Electron Microscopy (TEM)

The structure of the graphite and the GICs flakes and their microstructures was determined using a transmission electron microscope (TEM). The transmission electron microscopy is a powerful technique for the characterization of materials at the nanoscale. With the TEM analysis electron beam is passed through a very thin sample. The use of TEM micro-structural analysis permits to achieve very high spatial resolution. The observations were carried out by TEM FEI Tecnai Spirit Twin G12 with LaB6 emission source using spot size 1. The images were acquired by Fei Eagle $4000x4000$ CCD camera, mounted on the same axis. All the compounds analyzed were subjected to sonication by an ultrasonic bath, at room temperature.

1.3.2 Structural Analysis

1.3.2.1 Wide Angle X-ray Diffraction (WAXD)

The use of the technique of X-ray diffraction at high angle (WAXD) allows the analysis of the structural characteristics of the GICs. Wide-angle X-ray diffraction (WAXD) measurements were conducted by Philips XPW diffractometer (Philips Analytical, Almelo, The Netherlands) with Cu Ka radiation (1.542 Å) filtered by nickel. The scanning rate was $0.02 \,^{\text{deg}}/\text{s}$, and the scanning angle was from 5 to $45°$ for all compounds. From this technique is possible to evaluate the shift of the characteristic signals of the graphite diffractogram and the eventual presence/absence of the others signals.
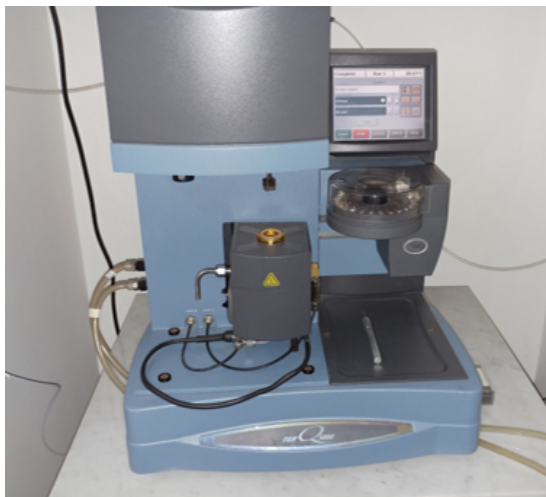
Figure 1.4: TGA: TA Q5000 equipped with infrared furnace heating

1.3.2.2   Micro - Raman Spectroscopy (μ-RS)

Micro-Raman (μ-RS) spectroscopy were used to analyze the chemical structure of pure graphite and "as prepared" graphite bisulfates. A Jobin-Yvon system from Horiba ISA, with a TriAx 180 monochromator, equipped with a liquid-nitrogen-cooled charge-coupled detector was used for the μ-RS measurements. The grating of $1800\,^{\text{grooves}}/_{\text{mm}}$ allows a final spectral resolution of $4\,\text{cm}^{-1}$. The spectra were recorded in air at room temperature using a $17\,\text{mW}$ He-Ne laser source (wavelength $632.8\,\text{nm}$). The spectrum accumulation time was $120\,\text{s}$. The laser light was focused to a $2\,\mu\text{m}$ spot size on the sample through an Olympus microscope with $100\times$ optical objective. The spectra obtained were analyzed in terms of convoluted Lorentzian functions by using a best-fitting routine of GRAMS/AI (2001, Thermo Electron) program, which is based on the Levenberg-Marquardt nonlinear least-square methods.

1.3.2.3   Fourier Transform Infrared Spectroscopy (FT-IR)

FT-IR spectroscopy were used to analyze the chemical structure of pure graphite and graphite bisulfates. FT-IR were recorded in transmission mode with a Perkin Elmer Frontier FT-IR spectrometer, in the range $4000 - 800\,\text{cm}^{-1}$ with $4\,\text{cm}^{-1}$ resolution and 6 scans. The KBr pressed disc technique (1 mg of sample and $160\,\text{mg}$ of KBr) was used. The KBr was first heated in a furnace overnight at $120\,°\text{C}$ to minimize the amount of the adsorbed water.

1.3.3 Thermal Behavior

1.3.3.1 Thermogravimetric Analysis (TGA)

The thermal expansion threshold of the different intercalation compounds was measured by means of a thermogravimetric analysis (TGA). The instrument used was a TA Q5000 equipped with an infrared furnace heating (shown in Figure 1.4). Thermogravimetry consists of recording the variation of mass of a sample as a function of time and/or temperature in a controlled atmosphere. The measurements were carried out at a heating rate of $10\,^{\circ}C/\text{min}$ from $30\,^{\circ}C$ to $800\,^{\circ}C$, using about $1.0/1.8\,\text{mg}$ of the sample in alumina crucible placed in a platinum pan. Such method, illustrated in Figure 1.5) has been used to prevent the leakage of the sample during the expansion phenomenon [8]. The experiments were performed in a Nitrogen atmosphere at flow rate of $25\,\text{mL/min}$. The temperature at which the expansion occurs is determined from thermograms. This specific temperature corresponds to the abscissa of the starting weight loss of the thermograms.

Figure 1.5: TGA setup: alumina crucible placed in platinum pan

References

[1] L.B. Ebert, *Intercalation compounds of graphite*, Annual Review of Materials Science 6.1, 181-211, **(1976)**

[2] A. Mills, et al., *Thermal conductivity enhancement of phase change materials using a graphite matrix*, Applied Thermal Engineering 26.14, 1652-1661, **(2006)**

[3] W.S. Hummers and R.E. Offeman, *Preparation of graphitic oxide*, Journal of the American Chemical 80, 1339 **(1958)**

[4] R.U. Lemieuxan and E. Von Rudloff, *Periodate-Permanganate oxidations I. oxidation of olefins*, Canadian Journal Of Chemistry 33(11), 1701-1709, **(1955)**

[5] M. Yang, S. Moriyama and M. Higuchi1, *Selective Edge Modification in Graphene and Graphite by Chemical Oxidation,* Journal of Nanoscience and Nanotechnology 14, 2974–2978, **(2014)**

[6] B.C. Brodie, *On the Atomic Weight of Graphite*, Philosophical Transactions of the Royal Society of London 149, 249-259, **(1859)**

[7] L. Staudenmaier, *Verfahren zur Darstellung der Graphitsäure,* Ber Dtsch Chem Ges, 1481, **(1898)**

[8] M. Salvatore, G. Carotenuto, S. De Nicola, C. Camerlingo, V. Ambrogi, C. Carfagna, *Synthesis and characterization of high-filled intercalated graphite bisulphate*, Nanoscale Research Letters, 12:167, **(2017)**

[9] G. Carotenuto, S. De Nicola, M. Palomba, D. Pullini, A. Horsewell, T.W. Hansen, & L. Nicolais, *Mechanical properties of low-density polyethylene filled by graphite nanoplatelets*, Nanotechnology, 23(48), 485705, **(2012)**

[10] Celzard, A., et al., *Electrical conductivity of anisotropic expanded graphite-based monoliths.* Journal of Physics D: Applied Physics, 33-23, 3094, **(2000)**

[11] W. Wang, X.Yang, Y.Fang, J. Ding, J. Yan, *Preparation and thermal properties of polyethylene glycol/expanded graphite blends for energy storage*, Applied Energy, 86(9), 1479-1483, **(2009)**

[12] M.J. McAllister, J.L. Li, D.H. Adamson, H.C. Schniepp, A.A. Abdala, J. Liu, O.M. Herrera-Alonso, D. L. Milius, R. Car, R.K. Prud'homme and I. A. Aksay, *Single Sheet Functionalized Graphene by Oxidation and Thermal Expansion of Graphite*, Chem. Mater. 19, 4396-4404 **(2007)**

[13] D.D.L. Chung, *Review of exfoliation of graphite*, Journal of materials science 22, 4190-4198, **(1987)**

[14] O.Y. Kwon, S.W. Choi, K.W. Park, & Y.B. Kwon, *The preparation of exfoliated graphite by using microwav*e, Journal of Industrial and Engineering Chemistry, 9(6), 743-747, **(2003)**

Chapter 2

Effect of Time - Temperature Conditions

In order to search for the best reaction conditions, it has been analyzed the most common system used in the literature [1, 2] to obtain graphite bisulfate: H_2SO_4/HNO_3. A preliminary time-temperature study has been performed on this system. Three different reaction temperatures (25 °C, 40 °C, 60 °C) and four different reaction times (1, 2, 3 and 4 hours) were used. The sample codes are reported in the Table 1.9 in the previous chapter. In order to confirm the intercalation had been actually achieved, an expansion test, by microwaves, was done for all GICs prepared. For all the samples the expansion phenomenon was observed (an example is reported in Figure 2.1) after a few seconds of heating $(5-10\,\text{s})$ with a strong increment in volume (about 300 %), as found in the literature [3, 4]. This result is the first confirmation of the graphite intercalation achieved.

2.1 Morphological Analysis

2.1.1 USB Microscopy

To observe the morphology of obtained GICs, immediately after the chemical reaction, a USB microscope was used. It is a small, portable microscope that can be linked to PC via USB. With this technique it is possible to observe the differences between morphology of the natural graphite, graphite intercalation compounds and expanded compounds. All the recorded images are very similar. Here, there are reported two of the twelve samples prepared: natural graphite and the GIC *AI_25_1h* as an example. As visible from Figure 2.2, the natural graphite flakes (size $\sim 1\,\text{mm}$) appear still and black. The samples images taken after intercalation and after expansion are reported in Figure 2.3 and 2.4 respectively. Figure 2.3 shows irregular flakes boundary compared with natural graphite flakes. Some flakes seem to be expanded (circled in red). From the
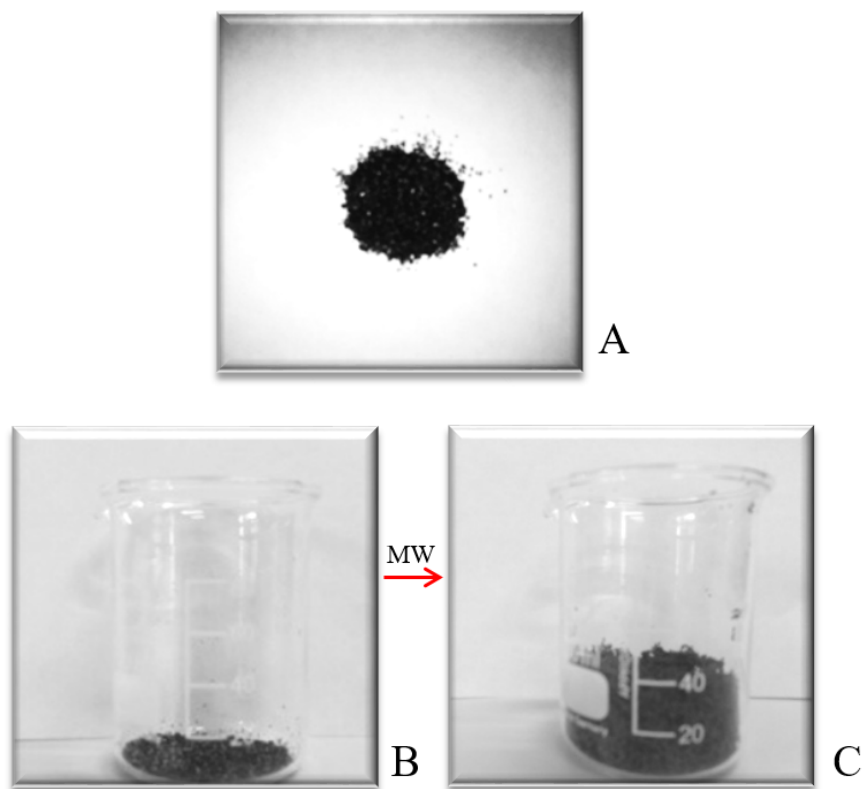
Figure 2.1: Expansion Test (A: Starting Natural Graphite; B: Expandable Graphite, C: Expanded Graphite)
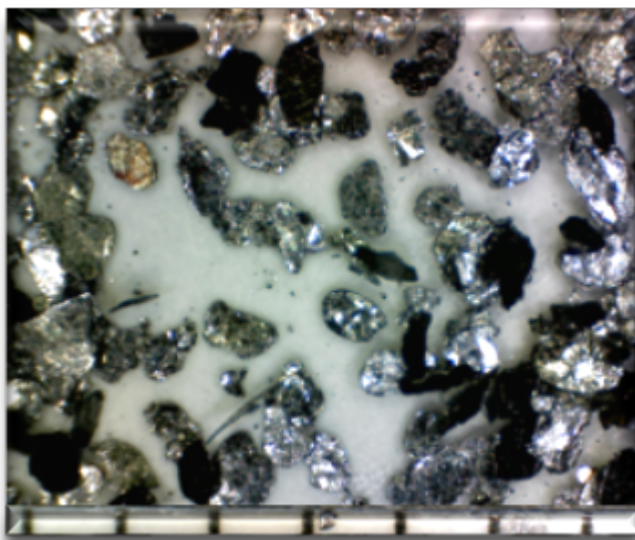
Figure 2.2: USB images of Natural Graphite flakes

Figure 2.4, it can be observed the expansion phenomenon. The flakes are better expanded and have achieved a worm-like shape, typical of an expanded GICs [5], and their size clearly increased compared to that of unexpanded flake. From this analysis we can extract only few and qualitative information. To understand the morphology of the obtained compounds it is necessary to analyze the images obtained by means of electron microscope.

2.1.2 Scanning Electron Microscopy (SEM)

The morphology of the GICs obtained using H_2SO_4/HNO_3 mixture, intercalation degree, differences produced due to different reaction temperatures and times, and others eventual effect of the chemical treatment, were determined by the scanning electron microscope (SEM). In Figure 2.5 the SEM micrographs at two different magnifications ($100X$ and $500X$) of starting natural graphite are reported. Figures 2.6, 2.7, 2.8 and 2.9 show a comparison between the micrographs of a GICs flake obtained at 25 °C, 40 °C, 60 °C for 1, 2, 3 and 4 hours of reaction respectively. All images are taken at magnification of $400X$ or $500X$ depending on the size of the flake. First, we can observe that the intercalation process increased the distance between the graphite layers, for all the considered temperatures and reaction times. From Figure 2.6 it is evident that 1 hour of reaction is enough to achieve good intercalation. Longer treatment times are not useful to get a better intercalation, as visible from Figures 2.7, 2.8, 2.9. In fact, from these images, it seems that the best intercalated compound is the first GIC (*AI_25_1h*) prepared with less severe conditions.

Figure 2.3: USB images of *AI_25_1h* after intercalation reaction

Figure 2.4: USB images of *AI_25_1h* after expansion by microwaves
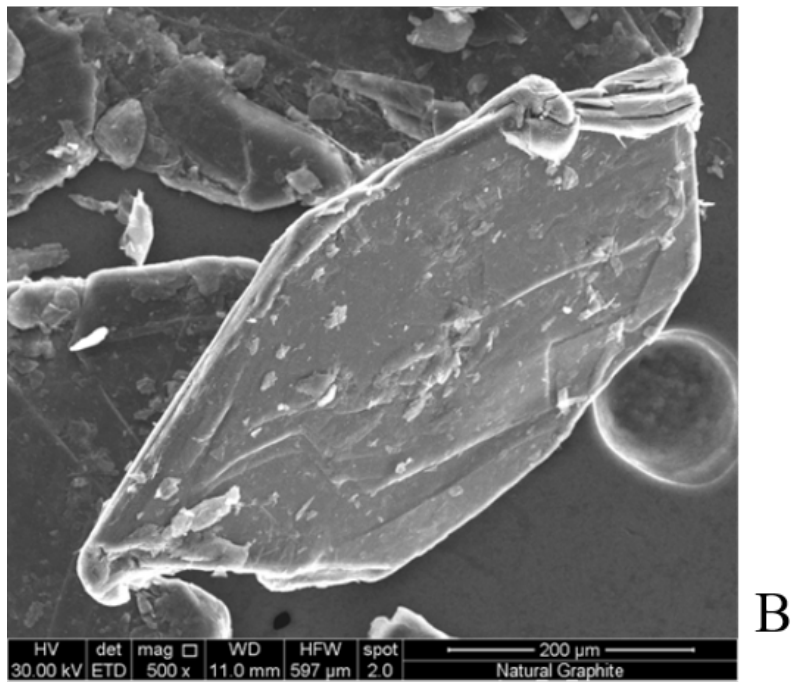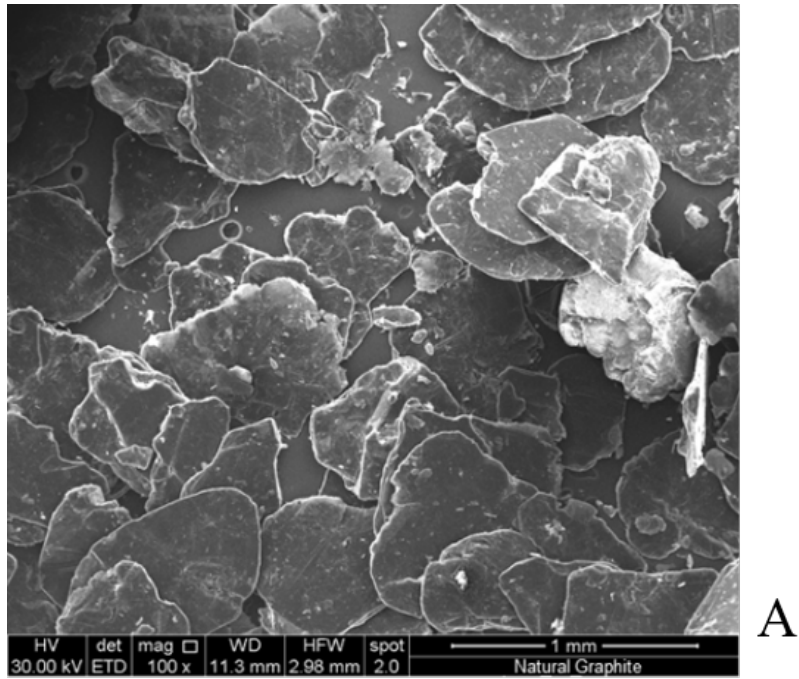
Figure 2.5: Scanning electron micrographs of Natural Graphite (magnification A: 100X, B: 500X)
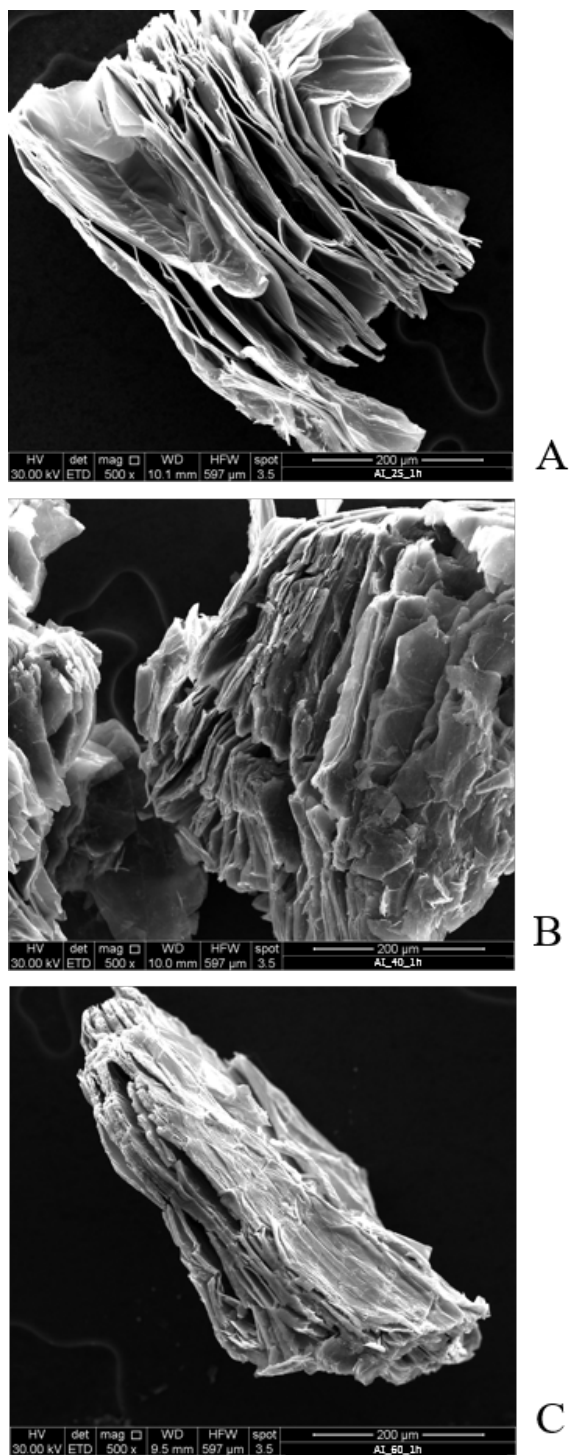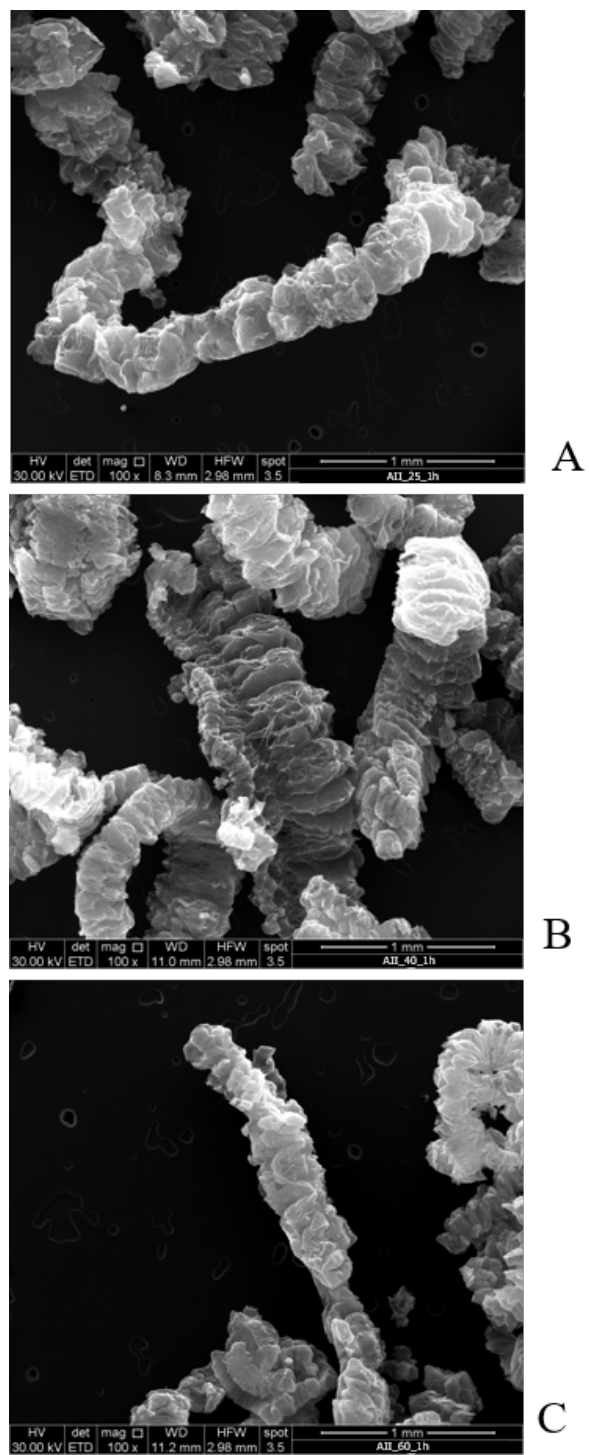
Figure 2.6: Scanning electron micrographs of GICs obtained from 1 hour of reaction at different Temperatures: A: 25 °C, B: 40 °C, C: 60 °C (magnification 500X)
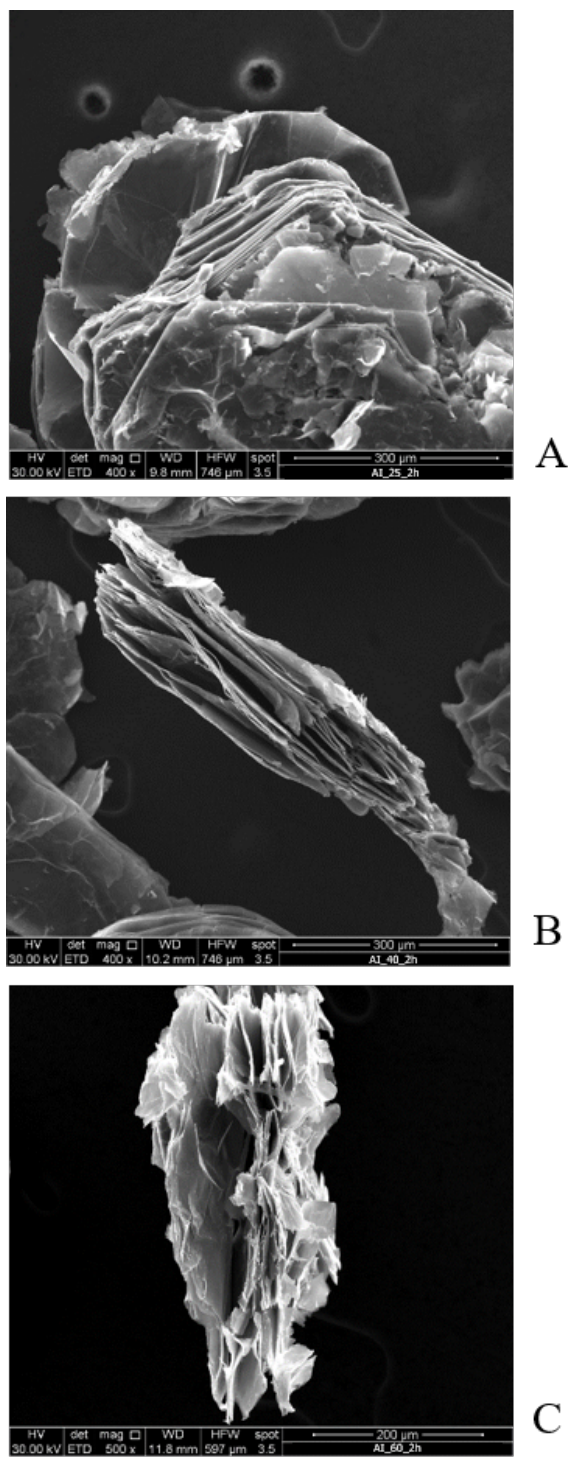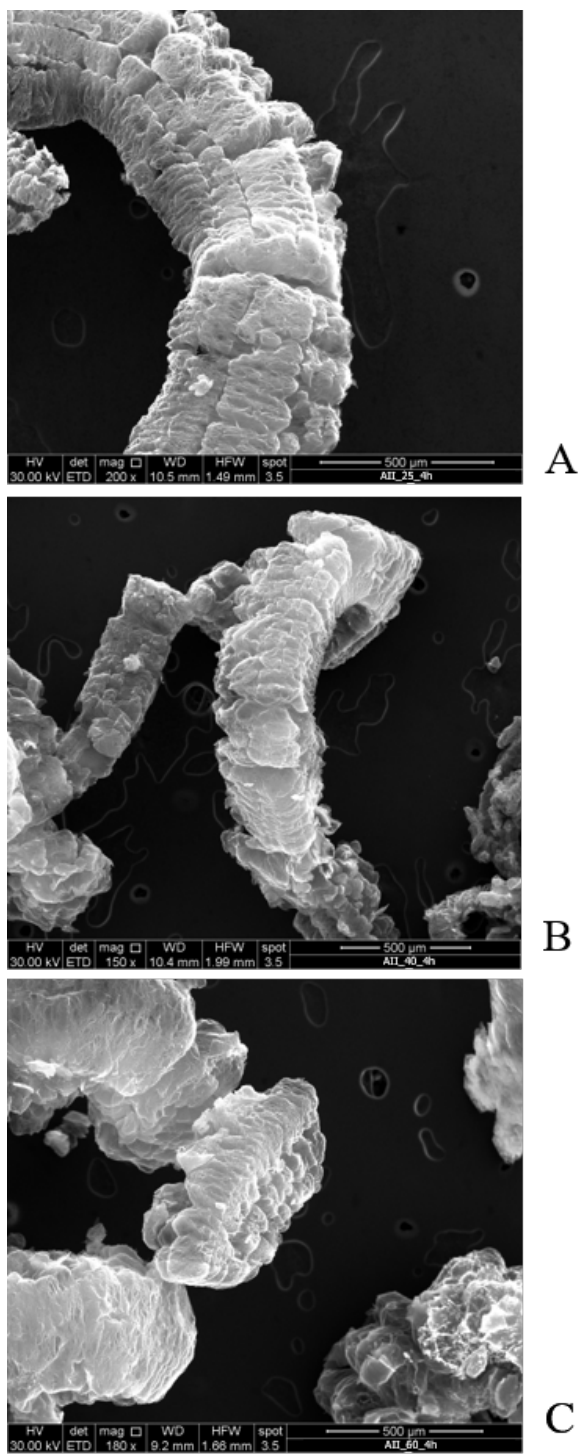
Figure 2.7: Scanning electron micrographs of GICs obtained from 2 hours of reaction at different Temperatures: A: 25 ˚C, B: 40 ˚C, C: 60 ˚C (magnification A, B: 400X and C:500X)
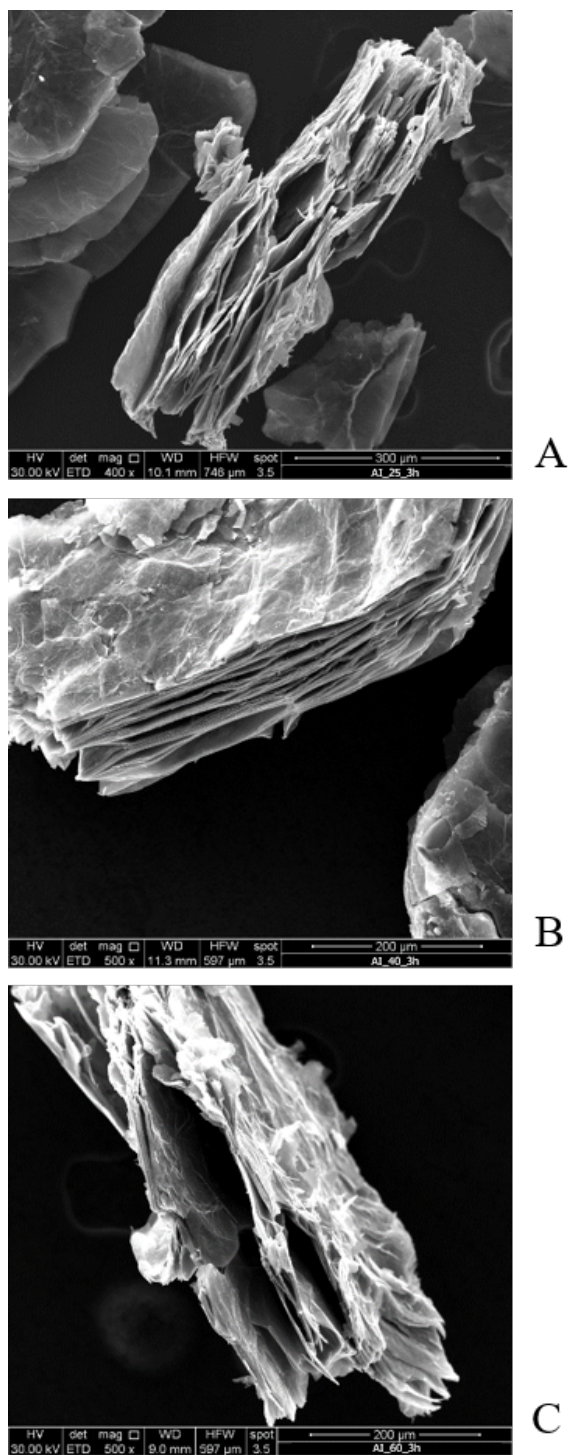
Figure 2.8: Scanning electron micrographs of GICs obtained from 3 hours of reaction at different Temperatures: A: 25 ℃, B: 40 ℃, C: 60 ℃ (magnification A: 400X and B, C:500X)
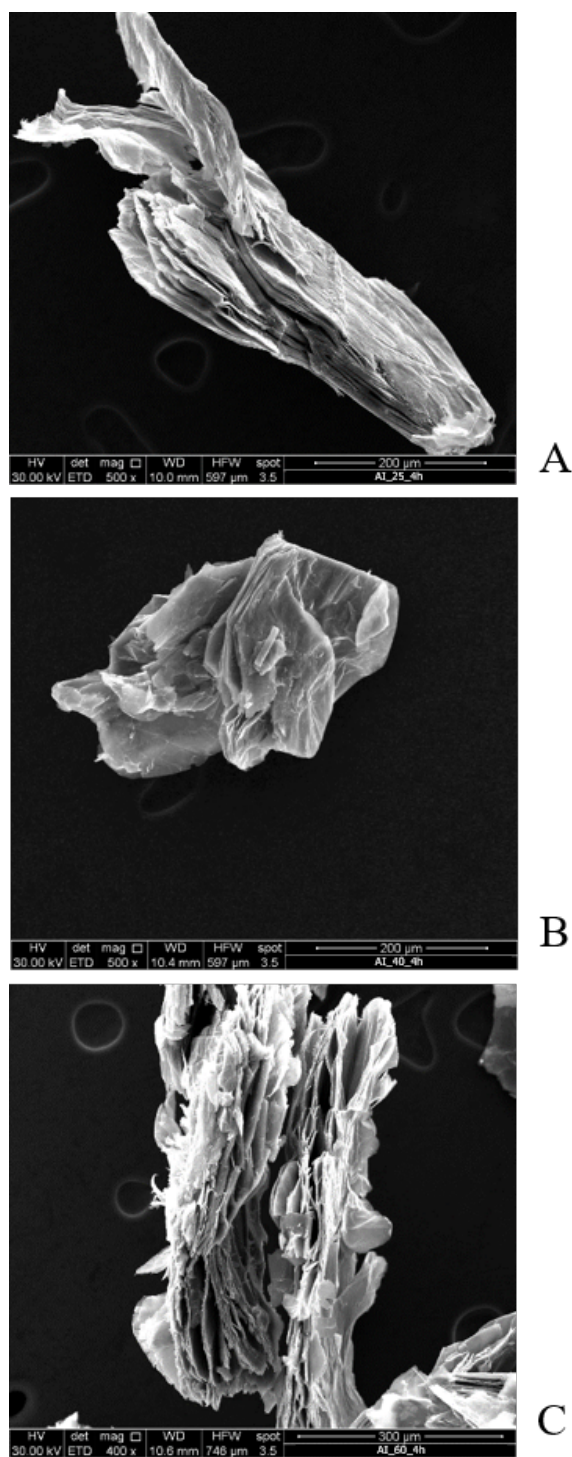
Figure 2.9: Scanning electron micrographs of GICs obtained from 4 hours of reaction at different Temperatures: A: 25 °C, B: 40 °C, C: 60 °C (magnification A, B: 500X and C:400X)

Energy Dispersive X-ray Spectroscopy (EDS)

The presence of the intercalating agent inside the GICs prepared, has been tested by the Energy Dispersive X-ray Spectroscopy (EDS). EDS micro-analysis was carried out on small sample areas to determine nature and percentage of the elements present in the flake. As an example the data of EDS spectra from graphite and GIC obtained by HNO_3 (*AI_40_1h*) are reported. All prepared samples showed qualitatively the same result. In Figure 2.10 A and B the positions where EDS analysis has been performed on the graphite and on the GIC (HNO_3) surface, are showed respectively. The elemental composition for each EDS spectrum is reported in Table 2.1. In natural graphite it can be clearly seen only the presence of the element Carbon (besides some impurity). EDS spectra of the other GICs samples indicated the presence of a significant quantity of Sulfur and Oxygen due to the oxidation/intercalation process, in addition to the presence of Carbon.

Table 2.1: EDS analysis: elemental composition. Results in weight %

	SPECTRUM	C	O	S	Other	Total
Graphite (Figure 2.10 A)	Spectrum 1	100	-	-	-	100
	Spectrum 2	99.50	-	-	0.50	100
	Spectrum 3	99.56	-	-	0.44	100
GIC (HNO_3) (Figure 2.10 B)	Spectrum 1	75.48	21.83	2.32	0.37	100
	Spectrum 2	70.37	21.46	7.93	0.31	100

Morphology of the Expanded Samples

The GICs have been expanded by microwave oven. SEM has been used to analyze morphology of samples which have undergone thermal expansion. Figures 2.11 and 2.12 show a comparison between the micrographs of expanded GICs obtained at 25 °C, 40 °C, 60 °C for 1, and 4 hours respectively. Images have been taken at magnification between $100X - 200X$ depending on the size of the flake under investigation. First, we can observe the morphological changes undergone by the flakes after the thermal shock.   The comparison of SEM images before and after the treatment by microwave, suggests that graphite crystals are converted to very porous filaments with formation of structural defects and bubbles. It is noticeable that the unidirectional expansion induced by the microwaves resulted in a sort of worm-like filament, that is, a long, porous, deformed cylinder-like structure. The expansion is closely related with the intercalation achieved in the step 1 (intercalation reaction) [6]. In this preliminary study, these information have been used to choose the best intercalated compounds. The expanded GICs analysis seems to confirm the result discussed in the section 2.1.2. From the morphology analysis it seems that the lower temperature and time of reaction are the best condition to obtain the GICs.
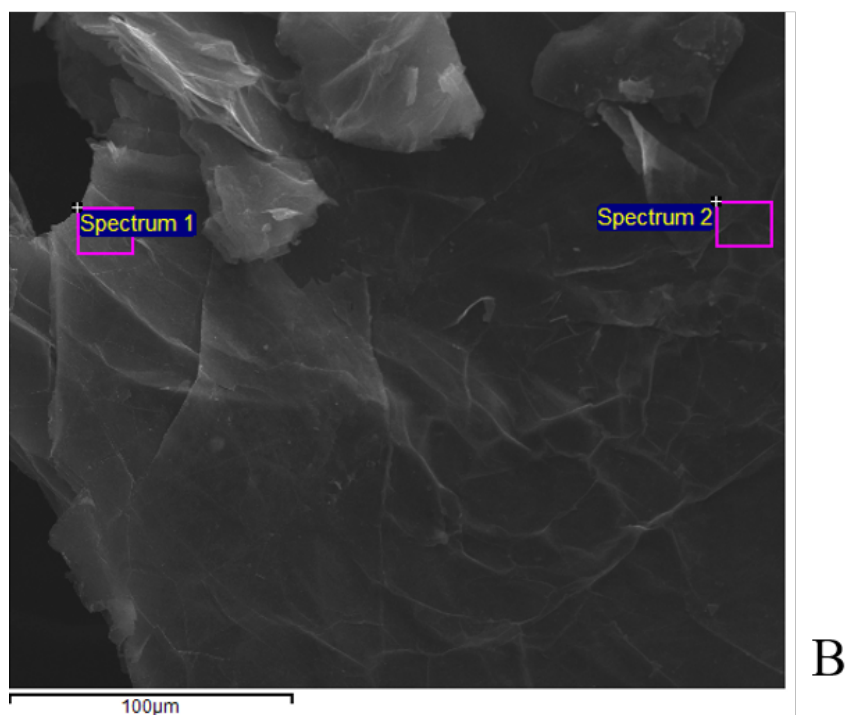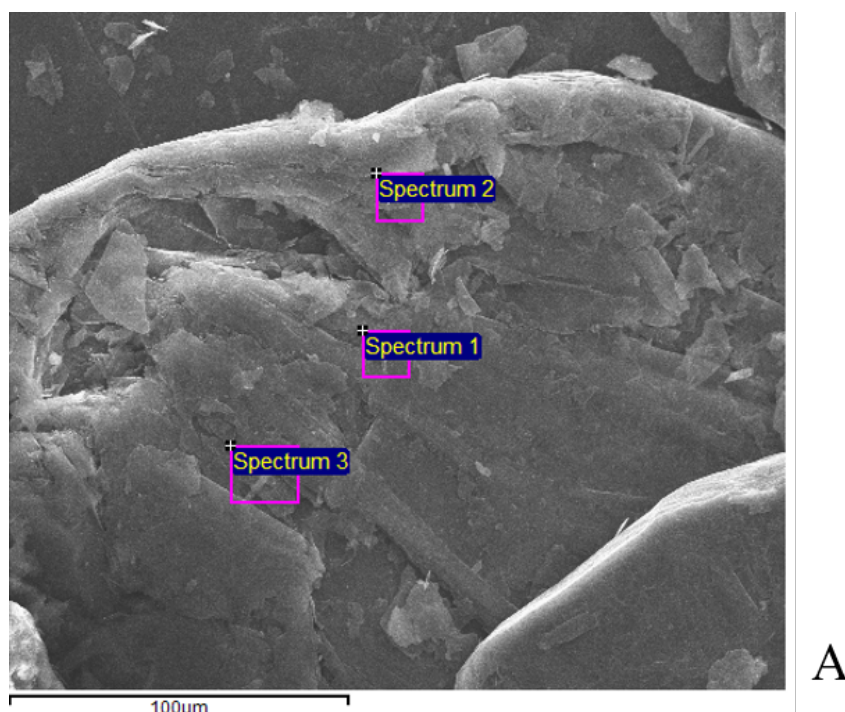
Figure 2.10: Positions where EDS analysis has been performed on A: starting natural graphite and B: *AI_40_1h*

Figure 2.11: Scanning electron micrographs of expanded GICs obtained from 1 hour of reaction at different Temperatures: A: 25 ℃, B: 40 ℃, C: 60 ℃ (magnification 100X)

Figure 2.12: Scanning electron micrographs of expanded GICs obtained from 4 hour of reaction at different Temperatures: A: 25 ˚C, B: 40 ˚C, C: 60 ˚C (magnification A: 200X and B, C: 150X)

2.2   Spectroscopic Analysis

2.2.1   IR Spectroscopy

To study the oxidation and the functional groups presents in various intercalation compounds, FT-IR spectroscopy was performed on prepared samples and on starting natural graphite for comparison. The spectra obtained from the FT-IR analysis of the starting graphite flakes and of the intercalated compounds, are shown in Figure 2.13 A and B respectively, in range of wavenumber from $4000\,\mathrm{cm}^{-1}$ to $800\,\mathrm{cm}^{-1}$. All spectra are shifted arbitrarily along the y-axis to show different trends. As visible, the GICs spectra are remarkably different from that of natural graphite. Prepared GICs exhibit an oxidation signal due to the presence of hydroxyl groups $(-OH)$ at $3400\,\mathrm{cm}^{-1}$. The natural graphite also presents a light oxidation (indicated by a dashed line in Figure 2.13 A). The oxidation degree is quite similar for all spectra analyzed. All spectra also featured a clear signal at $1650\,\mathrm{cm}^{-1}$ ascribed to the $C = C$ double bond stretching vibration and $C - O$ bond stretching vibration at $1200\,\mathrm{cm}^{-1}$. No important differences can be seen in the spectra. This result shows there are not different peaks for the analyzed compounds.

2.3   Conclusions

In this preliminary study, the basic aim was to determine the best reaction conditions to obtain an intercalated compound. From the morphology and structural characterizations, it is possible to state that 1 hour at room temperature is enough to obtain a GIC with a good intercalation degree and, consequently, good expansion property. It is possible to assess that there are not reasons in using different time and temperature conditions. Indeed, in some cases, using more restrictive conditions seems to lead to a worse product. However, in order to perform the reactions at controlled temperatures, the subsequent reactions were performed at temperatures greater than room temperature. Depending on the reactivity of the oxidant, temperatures between 30 ˚C and 40 ˚C have been chosen.
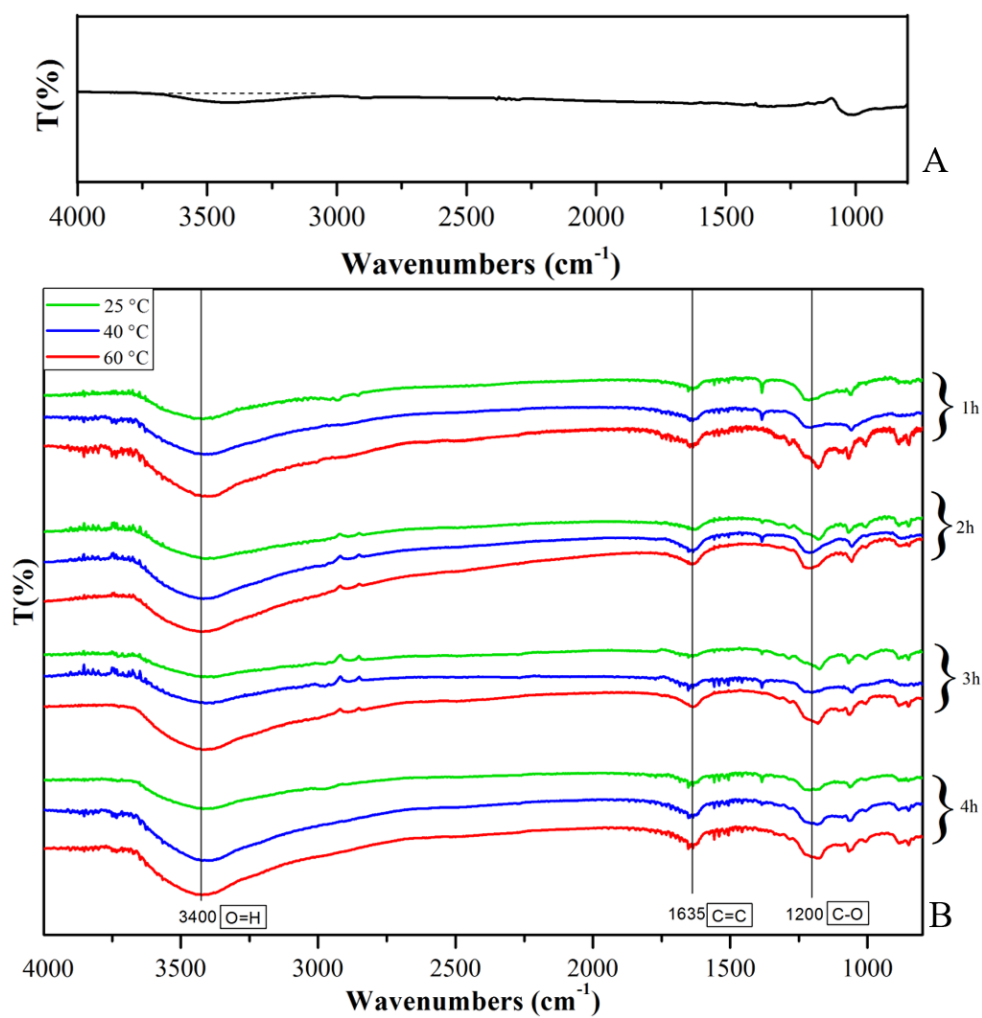
Figure 2.13: FT-IR spectra in transmittance of A: starting graphite and B: GICs in wavenumbers range of 4000 to 800 cm^{-1}. The curves are shifted arbitrarily along the y-axis

References

[1] L.B. Ebert, *Intercalation compounds of graphite*, Annual Review of Materials Science 6.1**, 181-211, **(1976)**

[2] A. Mills, et al., ***Thermal conductivity enhancement of phase change materials using a graphite matrix*, Applied Thermal Engineering 26.14, 1652-1661, **(2006)**

[3] Fire Carb, Expandable graphite, En 13 08;

[4] S.H. Anderson, D.D.L. Chung, *Exfoliation of Intercalated Graphite*, Carbon 22 (3), 253-263, **(1984)**

[5] W. Wang, X.Yang, Y.Fang, J. Ding, J. Yan, *Preparation and thermal properties of polyethylene glycol/expanded graphite blends for energy storage*, Applied Energy, 86(9), 1479-1483, **(2009)**

[6] G. Carotenuto, et al., *Laser-Induced Thermal Expansion of H2SO4-Intercalated Graphite Lattice*, The Journal of Physical Chemistry, 119.28, 15942-15947, **(2015)**

Chapter 3

Morphological and Structural Analysis

In this chapter it is addressed the problem of morphological and structural characterization of the different graphite bisulfates prepared.

3.1 Morphology of Graphite Bisulfates

Morphology of graphite flakes after the oxidation/intercalation treatment has been investigated by comparing SEM-micrographs of different GICs with that of the starting graphite flakes.

3.1.1 SEM Analysis

Here, micrographs of starting natural graphite, already shown in *Chapter 2*, are reported again for comparison. The images show that treatments with H_2SO_4/oxidant lead to intercalated graphite. In addition to the erosion phenomenon also a delamination and pre-expansion is clearly visible for some compounds. The image of a natural graphite single flake, reported in Figure 3.1, shows that the flake layers are really close to each other and the surface is flat and uniform. Figures 3.2 A and 3.2 B and 3.3 show the GICs obtained using HNO_3 and $K_2Cr_2O_7$ as oxidizers agent. In addition to intercalation, it is possible to observe a *delamination* phenomenon which can be ascribed to the strong oxidation effect. When KNO_3 is used as oxidizer (Figure 3.4 A and B), only a light intercalation phenomenon occurs. In this case, small white particles can be observed on the intercalated flakes, probably resulting from the KNO_3 crystals not dissolved during the chemical treatment [1]. Figure 3.5 shows an image of the GIC resulting from the reaction with H_2O_2 as oxidizing agent at different magnifications. In this case, a graphite pre-expansion phenomenon occurred during the intercalation process. Such a phenomenon is probably related to the H_2O_2 decomposition into H_2O and O_2 at room temperature [2]. Figures 3.6 A
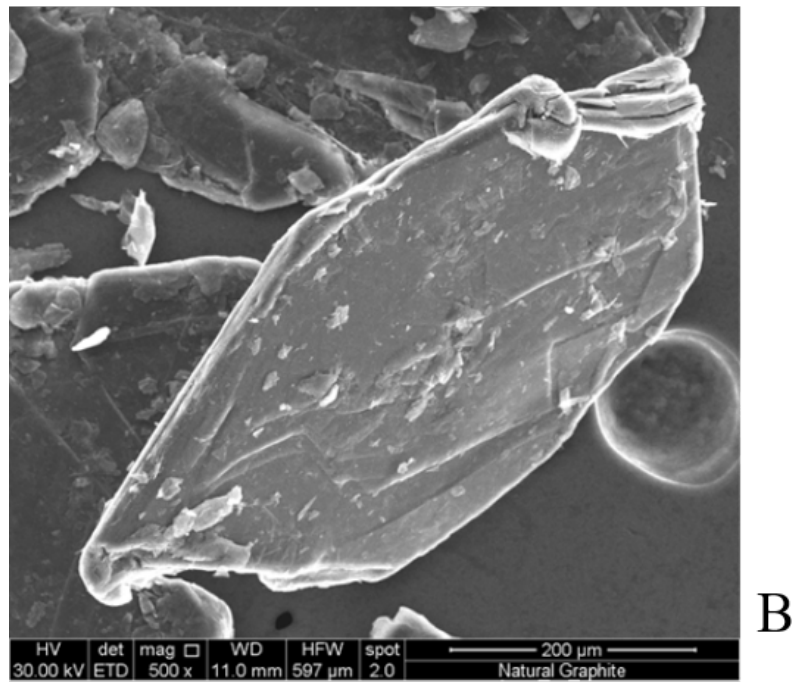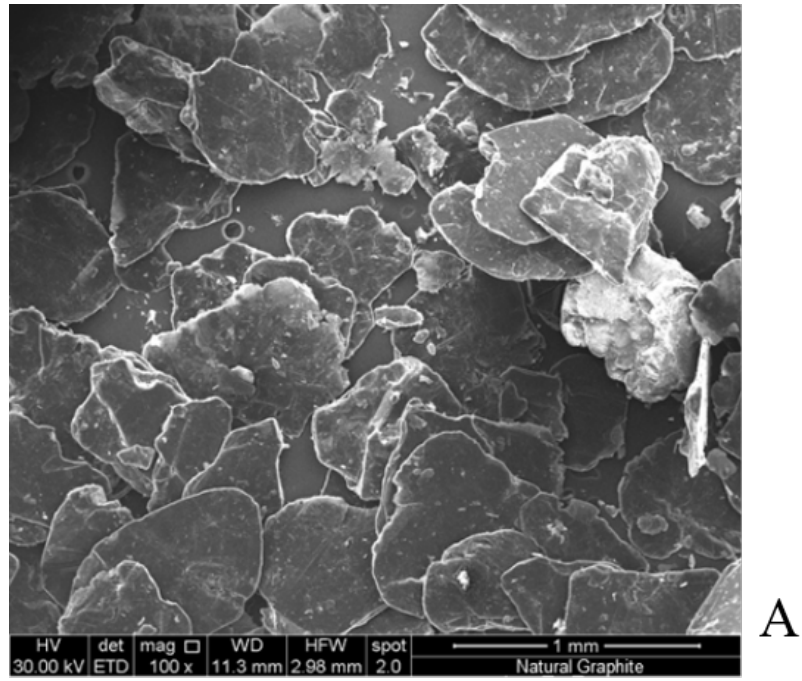
Figure 3.1: Scanning electron micrographs of Natural Graphite (magnification A: 100X, B: 500X)

Table 3.1: EDS analysis: elemental composition. Results in weight %

	SPECTRUM	**C**	**O**	**S**	**other**	**Total**
Graphite (Figure 3.9 A)	Spectrum 1	100	-	-	-	100
	Spectrum 2	99.50	-	-	0.50	100
	Spectrum 3	99.56	-	-	0.44	100
HNO_3 **- GIC** (Figure 3.9 B)	Spectrum 1	75.48	21.83	2.32	0.37	100
	Spectrum 2	70.37	21.46	7.93	0.31	100
KNO_3 **- GIC** (Figure 3.10 A)	Spectrum 1	73.39	23.18	2.75	0.66	100
H_2O_2 **- GIC** (Figure 3.10 B)	Spectrum 1	85.27	11.39	3.01	0.33	100
$KMnO_4$ **- GIC** (Figure3.11 A)	Spectrum 1	90.42	8.23	0.83	0.52	100
$K_2Cr_2O_7$ **- GIC** (Figure 3.11 B)	Spectrum 1	72.19	16.69	6.40	1.73	100

and B and 3.7 show the images of GICs obtained from $KMnO_4$ and $NaIO_4$, respectively. In this case it is possible to observe the erosion of the flakes boundary. This morphology is strictly influenced by the intercalation process although a layer-separation is not noticeable as in the others samples. The GIC obtained using $NaClO_3$ as oxidizing agent (Figure 3.8 A and B), shows a strong intercalation phenomenon. From the SEM image it is possible to recognize multiple layers forming the flake [1].

EDS Microanalysis

To confirm the presence of the intercalating agent inside the compounds flakes, EDS microanalysis was carried out on small sample areas. In this way it can be determine the nature and the percentage of the elements present in the GICs. EDS analysis has been performed also on the natural graphite flakes to have a comparison with the starting material (Figure 3.9). The positions where EDS analysis has been performed are indicated in Figures 3.9 A 3.10, 3.11. The spectra collected on natural graphite show only the presence of the element Carbon (besides some impurity). All EDS analysis performed on the GICs samples detected a significant quantity of Sulfur and Oxygen due to the oxidation/intercalation process. The elemental composition for each EDS spectrum is reported in Table 3.1.
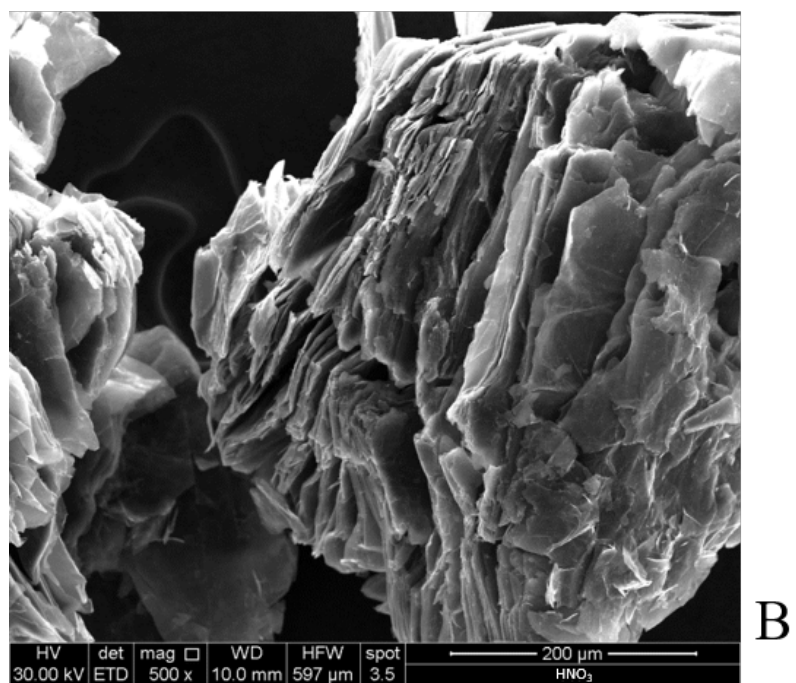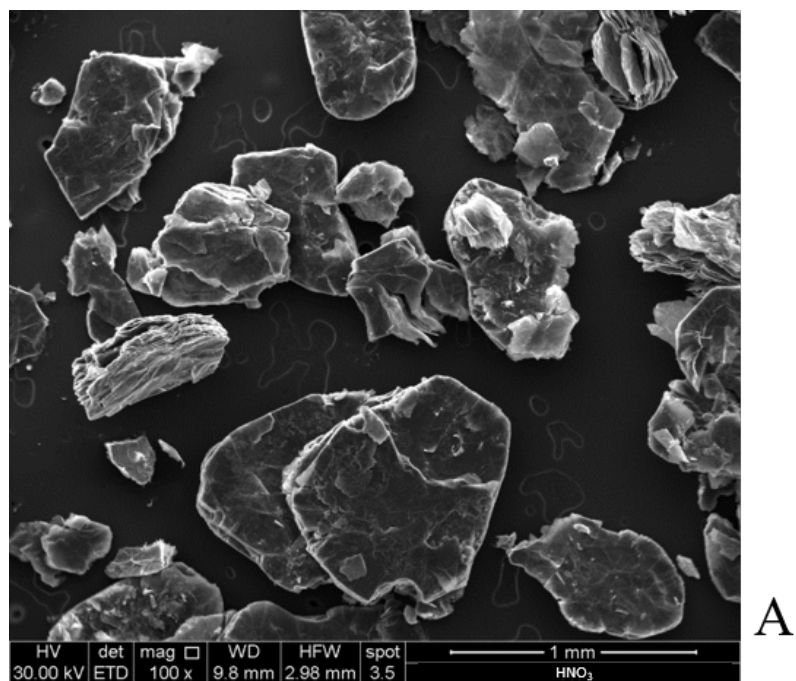
Figure 3.2: Scanning electron micrographs of HNO_3 - GIC (magnification A: 100X, B: 500X)

HV	det	mag □	WD	HFW	spot	200 μm
30.00 kV	ETD	500 x	10.2 mm	597 μm	3.0	$K_2Cr_2O_7$
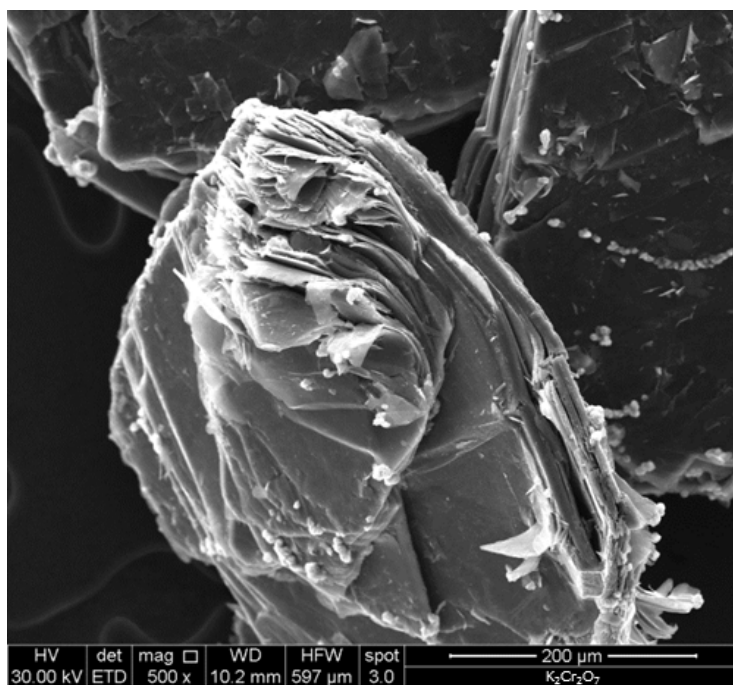
Figure 3.3: Scanning electron micrographs of $K_2Cr_2O_7$ - GIC, (magnification 500X)
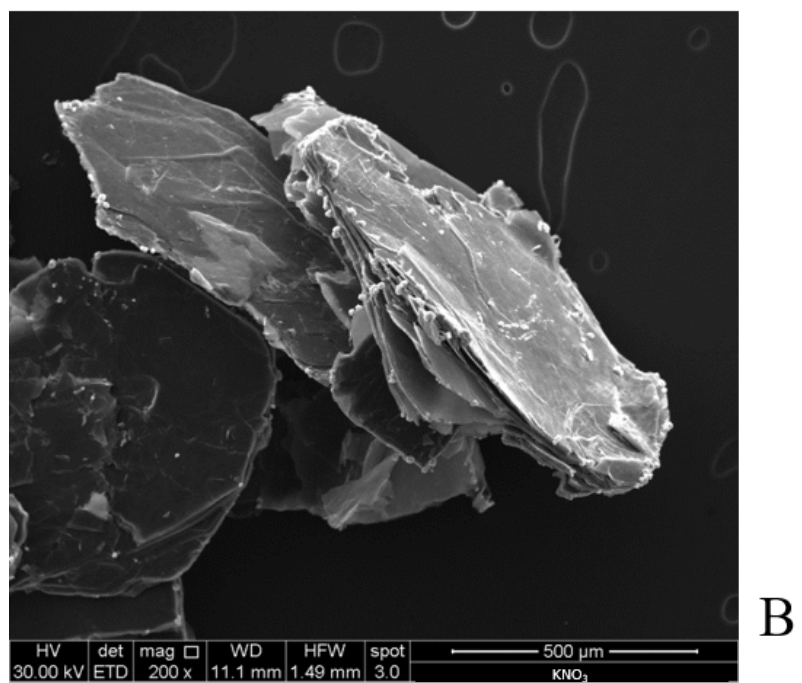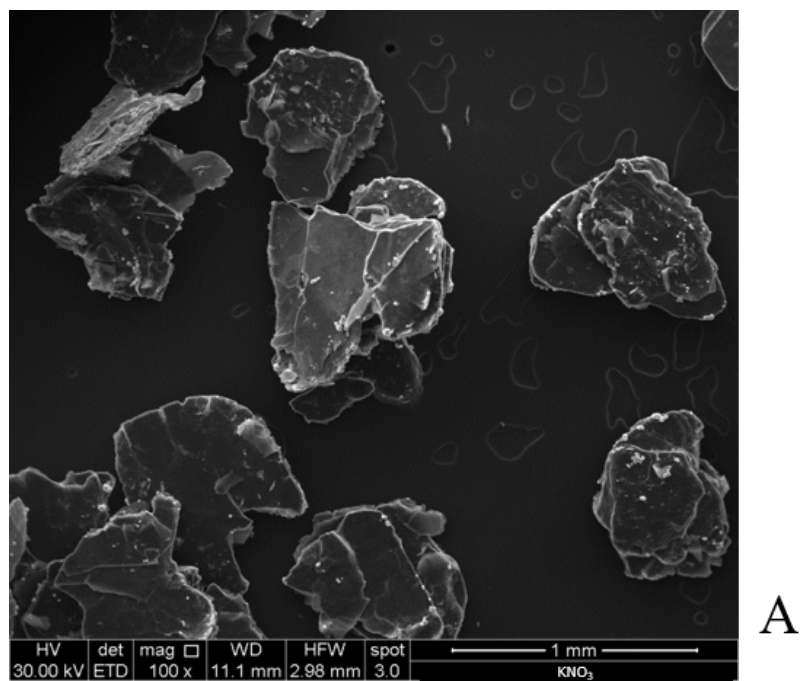
Figure 3.4: Scanning electron micrographs of KNO_3 - GIC (magnification A: 100X, B: 200X)

| HV | det | mag □ | WD | HFW | spot | 1 mm |
| 30.00 kV | ETD | 100 x | 10.4 mm | 2.98 mm | 3.0 | H_2O_2 |

A

| HV | det | mag □ | WD | HFW | spot | 300 μm |
| 30.00 kV | ETD | 400 x | 10.2 mm | 746 μm | 3.0 | H_2O_2 |

B
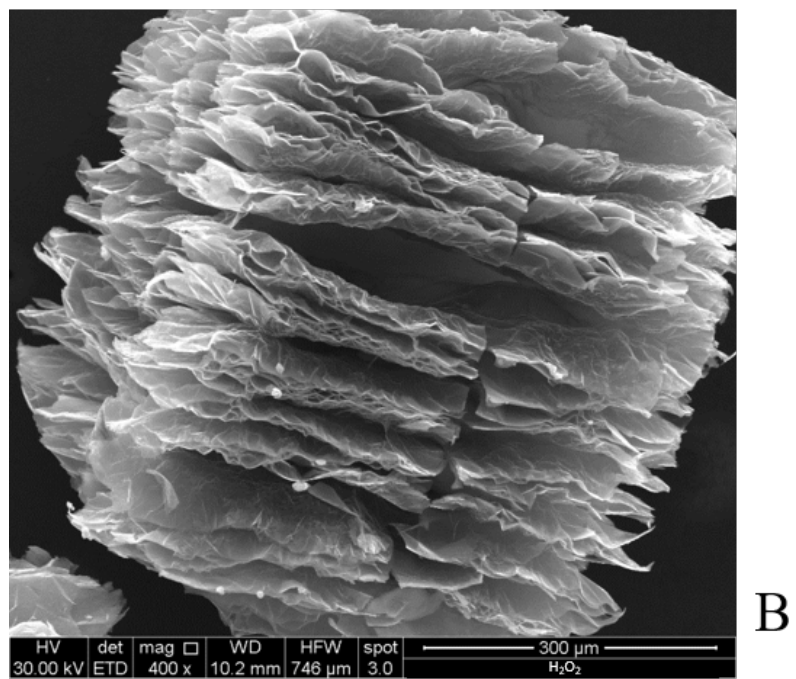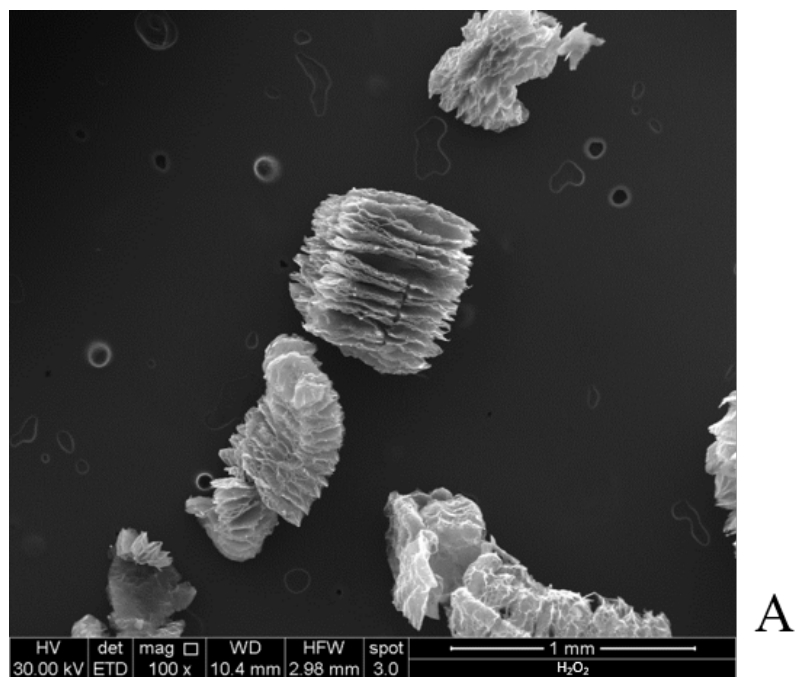
Figure 3.5: Scanning electron micrographs of H_2O_2 - GIC (magnification A: 100X, B: 400X)
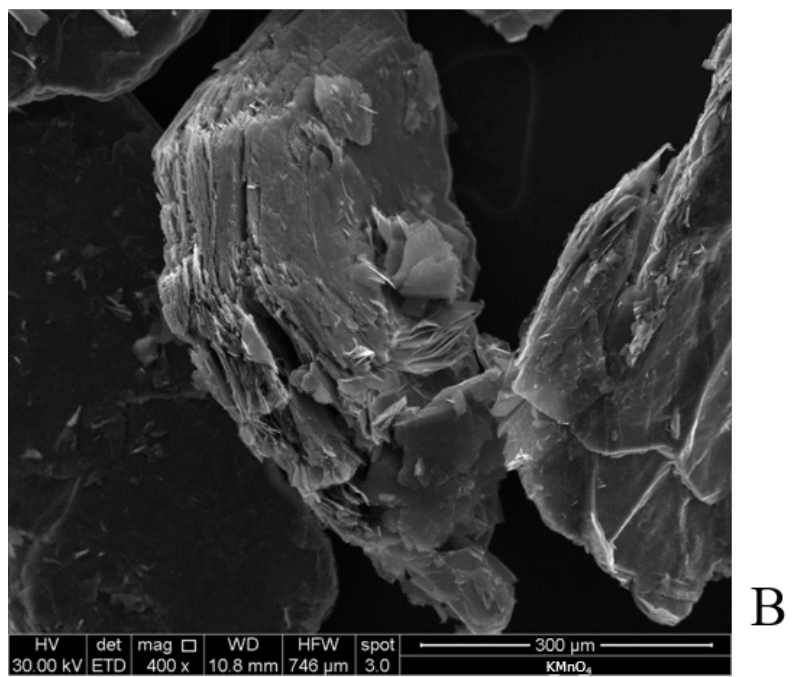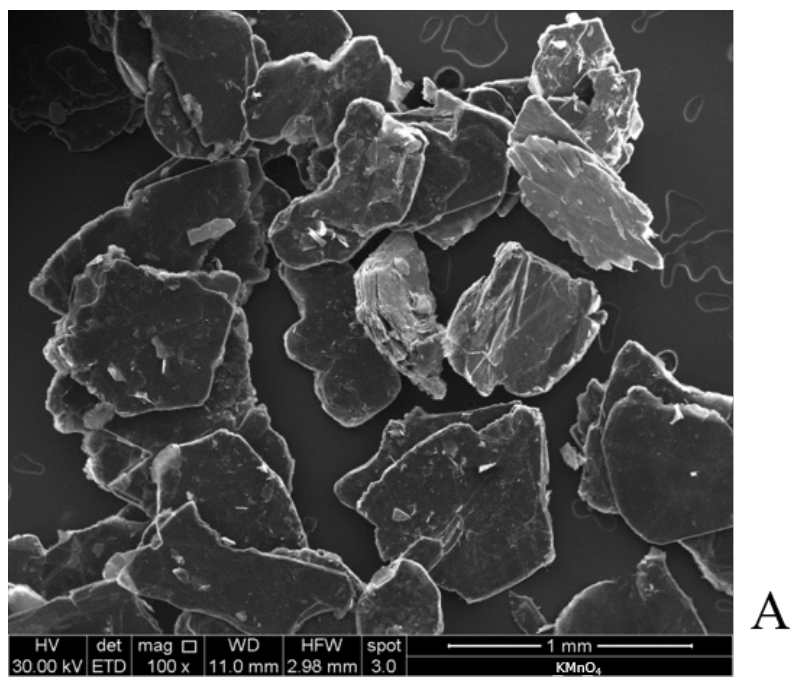
Figure 3.6: Scanning electron micrographs of $KMnO_4$ - GIC (magnification A: 100X, B: 400X)
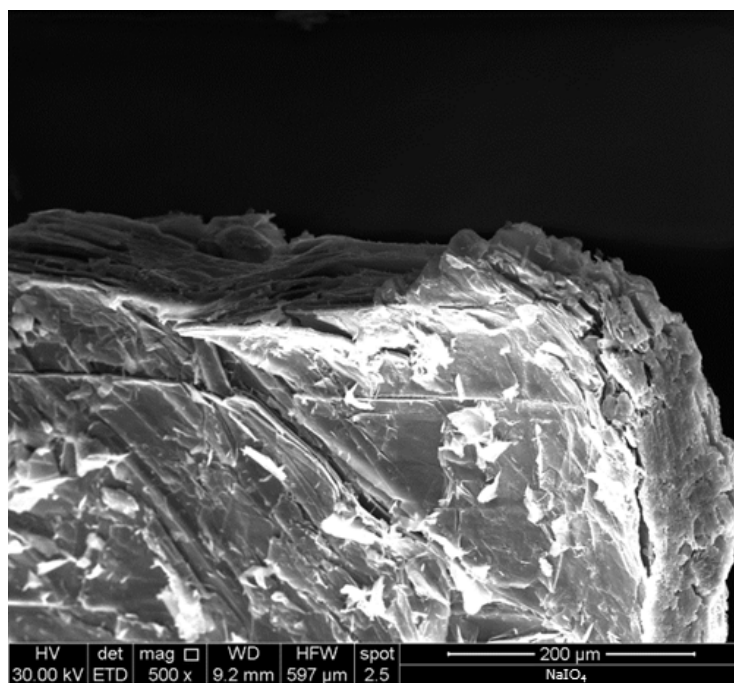
Figure 3.7: Scanning electron micrographs of $NaIO_4$ - GIC, (magnification 500X)
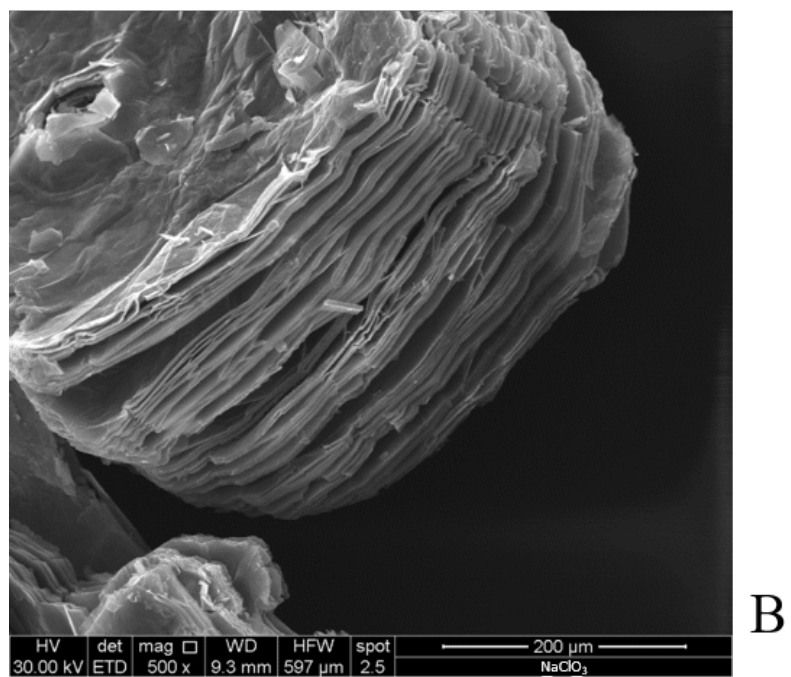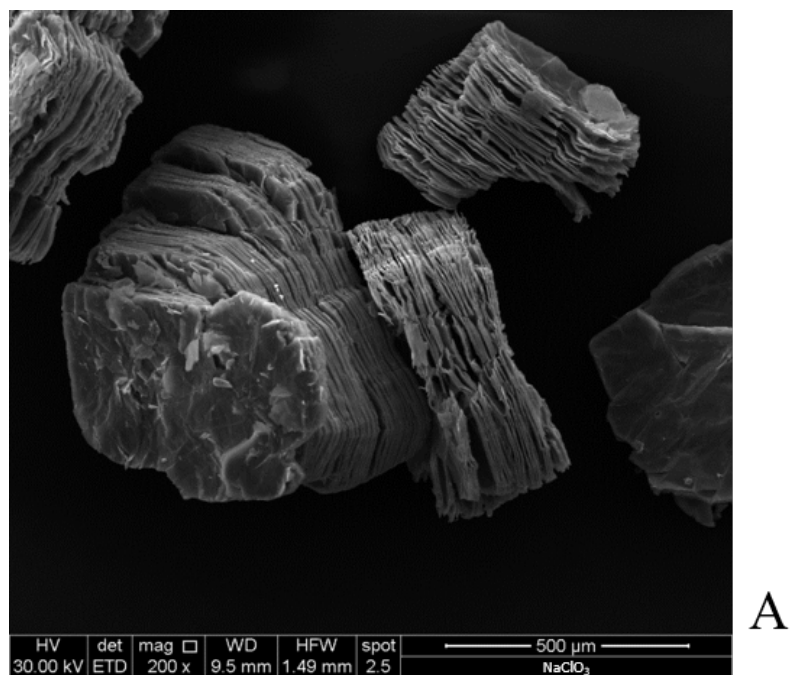
Figure 3.8: Scanning electron micrographs of $NaClO_3$ - GIC (magnification A: 200X, B: 500X)
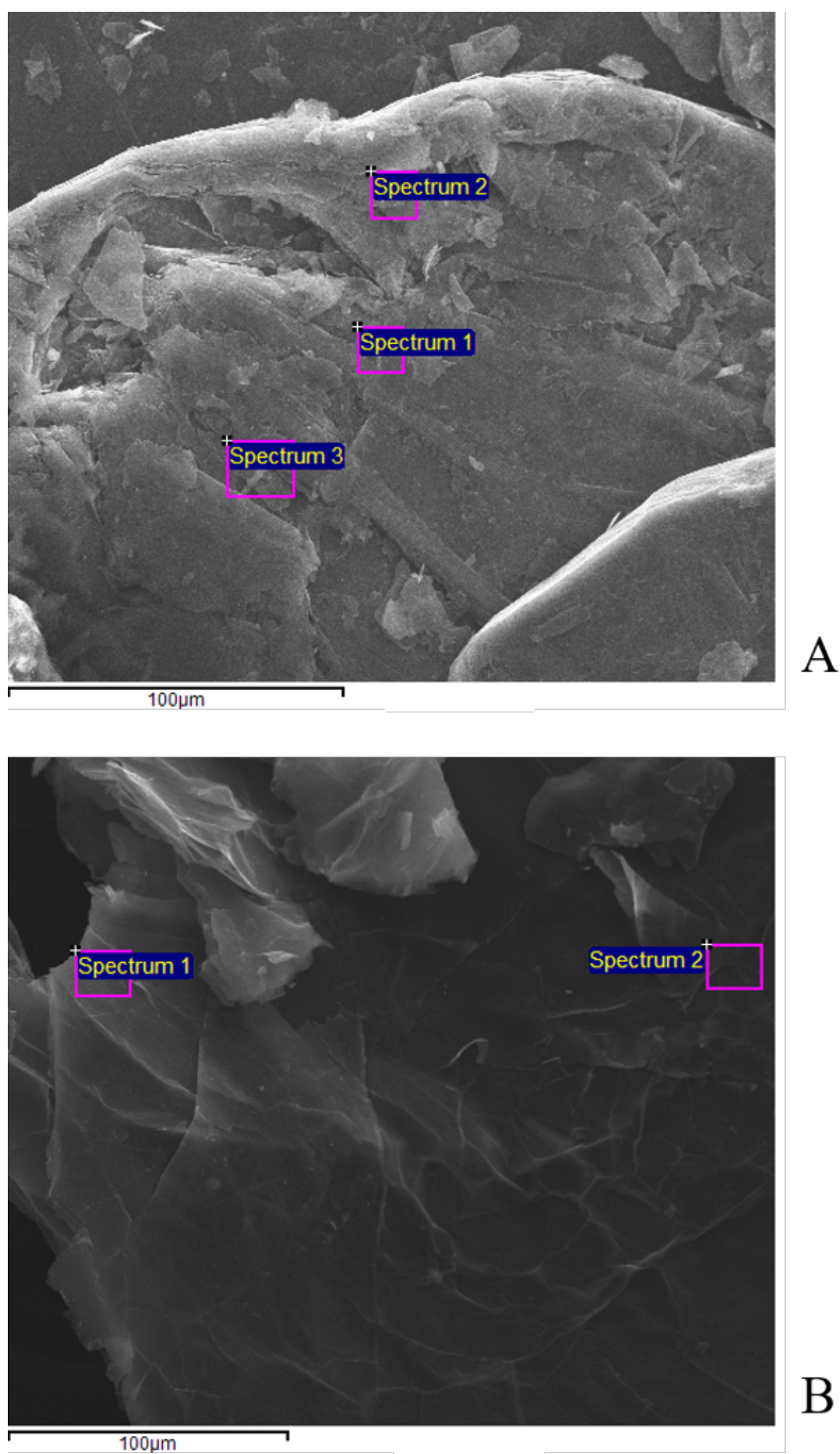
Figure 3.9: Positions where EDS analysis has been performed on A: starting Natural Graphite and B: HNO_3 - GIC
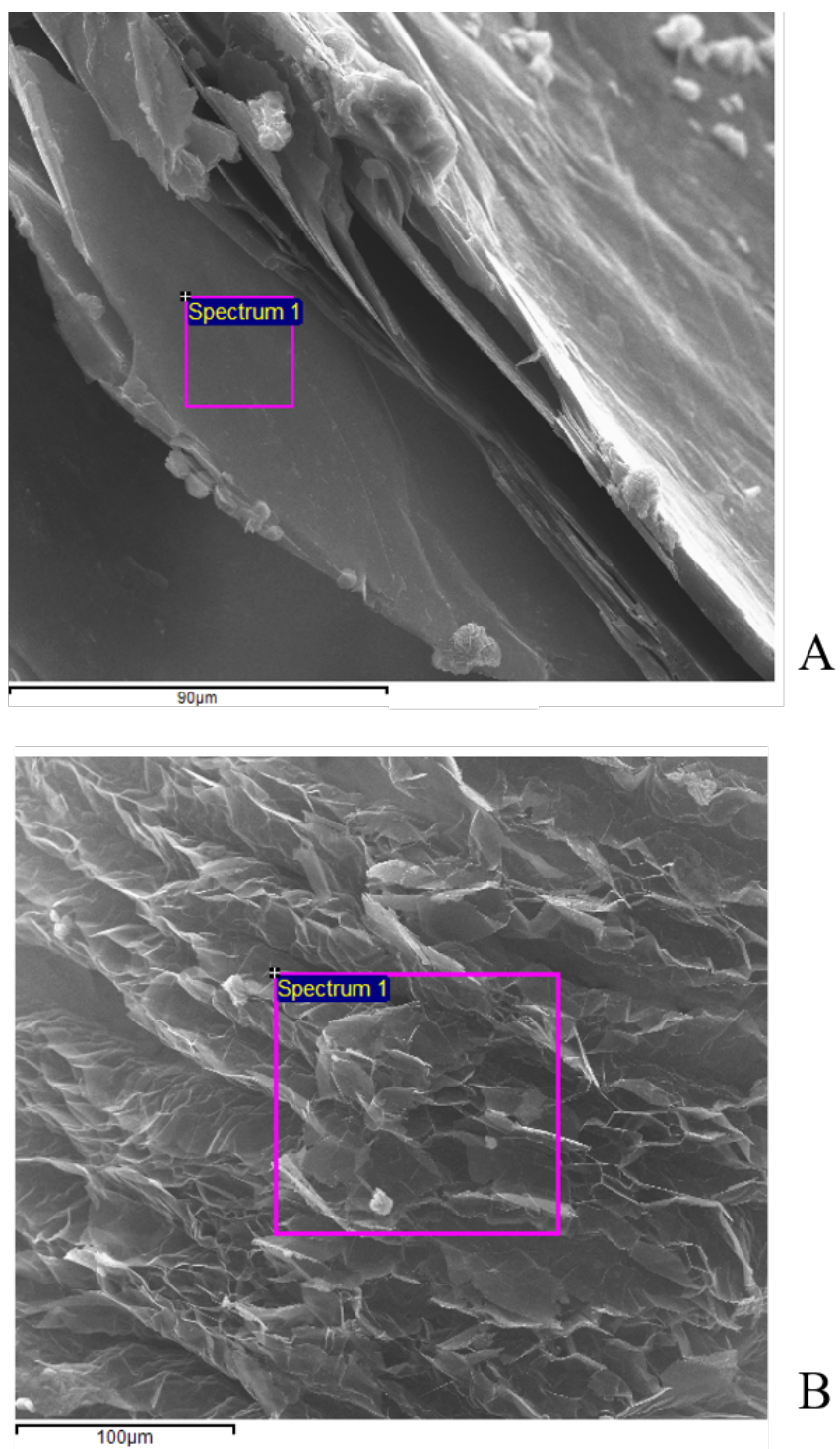
Figure 3.10: Positions where EDS analysis has been performed on A: KNO_3 - GIC and B: H_2O_2 - GIC
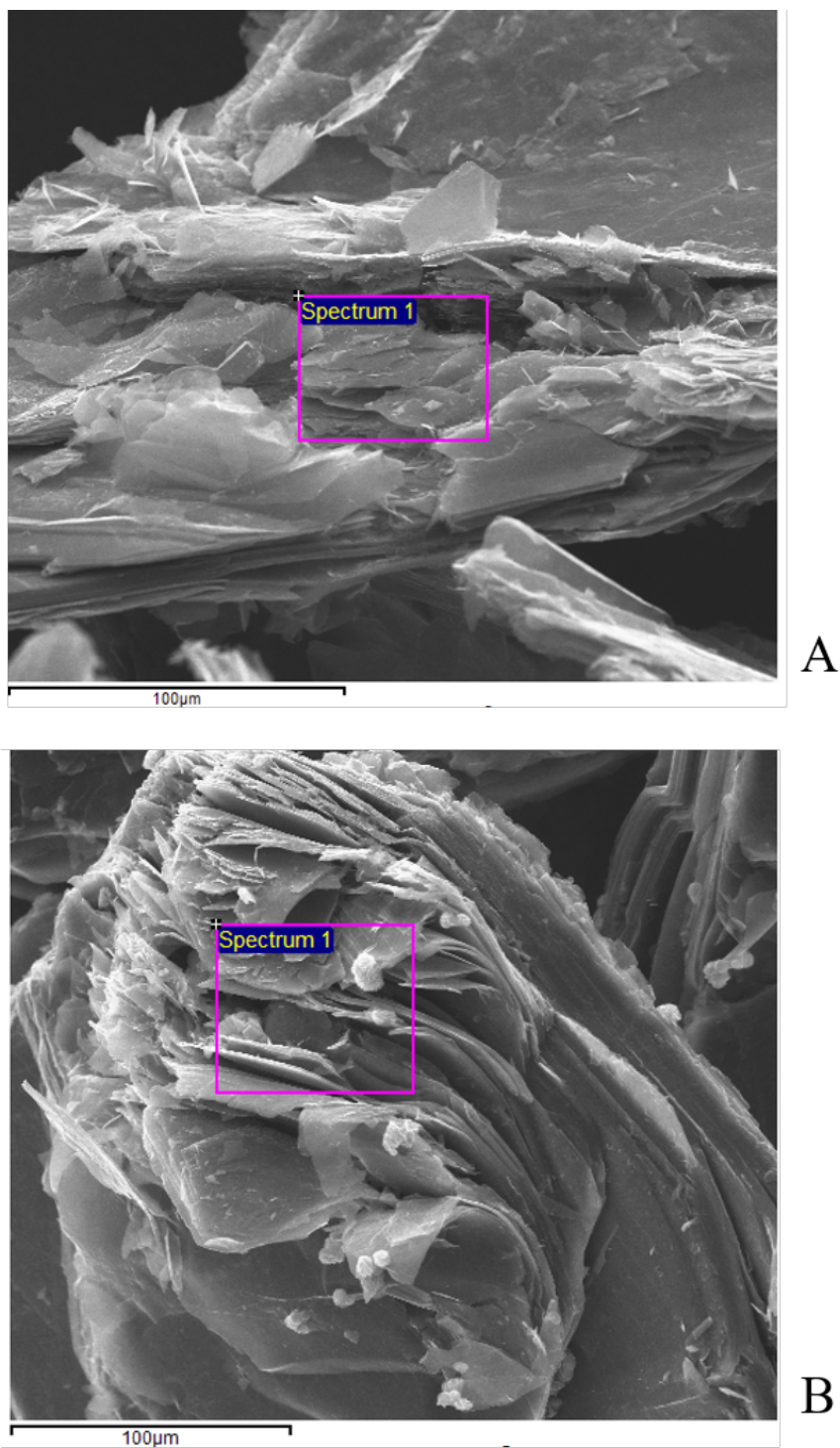
Figure 3.11: Positions where EDS analysis has been performed on A: $KMnO_4$ - GIC and B: $K_2Cr_2O_7$ - GIC
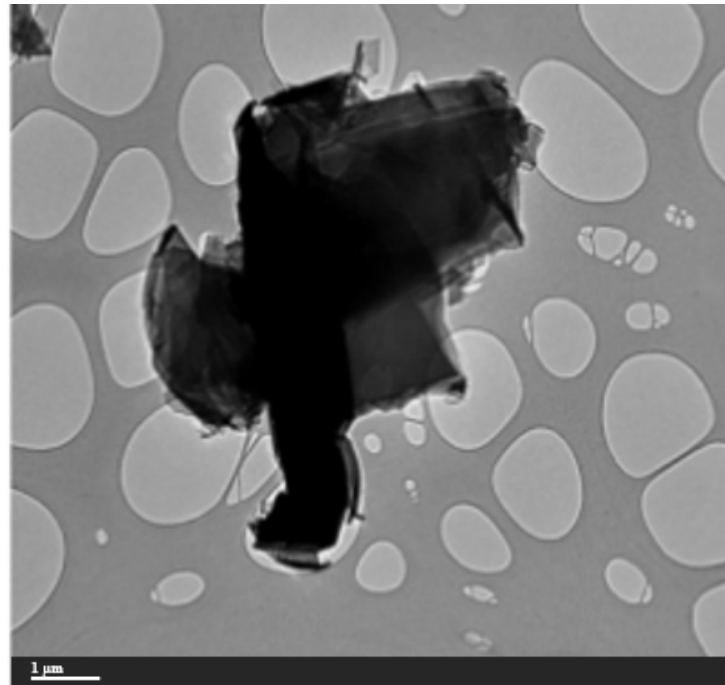
Figure 3.12: Transmission electron micrograph of Natural graphite [3]

3.1.2 TEM Analysis

For further morphology characterization, a Transmission Electron Microscopy (TEM) analysis was performed. The TEM image of graphite (shown in Figure 3.12), shows its graphitic structure as large thick dark flakes [3]. TEM samples have been prepared by pipetting the GICs dispersion onto a mesh grid. Here, as an example, I report three of the seven sample analyzed, in particular the micrographs obtained from KNO_3 - GIC, H_2O_2 - GIC and $KMNO_4$ - GIC are shown in Figure 3.13 A, B and C respectively. All samples analyzed show the same principal characteristics. Comparing the images reported in Figures 3.13 A and C with Figure 3.12, it is evident the intercalation phenomenon, it is possible to observe the increased distance between the graphite layers. Furthermore, from Figures 3.13 A and B, we can notice another effect of the intercalation, some layer are partially "rolled up" on their two edges. This morphology is quite similar to that found in the TEM images of the carbon nanoscrolls reported in literature [5, 5].
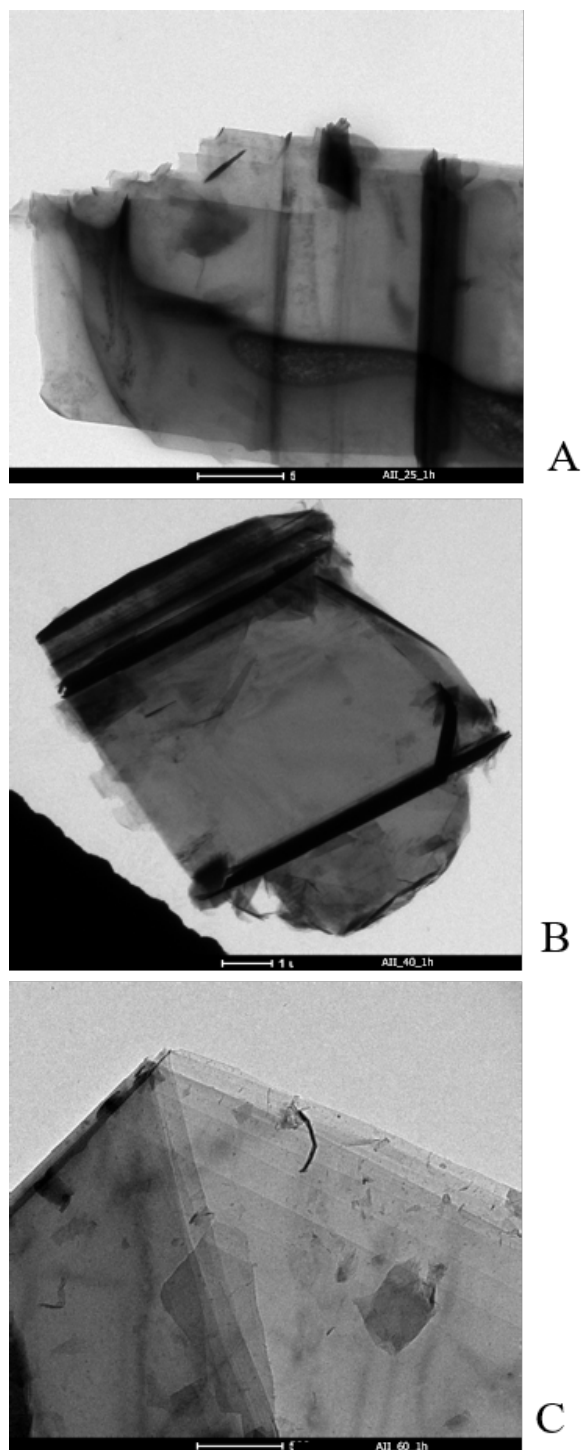
Figure 3.13: Transmission electron micrograph of A: KNO_3 - GIC; B: H_2O_2 - GIC; C: $KMNO_4$ - GIC

Figure 3.14: XRD (002) peak Starting Natural Graphite (range of 2θ from 5°
to 50°). The curves are shifted arbitrarily along the y-axis

3.2 Crystallographic Structure of Graphite Bisulfate

3.2.1 X-Ray Analysis

The structural characteristics of the obtained GICs can be evaluated by comparing XRD diffractograms of pure graphite and GICs. Figure 3.14, shows the diffractogram of natural graphite while Figure 3.15 shows a portion of the same diffractogram compared with those of the GICs prepared from the different oxidizing agents. As visible, the signal of GICs is significantly different from that of natural graphite. The (002) signal, which is the only one visible in the XRD pattern of natural graphite, represents reflections in the perpendicular direction (z-axis) of the graphite hexagonal planes [6, 7]. The (002) peak in the GICs X-ray diffractograms is clearly broadened compared to that of the pure graphite. Furthermore, the (002) peak results shifted to lower angles for all studied GICs compared to the pure graphite case. This result is probably due to the presence of defects in the GICs crystal lattice. This effect depends on the obtained intercalation and on the kind of oxidizing agents used in the reaction [1]. In
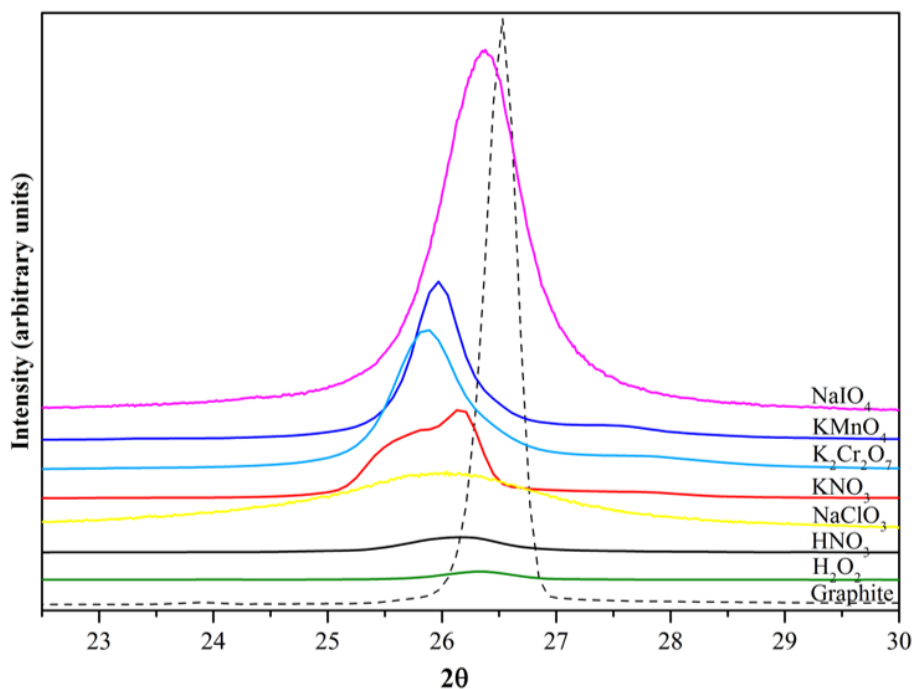
Figure 3.15: XRD (002) peak of Starting Graphite and GICs (range of 2θ from 22.5° to 32.5°). The curves are shifted arbitrarily along the y-axis

particular, the X-ray diffractograms of GICs obtained using $NaClO_3$, KNO_3 and $K_2Cr_2O_7$ as oxidizing agents show the maximum shift of the (002) peak. The XRD spectra of GICs by HNO_3 and H_2O_2 exhibit maximum broadening of the (002) peak [2]. As it can be seen from the corresponding SEM images (Figures 3.2 and 3.5 respectively) the samples appear to be better expanded compared to the other GICs. I ascribe the better expansion to the instability of the HNO_3 and H_2O_2 oxidants which results in gas formation during the intercalation reactions.

Bibliography

[1] M. Salvatore, G. Carotenuto, S. De Nicola, C. Camerlingo, V. Ambrogi, C. Carfagna, *Synthesis and characterization of high-filled intercalated graphite bisulphate*, Nanoscale Research Letters, 12:167, **(2017)**

[2] M. Salvatore, G. Carotenuto, V. Ambrogi, C. Carfagna, *Synthesis of H2SO4-intercaleted graphite flakes based on different oxidizing agents*, XI Convegno nazionale Materiali Nanofasici, pp 159-160, **(2015)**

[3] C.M. Willemse, K. Tlhomelang, N. Jahed, P.G. Baker, & E.I. Iwuoha, *Metallo-graphene nanocomposite electrocatalytic platform for the determination of toxic metal ions*, Sensors, 11(4), 3970-3987, **(2011)**

[4] G. Carotenuto, A. Longo, S. De Nicola, C. Camerlingo, & L. Nicolais, *A simple mechanical technique to obtain carbon nanoscrolls from graphite nanoplatelets*, Nanoscale research letters, 8(1), 403, **(2013)**

[5] B. Jayasena, S. Subbiah, & C.D. Reddy, *Formation of Carbon Nanoscrolls During Wedge-Based Mechanical Exfoliation of HOPG*, Journal of Micro and Nano-Manufacturing, 2(1), 011003, **(2014)**

[6] P.S. Gaal, *Thermal conductivity 24: and thermal expansion*, 12th 24th CRC Press, Pennsylvania **(1999)**

[7] G. Sun, X. Li, Y. Qu, X. Wang, H. Yan, & Y. Zhang, *Preparation and characterization of graphite nanosheets from detonation technique*, Materials Letters, 62(4), 703-706, **(2008)**

Chapter 4

Spectroscopic Analysis

Characterization of the chemical structure of materials and products is reported in the next paragraphs.

4.1   Raman Spectroscopy

The μ-RS spectra obtained from the graphite intercalated compounds are reported in Figure 4.1 and compared with spectrum of pure graphite. In Figure 4.1 A, the spectrum region in the wavenumber range of $1200 - 1850\,cm^{-1}$ is considered, where a prominent peak (designated as G mode) is generated by graphite at about $1582\,cm^{-1}$. This peak is clearly visible in the spectrum of graphite, reported in the low part of the figure, and in all the other spectra, even if evident differences occur in the observed Raman response. The spectra in the Figure 4.1, are sorted in increasing degree of differentiation with respect to that of graphite. The spectra of samples obtained from KNO_3, $KMnO_4$, H_2O_2 look rather similar to that of graphite even if the higher intensity of Raman mode visible at about $1332\,cm^{-1}$ (D mode) manifests the occurrence of a relatively large amount of defects in the lattice [1]. For samples obtained from KNO_3, H_2O_2 and $KMnO_4$ the Raman G mode can be successfully fitted by a single Lorentzian function centered at about $1580\,cm^{-1}$. This is not the case of the other spectra (related to $K_2Cr_2O_7$, HNO_3, $NaIO_4$ and $NaClO_3$), where the fit require two distinct components, represented by Lorentzian functions centered at about $1580\,cm^{-1}$ and $1600\,cm^{-1}$, respectively. Two dotted lines indicates these positions in the Figure 4.1 A. The first component has a center value close to the G mode position of pristine graphite and is assigned to block of not intercalated graphite layers, while the $1600\,cm^{-1}$ mode is assigned to graphene layers next to an intercalant layer. The ratio of the intensity of this second component with respect to the intensity of $1580\,cm^{-1}$ mode, evaluated by the fit procedure, gradually increases from the value of 0.32 for sample $K_2Cr_2O_7$ to the value of 1.33 of sample $NaClO_3$, indicating a significant intercalation degree of the samples even if in different stage configurations. For
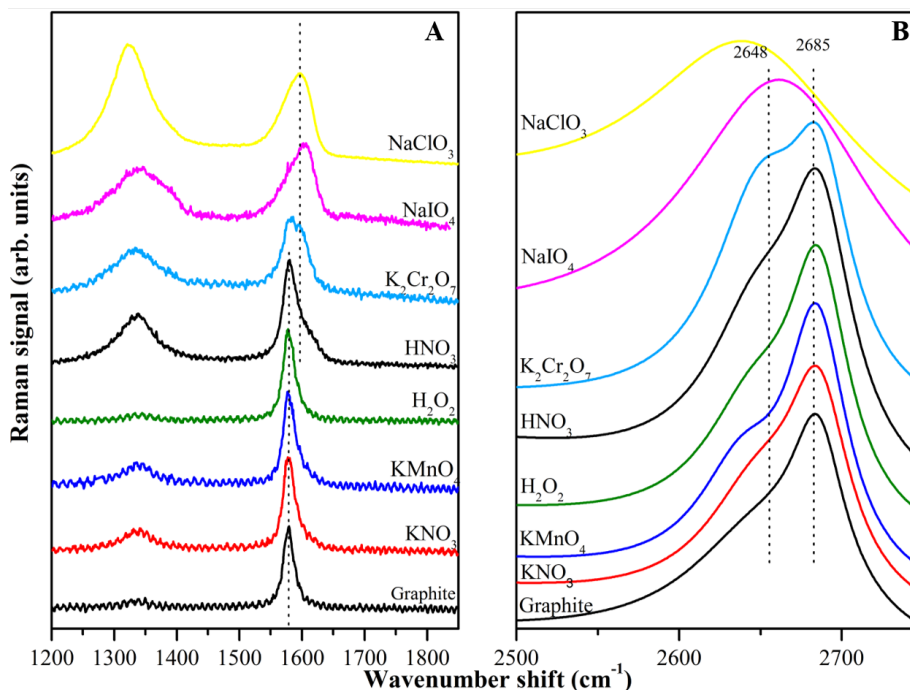
Figure 4.1: μ-RS of GICs in the spectral range of A: $1200 - 1850\,\mathrm{cm}^{-1}$ and B: $2500 - 2800\,\mathrm{cm}^{-1}$. The spectra are shifted arbitrarily along the y-axis. The dotted lines indicate the spectral position of the main components observed for A: G and B: 2D mode, respectively.

these compounds the intensity of the D mode (at $1332\,\mathrm{cm}^{-1}$) is also clearly observable in the Raman spectra (see Figure 4.1 A) and it is relatively larger than in the case of GICs before considered (KNO_3, $KMnO_4$, H_2O_2), indicating the occurrence of structural defects. This is also evidenced by the slight increase of both the position and the width of the G peak, that is a signature of increasing lattice defects [2]. It is worth to note that in the case of doping-like defects the increase of position of G mode with impurity degree is instead accompanied by an increasing stiffness [2]. This general behavior is confirmed by the Raman spectra in the wavenumber range of $2500 - 2800\,\mathrm{cm}^{-1}$, reported in Figure 4.1 B. In this range, graphite is characterized by a broad peak (designed as 2D mode) centered at about $2685\,\mathrm{cm}^{-1}$. Differently from the G mode, the position of this peak depends on the laser excitation wavelength (in our case $= 632.8\,\mathrm{nm}$) [2, 3, 4]. The differences with respect to graphite become gradually more significant when spectra of the sample obtained from $KNO_3$to that one derived from $NaClO_3$ are considered, in the order indicated in Figure 4.1 B. Besides the pristine graphite 2D mode (at $2685\,\mathrm{cm}^{-1}$), the fit of the experimental data requires an additional component at about $2648\,\mathrm{cm}^{-1}$ with increasing intensity.

This mode becomes the prevalent one in the samples obtained by using $NaIO_4$ and $NaClO_3$ as oxidizers. Two dotted lines represent the position of these two modes in Figure 4.1 B. The observed shift of the 2D mode position to lower wavenumber values with respect to pristine graphite is a signature of presence of graphene sheets, indicating the formation of low stage GICs [5]. A large intercalation configuration in the $NaIO_4$ and $NaClO_3$ systems is inferred, because the Raman signal results generated by almost monolayers of graphene (low stage number). In the remaining samples intercalation process is also obtained, but with relative thicker layer blocks of graphite (high stage number) interposed to intercalated layers [6].

4.2 IR Spectroscopy

The oxidation of GICs samples was investigated by FT-IR spectroscopy. Figure 4.2 shows FT-IR spectra of prepared intercalation compounds in wavenumber range of $3800 - 500 \, \text{cm}^{-1}$, compared with spectrum of pure graphite. All spectra
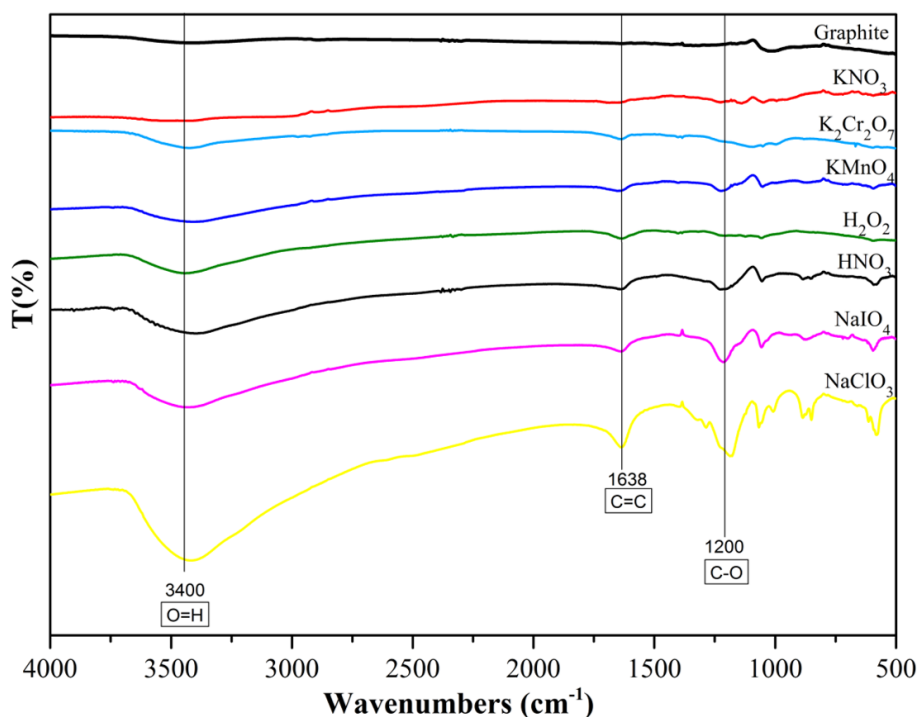
Figure 4.2: FT-IR spectra of pure graphite and GICs in wavenumbers range of 4000 to 500 cm^{-1}. The spectra are shifted arbitrarily along the y-axis

are shifted arbitrarily along the y-axis . Also in this case (like the spectra shown in *Chapter 2 - Effect of Time-Temperature Conditions*) it is visible that the GICs

spectra are remarkably different from that of natural graphite. They exhibit an oxidation signal due to the presence of hydroxyl groups $(-OH)$ at $3500\,\mathrm{cm}^{-1}$. The natural graphite also presents a light oxidation. The oxidation degree was depending on the type of oxidizer used, and has a maximum for $NaClO_3$ and a minimum for the KNO_3 oxidizer. All spectra also featured a clear signal at $1650\,\mathrm{cm}^{-1}$ascribed to the $C = C$ double bond stretching vibration and $C - O$ bond stretching vibration at $1200\,\mathrm{cm}^{-1}$[6].

References

[1] J.M. Benoit,J.P. Buisson, O. Chauvet, Q.C. Godon, S. Lefrant, *Low-frequency Raman studies of multiwalled carbon nanotubes: Experiments and theory*, Phys. Rev. b, 66, 013417, **(2002)**

[2] C. Casiraghi, S. Pisana, A.C. Ferrari, K.S. Novoselov, A.K. Geim, A.C. Ferrari, *Raman fingerprint of charged impurities in graphene*, App. Phys. Lett, 91, 233108 **(2007)**

[3] D. Roy, E. Angeles-Tactay, R.J.C. Brown, S.J. Spencer, T. Fry, T.A. Dunton, et al: *Synthesis and Raman spectroscopic characterization of carbon nanoscrolls*, Chem. Phys. Lett., 465, 254-257, **(2008)**

[4] L.G. Cancado, A. Jorio, E.H. Martins Ferreira, F. Stavale, C.A. Achete, R.B. Capaz, et al. *Quantifying defects in graphene via Raman spectroscopy at different excitation energies*, Nano Lett. 11, 3190-3196, **(2011)**

[5] G. Carotenuto, A. Longo, S. De Nicola, C. Camerlingo, & L. Nicolais, *A simple mechanical technique to obtain carbon nanoscrolls from graphite nanoplatelets*, Nanoscale research letters, 8(1), 403, **(2013)**

[6] M. Salvatore, G. Carotenuto, S. De Nicola, C. Camerlingo, V. Ambrogi, C. Carfagna, *Synthesis and characterization of high-filled intercalated graphite bisulphate*, Nanoscale Research Letters, 12:167, **(2017)**

Chapter 5

Expansion and Thermal Behavior

In this section the expansion phenomenon is explained, it is shown the morphology of the *expanded graphite* obtained from the different graphite bisulfates prepared and it is reported the results of the thermogravimetric study.

Figure 5.1: Expanded Graphite

5.1 Expansion Phenomenon

As discussed in *Chapter 1*, graphite bisulfates have the ability to expand when a heating is applied to them. The thermal shock causes a violent reaction between

Carbon of the graphite and sulfuric acid molecules and HSO_4^- ions present in the graphite inter-layers [1]. Intercalating agent and graphite react according to the following scheme [2, 3].

$$C + 2H_2SO_4 \rightarrow CO_2 + 2SO_2 + 2H_2O \quad (2)$$
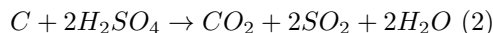
This reaction occurs with a gas release, which in turn determines a strong inter-layer distancing, the more this phenomenon is intense, the higher the intercalation degree becomes. The product of this reaction is named *expanded graphite*. The resulting morphology is very different from that of the GICs, that results in a substantial volumetric expansion. As we will see in this chapter, the resultant materials have a worm-like shape [4, 5]. During this process the graphite crystals are converted to very porous filaments by an uniaxial expansion mechanism involving the graphite crystal lattice. Such expansion is due to the mixture of gases produced in the crystal lattice by the reaction of carbon with H_2SO_4 [7].

5.2   Morphology of Expanded Compounds

After the expansion by microwave, a SEM analysis was performed on the obteined expanded graphite. Following Figures (from 5.2 to 5.8) show a comparison between GIC before and after heating for all compounds prepared. The micrographs are taken for each sample at the same magnification to show immediately the strong differences in morphology and structure. For all samples it is very noticeable the increase in volume and the difference in structure. The graphite bisulfates consists of flakes with an intercalated layered structure with galleries or small spaces between layers. The expanded graphite bisulphates have a worm-like shape with a lot of porous and defects. This result represent a confirmation of the obteined intercalation during the step 1.   Only the sample H_2O_2 show a different behavior. Indeed, its volume doesn't really change. This result is probably due to the pre-expansion phenomenon occurred during the step 1 and caused by H_2O_2 decomposition to H_2O and O_2 (as already discussed in *Chapter 3* - Morphology and Structure). Heating by means of a microwave oven permits to obtain the expansion very quickly (just a few seconds) and very easily [8]. However, the expansion phenomenon occurs also using other heating methods, such as in a tube furnace at very high temperature (1000 °C) or on the flame, or with resistance and induction heating. Consequently, the GICs expand also in a TGA furnace, in this way it has been possible to control and compare the behaviors of different GICs during the expansion phenomenon.
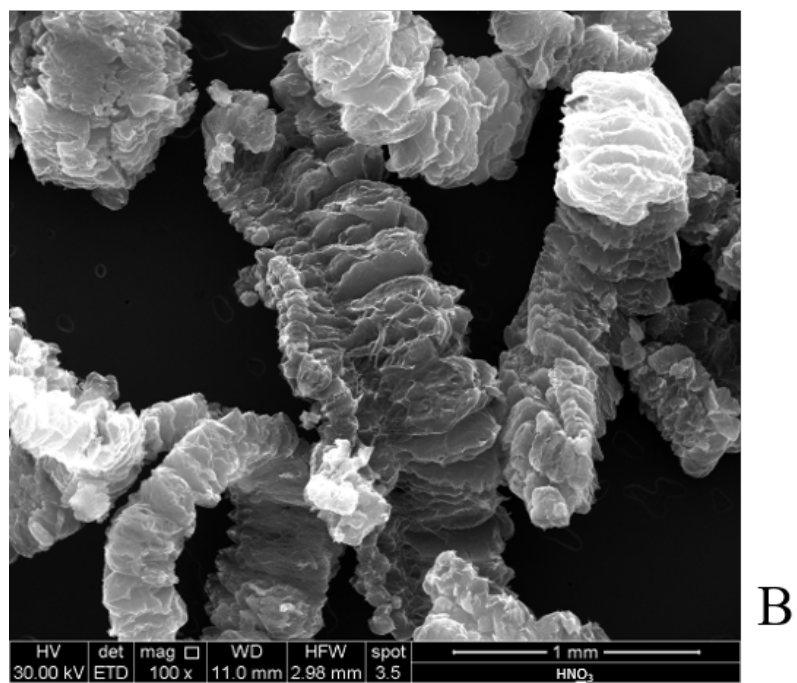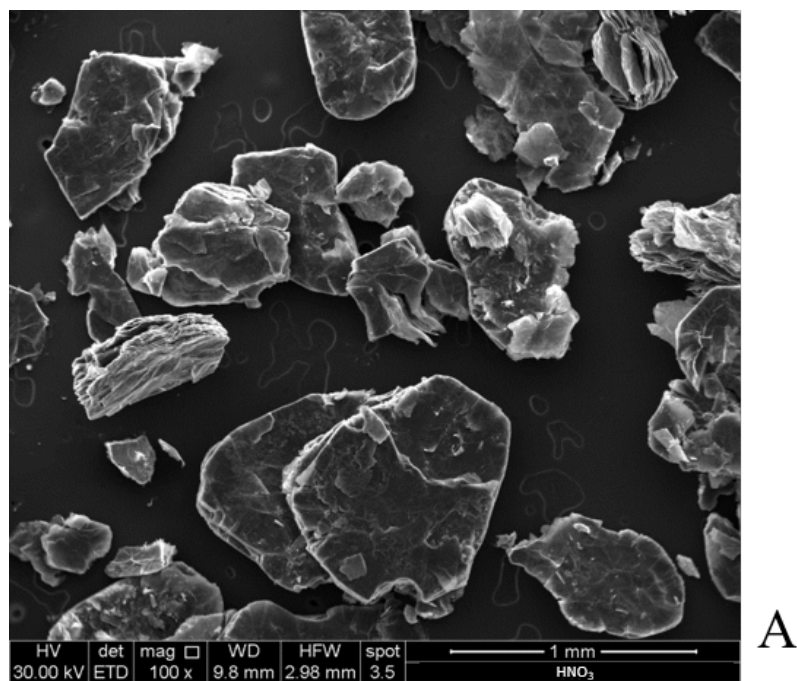
Figure 5.2: Scanning electron micrographs of HNO_3 - GIC, A: before heating and B: after heating (magnification 100X)
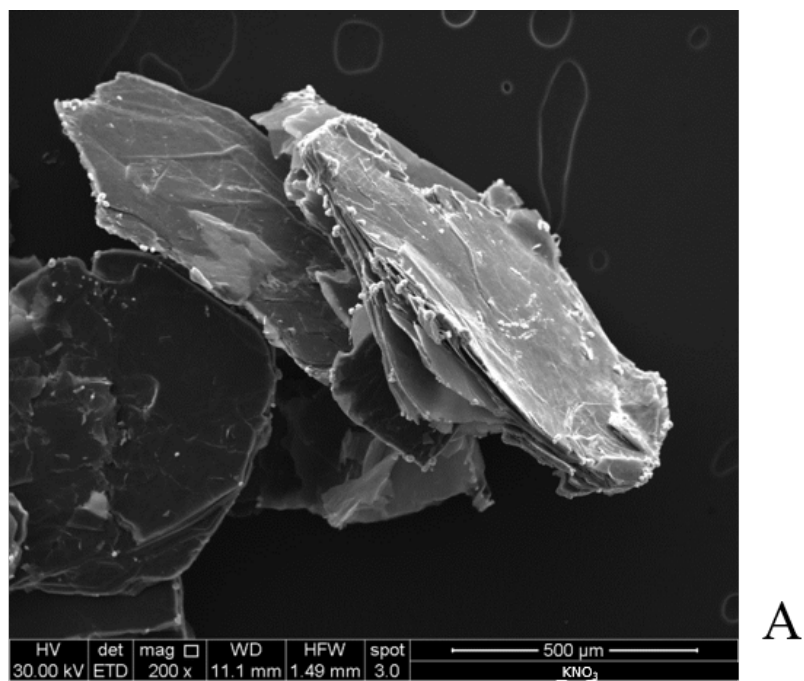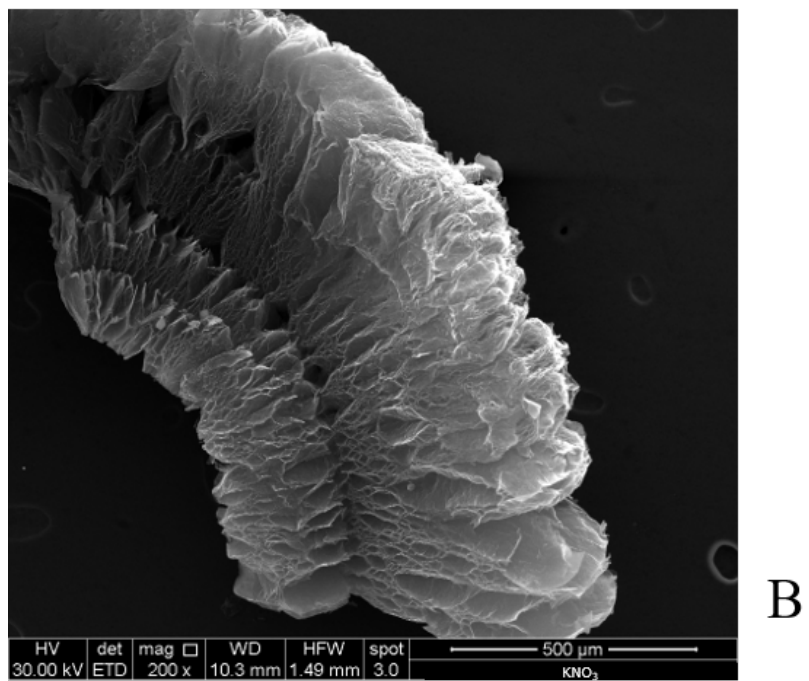
Figure 5.3: Scanning electron micrographs of KNO_3 - GIC A: before heating and B: after heating (magnification 200X)
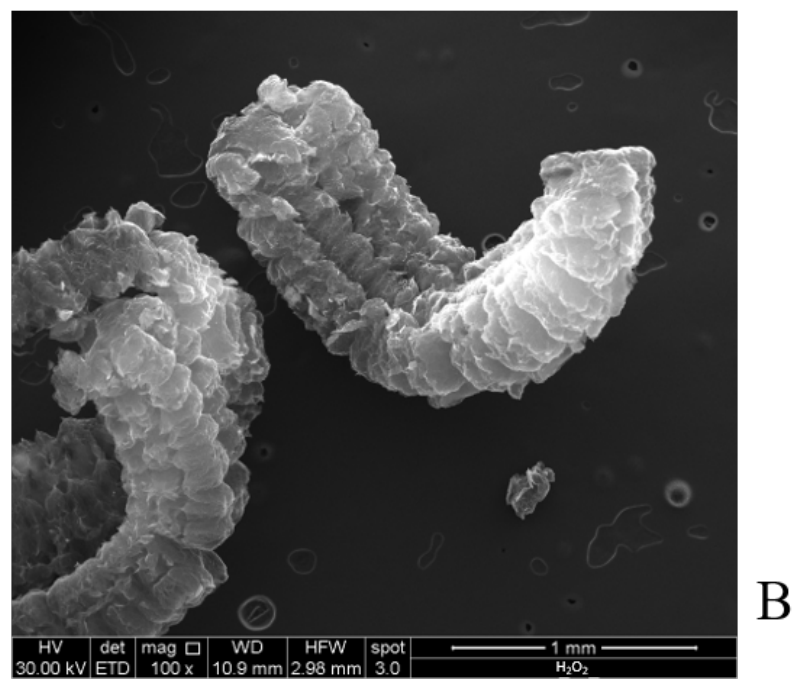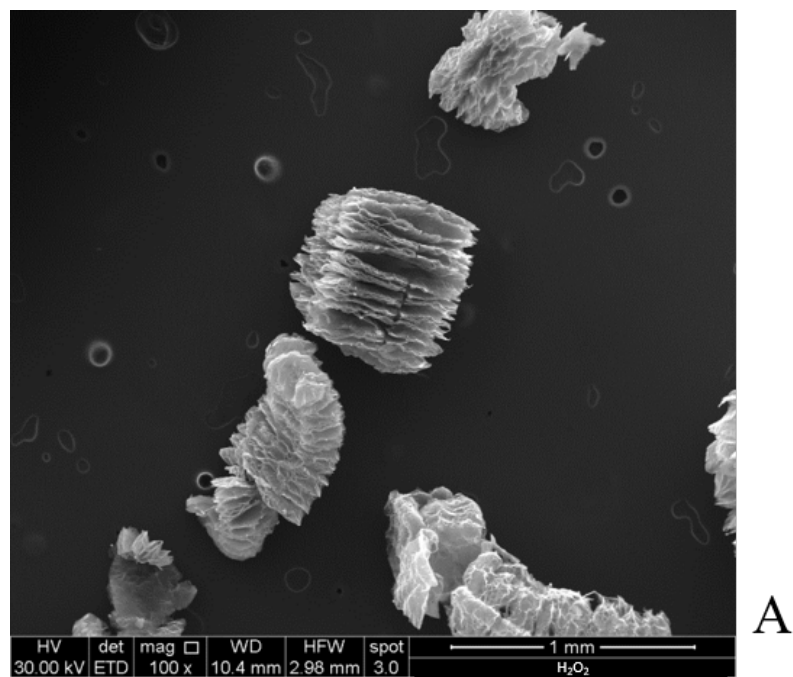
Figure 5.4: Scanning electron micrographs of H_2O_2 - GIC A: before heating and B: after heating (magnification 100X)
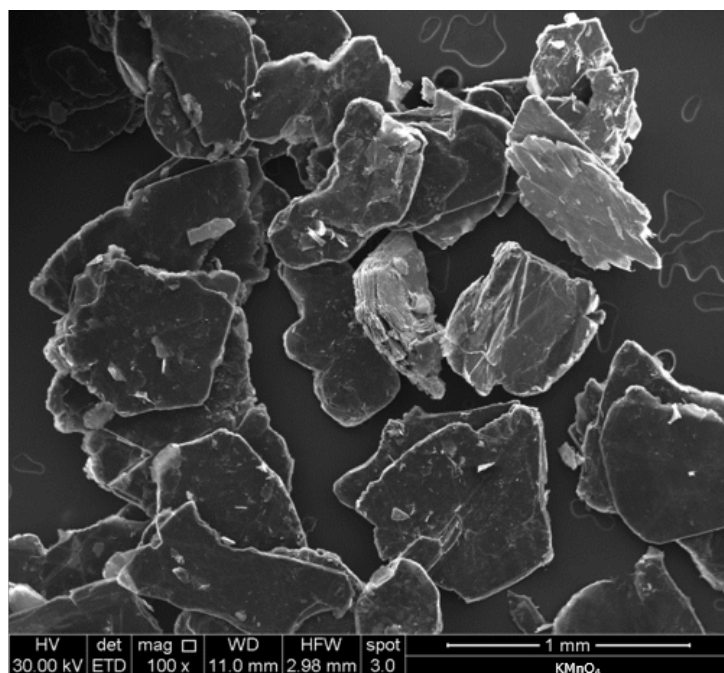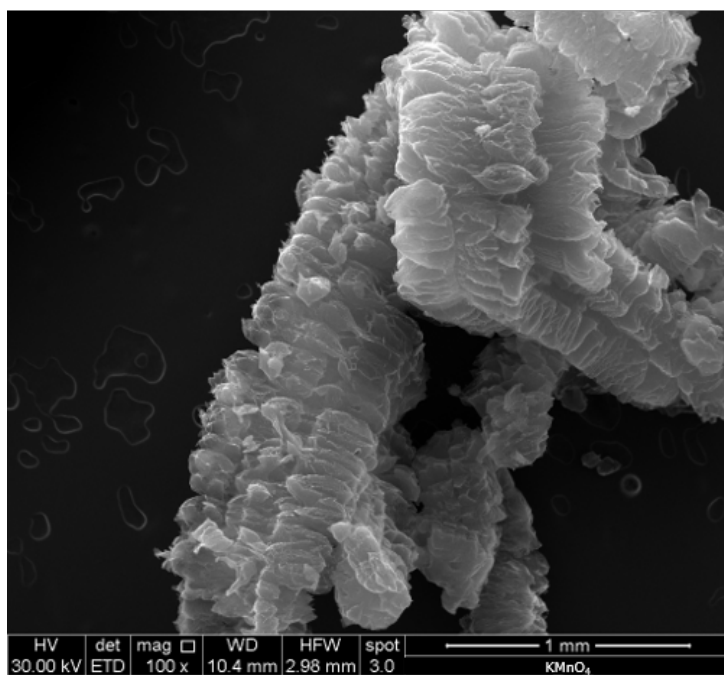
Figure 5.5: Scanning electron micrographs of $KMnO_4$ - GIC A: before heating and B: after heating (magnification 100X)
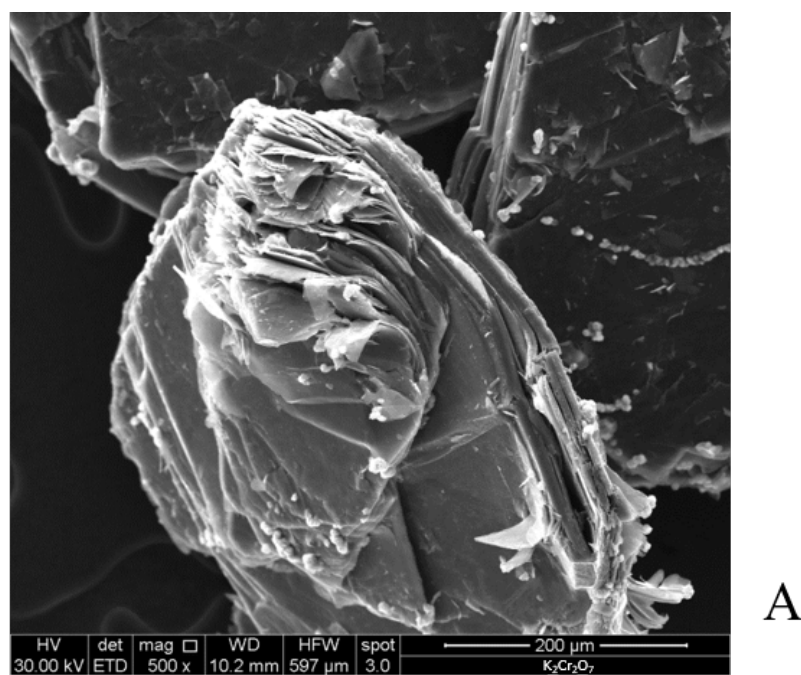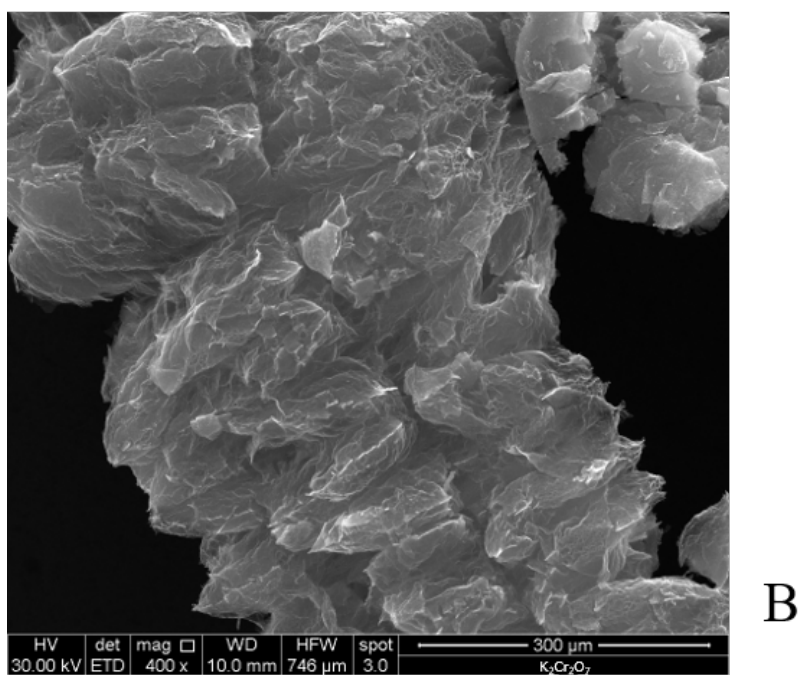
Figure 5.6: Scanning electron micrographs of $K_2Cr_2O_7$ - GIC A: before heating and B: after heating (magnification A: 500X, B: 400X)
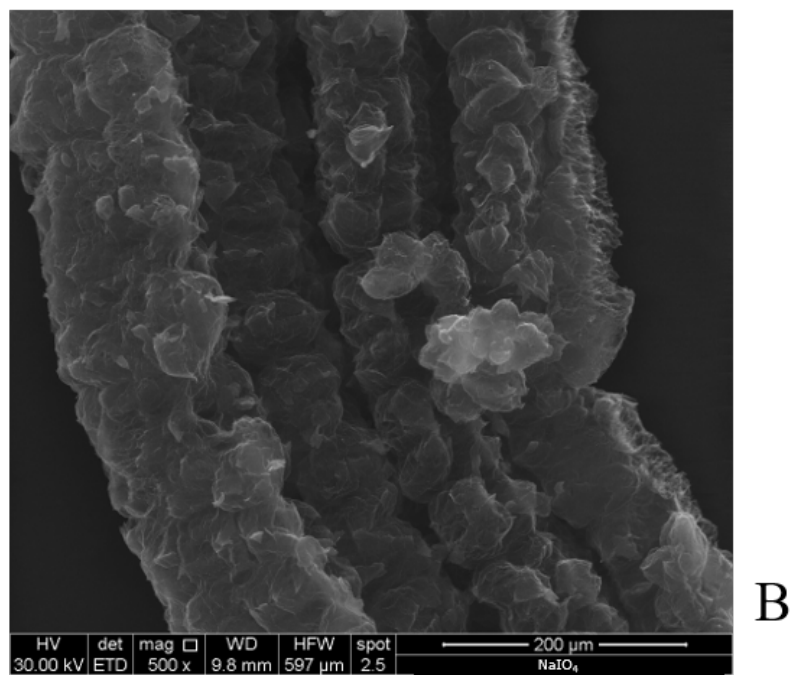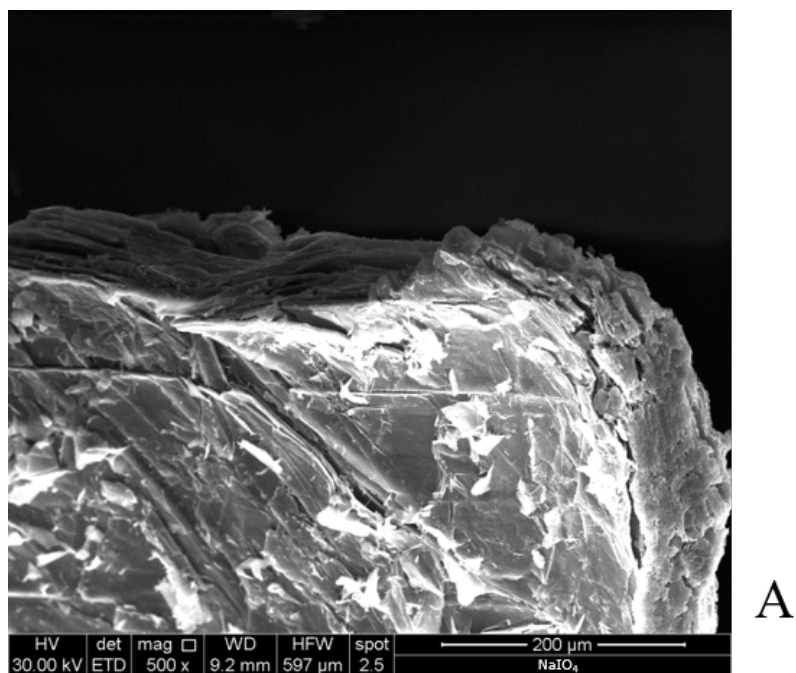
Figure 5.7: Scanning electron micrographs of $NaIO_4$ - GIC A: before heating and B: after heating (magnification 500X)
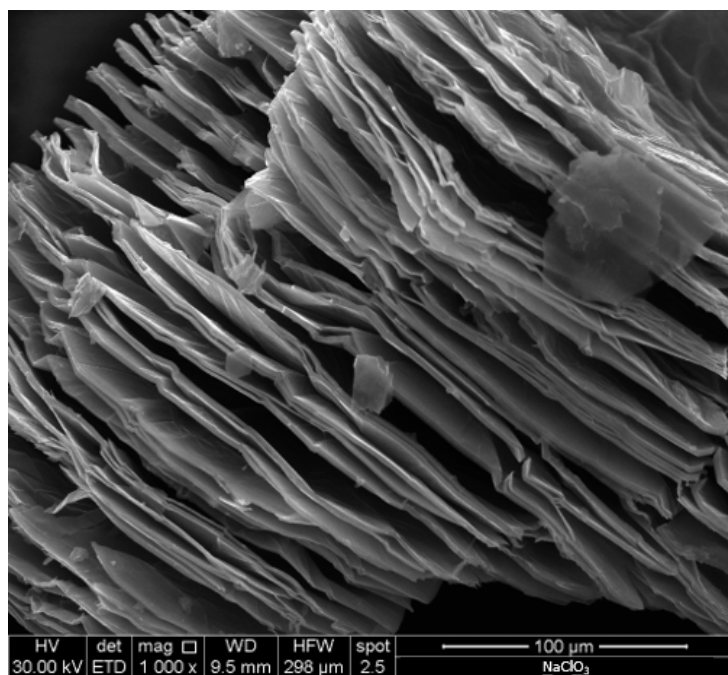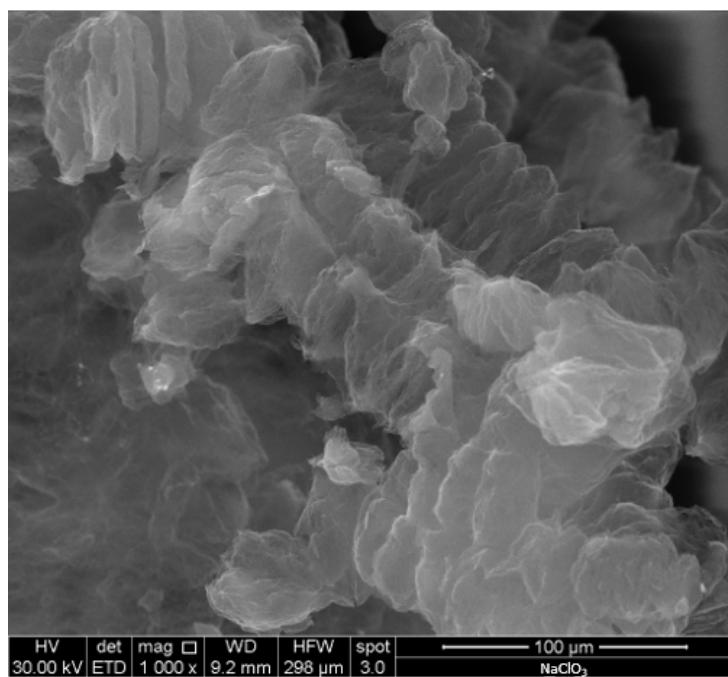
Figure 5.8: Scanning electron micrographs of $NaClO_3$ - GIC A: before heating and B: after heating (magnification 1000X)

5.3   Thermogravimetric Analysis

The thermogravimetric behavior of different GICs was evaluated by TGA analysis (Figure 5.9). All thermogravimetric curves were recorded between 30 and 800 °C by heating the samples at 10 °C/min under a inert atmosphere (nitrogen). The weight loss, due to the gas released, can be clearly seen for all the considered samples. From all curves, it is possible to observe a double steps of weight loss with different rates. This phenomenon is much evident for the $NaClO_3$-GIC (that has a considerable weight loss). Probably the fastest weight loss occurs in correspondence of the explosive reaction, here the greatest amount of gas is emitted [9]. After that the residual gas produced from the reaction, will continue to escape slower causing the further weight loss [10]. The weight loss ranged from 3 %, for KNO_3, up to 52 % for $NaClO_3$ (Table 5.1). It is important to notice that the order of data in Table 5.1 in increasing degree of weight loss, is the same as that used to tabulate μ-RS results in *Chapter 4*, and it clearly indicates that highest intercalation degree corresponds to higher weight loss.

Table 5.1: Weight loss percentage of starting Natural Graphite and GICs

SAMPLE	WEIGHT LOSS
Natural graphite	0 %
KNO_3	3 %
$KMnO_4$	7 %
H_2O_2	10 %
HNO_3	17 %
$K_2Cr_2O_7$	18 %
$NaIO_4$	30 %
$NaClO_3$	52 %
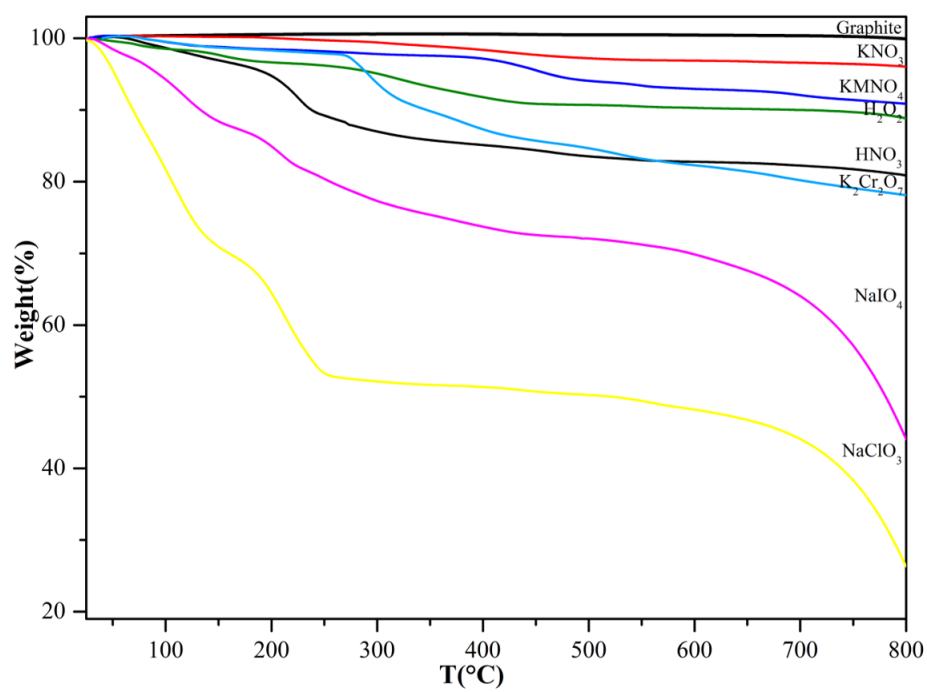
Figure 5.9: TGA curves of starting Natural Graphite and Graphite Intercalation Compounds

References

[1] D.D.L. Chung, *Review: Exfoliation of graphite*, J. of Materials Sci 22, 4190–4198, **(1987)**

[2] G. Camino, S. Duquensne, R. Delobel, B. Eling, C. Lindsay, T. Roels, *Mechanism of expandable graphite fire retardant action in polyurethanes*, ACS Symposium series 797, 90–109, **(2001)**

[3] S. Duquesne, M. Le Bras, S. Bourbigot, R. Delobel, G. Camino, B. Eling, C. Lindsay, T. Roels, *Thermal degradation of polyurethan/expandable graphite coatings*, Polymer Degradation and Stability 74, 493–499 **(2001)**

[4] Celzard, A., et al., *Electrical conductivity of anisotropic expanded graphite-based monoliths.* Journal of Physics D: Applied Physics, 33-23, 3094, **(2000)**

[5] W. Wang, X.Yang, Y.Fang, J. Ding, J. Yan, *Preparation and thermal properties of polyethylene glycol/expanded graphite blends for energy storage*, Applied Energy, 86(9), 1479-1483, **(2009)**

[6] W. Wang, X.Yang, Y.Fang, J. Ding, J. Yan, *Preparation and thermal properties of polyethylene glycol/expanded graphite blends for energy storage*, Applied Energy, 86(9), 1479-1483, **(2009)**

[7] G. Carotenuto, S. De Nicola, M. Palomba, D. Pullini, A. Horsewell, T.W. Hansen, & L. Nicolais, *Mechanical properties of low-density polyethylene filled by graphite nanoplatelets*, Nanotechnology, 23(48), 485705, **(2012)**

[8] O.Y. Kwon, S.W. Choi, K.W. Park, & Y.B. Kwon, *The preparation of exfoliated graphite by using microwave*, Journal of Industrial and Engineering Chemistry, 9(6), 743-747, **(2003)**

[9] M. Salvatore, G. Carotenuto, V. Ambrogi, C. Carfagna, *Synthesis of H2SO4-intercaleted graphite flakes based on different oxidizing agents*, XI Convegno nazionale Materiali Nanofasici, pp 159-160, **(2015)**

[10] M. Salvatore, G. Carotenuto, S. De Nicola, C. Camerlingo, V. Ambrogi, C. Carfagna, *Synthesis and characterization of high-filled intercalated graphite bisulphate*, Nanoscale Research Letters, 12:167, **(2017)**

Part I Conclusions

In Part I new chemical routes for synthesizing highly intercalated graphite bisulfate are presented and described. First the preliminary study has been described, where best reaction conditions to obtain an intercalated compound has been found. The result of the this study has been that the time of 1 hour and room temperature are enough to obtain a graphite bisulfate with a good intercalation degree. However, to perform the reactions under controlled temperatures, temperatures between 30 °C and 40 °C have been chosen, depending on the reactivity of the oxidant. The reaction schemes uses different auxiliary reagent (oxidizing agent): nitric acid, potassium nitrate, potassium dichromate, potassium permanganate, sodium periodate, sodium chlorate, and hydrogen peroxide. Micro Raman spectroscopy analysis of products has shown that samples treated by $NaIO_4$ and $NaClO_3$ lead to final products with the highest intercalation degree, which is consistent with the weight loss from the TGA data. Furthermore, according to FT- IR data, $(-OH)$ is the only oxygen-containing group generated during the intercalation process. EDS elemental analysis allowed to asses the presence of Sulfur and Oxygen characterizing the oxidation/intercalation process. The SEM micrographs, FT-IR analysis, Micro-Raman spectroscopy, TGA thermograms and calculated weight loss (from TGA analysis), confirm that the GIC, obtained using KNO_3 as oxidizer, is the most similar to natural graphite, whereas GIC based on $NaClO_3$ seems to have a higher intercalation degree.

Part II

Graphite Intercalation by FeCl$_3$

Chapter 6

Iron(III) Chloride - GIC

6.1 A Magnetic GIC

The literature [1] shows that a magnetic GIC is obtained by chemical reduction of the intercalation compound $FeCl_3$ - GIC through a potassium-naphthalene complex in tetrahidrofuran. The $FeCl_3$ - GIC compound used as starting material is synthesized by heating a mixture of iron (III) chloride anhydrous with natural graphite. Subsequently, the $FeCl_3$ - GIC is added to the solution K - naphthalene - THF in order to completely reduce the intercalated $FeCl_3$. In the literature are reported the XRD diffractograms performed on either the compounds at different reaction times. The spectra show diffraction peaks attributed to reaction products which are the metallic Fe and potassium chloride. The peaks attributable to metallic Fe are weak due to the small size of the particles. They do not found signals due to $FeCl_3$ - GIC compounds, indicating that the property was completely destroyed. The reaction products that are formed are very stable, it is not observed the oxidation of iron. Such stability could means that the products are englobed in the graphite matrix. When the final product is heated to high temperatures (in inert atmosphere) an appreciable exfoliation of the flakes was observed. The authors attribute this exfoliation phenomenon in the presence of THF molecules in the matrix. The conclusion of this study is that the particles of metallic Fe, formed during the reaction of reduction of the compound $FeCl_3$ - GIC, are stable because embedded in the graphite matrix. This result is important because the resulting product could be magnetic. In this section it is explained the method developed to obtain a magnetic expanded graphite in a very easy way. The research is turning to the production of this type of intercalation compound: graphite matrix with inclusions of metallic Fe starting from natural graphite and iron (III) chloride.

6.2   FeCl$_3$ - GIC Materials and Methods

6.2.1   Materials

The materials used to prepare FeCl$_3$ - GIC samples are:

1. Natural Graphite in flakes form (supplied by Sigma-Aldrich). Its characteristics are summarize in *Chapter 1 - Materials and Methods.*

2. Iron(III) Chloride, supplied by Sigma-Aldrich (see Table 6.1 for characteristics).

Table 6.1: Iron (III) Chloride properties

Reagent	Iron(III)Chloride FeCl3
Producer	ALDRICH
Vapor Pressure	1 mmHgat (194 ℃)
Form	powder or crystals
Assay	99.9 % trace metals basis
MP	304 ℃ (lit.)

6.2.2   Preparation Method and Technical Analysis

First a solid mixture of the starting products has been prepared. After that it was observed that heating the solid mixture by microwave oven, it generate an instant expansion phenomenon of the graphite. Indeed, after heating for few seconds, the product is morphologically different from the starting one. The reaction product in the microwave oven has been used to create a coating for LDPE film. Only a preliminary characterization has been performed on these samples. The achieved materials have been characterized regarding their morphology by scanning electron microscopy (SEM) and Energy Dispersive X-ray Spectroscopy (EDS). The thermal degradation of the FeCl$_3$ has been study using thermogravimetric analysis (TGA). Instruments used are the same described in *Chapter 1 - Materials and Methods.*

6.3   Preliminary Characterization

The samples prepared respond to the magnetic field, although very weakly (see Figure 6.2). Figure 6.2 A, shows an image of the FeCl$_3$ - GIC prepared by the method discussed in the previous section, placed in a plastic case. In Figure 6.2 B, a small neodymium magnet has been approached to the case. From this image it is evident the sample response to the magnetic field induced by the magnet, indeed it is attracted to the case side. On the samples obtained it has been performed a morphological analysis using a scanning electron microscope SEM. Figure 6.3 A, B and C shows the micrographs taken from the same
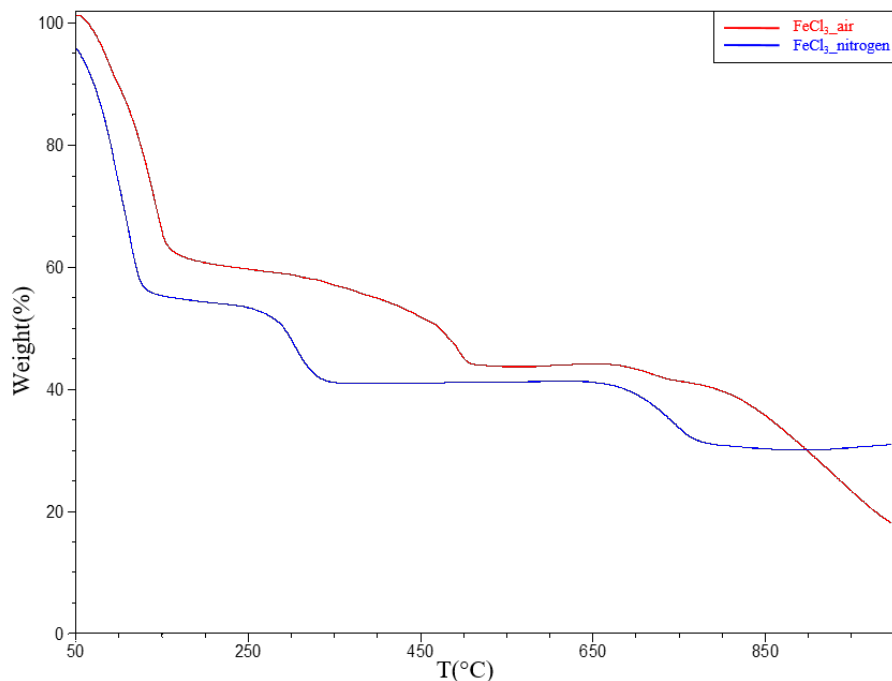
Figure 6.1: Thermal Degradation of FeCl$_3$ under air (red) and nitrogen (blue) fluxing

sample at three different magnifications: $150X$, $200X$ and $600X$ respectively. Images show a morphology characteristic of the expanded graphite, as discussed previously (a worm-like shape with a lot of porous and defects). From these micrographs it is evident also the presence of white, small particles of different nature from the graphite, probably $FeCl_2$ [2] or metallic Fe coming from the thermal decomposition of $FeCl_3$ (see Figure 6.1) . To confirm the particles nature, EDS analysis has been carried out on small samples areas. The positions where EDS analysis has been performed are indicated in Figure 6.4 . The elemental composition for each EDS spectrum is reported in Table 6.2. EDS analysis performed on the FeCl$_3$ - GICs samples has confirmed the iron content in these samples. As visible from the Figure 6.4, the sample area where the Spectrum 2 has been collected (circled in red in the Figure), is full of particles. The elemental composition of this spectrum shows the highest iron content.
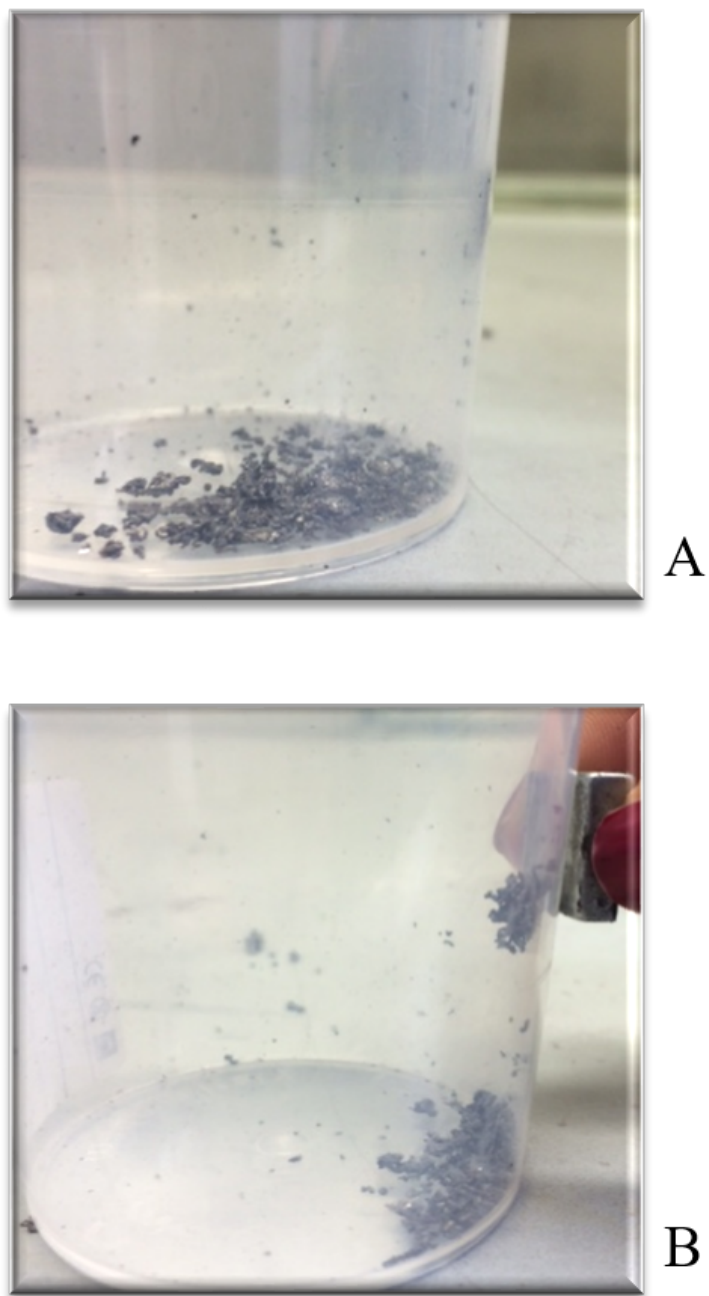
Figure 6.2: A: FeCl$_3$ - GIC after heating by microwave and B: FeCl$_3$ - GIC response to the magnetic field
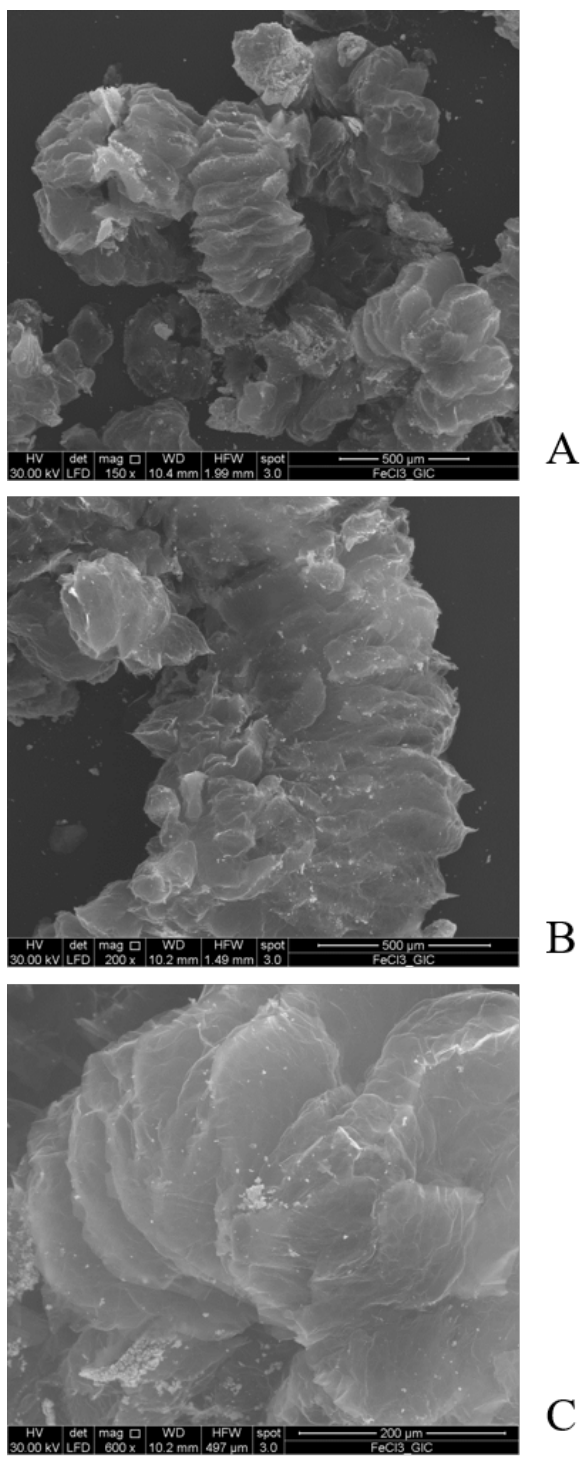
Figure 6.3: Scanning electron micrographs of FeCl$_3$ - GIC (magnification A: 150X, B: 200X and C: 600X)
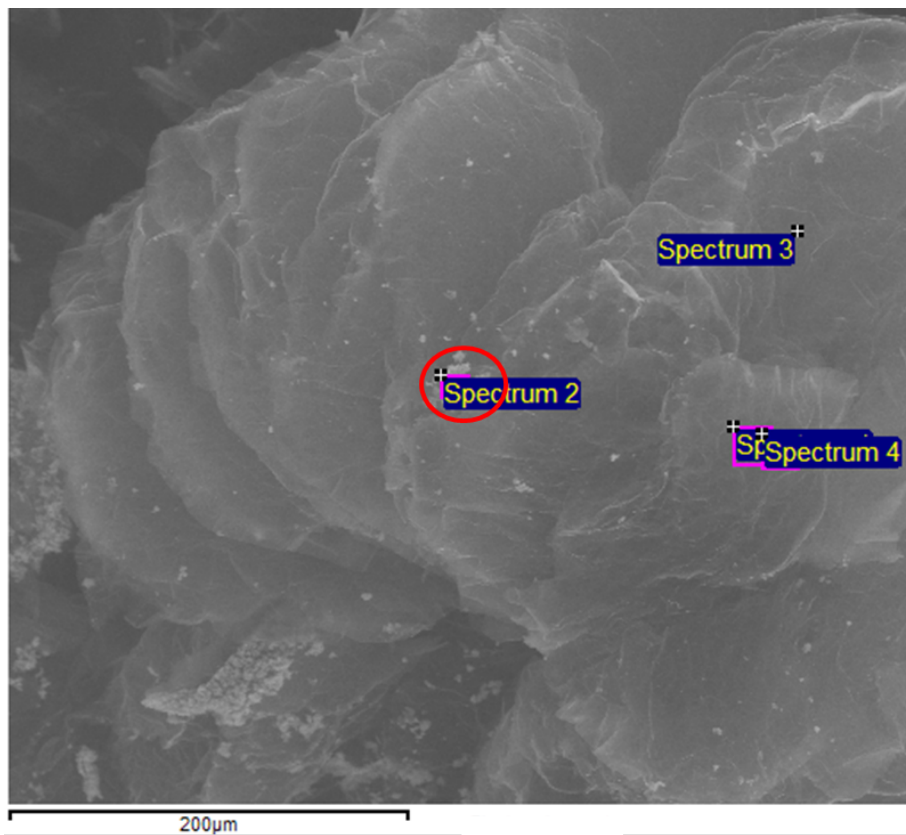
Figure 6.4: Positions where EDS analysis has been performed on FeCl$_3$ - GIC

Table 6.2: EDS analysis: elemental composition. Results in weight %. (Figure 6.4)

	SPECTRUM	C	O	Fe	Cl	Other	Total
FeCl$_3$-GIC (Figure 6.4)	Spectrum 1	90.02	4.13	3.21	2.48	0.16	100
	Spectrum 2	60.13	20.00	18.52	1.35	/	100
	Spectrum 3	76.39	14.91	7.25	1.33	0.12	100
	Spectrum 4	89.71	4.21	3.25	2.44	0.39	100

Table 6.3: EDS analysis: elemental composition. Results in weight %

	SPECTRUM	**C**	**O**	**Fe**	**Total**
LDPE coated (Figure 6.5 B)	Spectrum 1	71.82	19.13	9.05	100
	Spectrum 2	96.89	2.87	0.24	100
	Spectrum 3	92.96	5.71	0.19	100
	Spectrum 4	97.18	2.82	/	100

6.4   LDPE Film Coated

Another result observed for these compounds, regards the LDPE film coating. The LDPE coated has been prepared by dispersing the reaction product $FeCl_3$ - GIC in acetone under sonication[3]. The obtained colloid was gently rubbed up on the surface of a well extent low-density polyethylene film (by hands, using a LDPE film counterface) up to achieve a very uniform coating . The adhesion property of the LDPE surface combined with the applied shear stress allowed to deposit a continuous coating whit a quite uniform thickness [4]. First, it has been observed that the film obtained responds to the magnetic field (although weaker than reaction product). From SEM micrograph (see Figure 6.5 A) it can be observe a uniform surface with some white particles. EDS analysis have been performed on small areas where is visible the presence of the particles (Figure 6.5 B, Spectrum 1, 2) but also where there are not particles (Figure 6.5 B, Spectrum 3 and 4). The Table 6.3 summarize the elemental composition, it confirms that the particles are formed by the element Fe, that is still present on the coated samples.

6.5   Future Work

This study needs more other analysis and consideration. In particular a structural investigations (X-ray diffractometry) of the samples is necessary to confirm the presence of metallic Fe. Furthermore, it will be performed a study of the electrical and magnetic properties of LDPE-coated films.
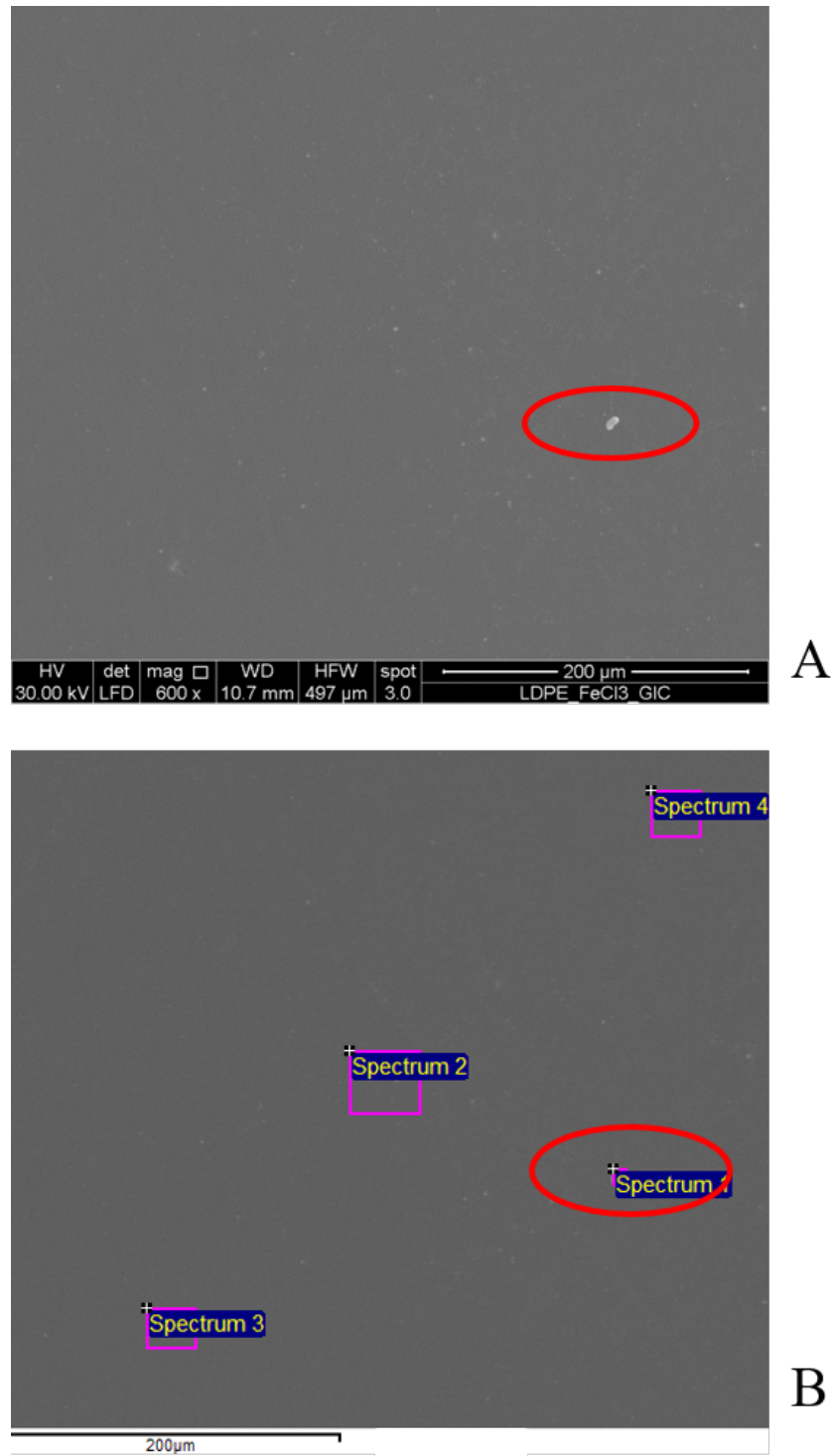
Figure 6.5: Scanning electron micrographs of LDPE coated with FeCl$_3$ - GIC (magnification 600X)

References

[1] A. Messaoudi, M. Inagaki and F. Beguin, *Chemical reduction of FeCl3–Graphite Intercalation Compounds with Potassium–Naphtalene Complex in Tetrahydrofuran*, J.MATER. CHEM., 1(5), 735-738, **(1991)**

[2] L. Wang, C. Guo, Y. Zhu, J. Zhou, L. Fan, & Y. Qian, *A FeCl 2-graphite sandwich composite with Cl doping in graphite layers: a new anode material for high-performance Li-ion batteries*, Nanoscale, 6(23), 14174-14179, **(2014)**

[3] G. Carotenuto, L. Nicolais, Wiley Encyclopedia of Composites, II edition, John Wiley and Sons, 1232, **(2012)**

[4] M. Palomba, M. Salvatore, G. Carotenuto, U. Coscia, G. Ambrosone, & S. De Nicola, Polymer-supported graphene obtained by a micromechanical tecnique based on shear-stress, Nanotechnology (IEEE-NANO), 2015 IEEE 15th International Conference, 485-488, **(2015)**

Conclusions

In this work two classes of Graphite Intercalation Compounds have been prepared and characterized: i) seven different graphite bisulfates, ii) graphite iron-chloride. Both with the property of expand under thermal heating (*Expandable Graphite*).

- To identify the best reaction conditions, a preliminary study of the effect of time and temperature conditions on the intercalating reactions, has been performed using the most common system reported in the literature to obtain graphite bisulfate: H_2SO_4/HNO_3. Three different reaction temperatures (25 °C, 40 °C, 60 °C) and four different reaction times (1, 2, 3 and 4 hours) were used.

- To obtain the best expandable graphite with the highest intercalation degree, seven different oxidizing agent (in a mixture with concentrated sulfuric acid) have been used. The graphite iron-chloride has been prepared to obtain an expendable graphite with magnetic property. The aim of this study was to find new chemical routes for synthesizing highly intercalated graphite bisulfate. The reaction schemes uses different auxiliary reagents (oxidizing agent): nitric acid, potassium nitrate, potassium dichromate, potassium permanganate, sodium periodate, sodium chlorate, and hydrogen peroxide. Graphite bisulfate (intercalated graphite with sulfuric acid) has been prepared by intercalation of graphite with sulfuric acid, in presence of an oxidizing agent by classical liquid-phase synthesis techniques. The intercalation reaction was performed in a glass-flask reactor (placed in a thermostatic bath), using air bubbling as homogenizing approach. The reaction time always was 1h and the H_2SO_4/oxidizing agent ratio was 9:1 by volume for all reactive mixtures. The reactions were stopped by adding deionized water to the systems. In order to evaluate the presence of delamination, and pre-expansion phenomena, and the achieved intercalation degree in the prepared samples, the obtained graphite intercalation compounds have been characterized by scanning electron microscopy (SEM), X-ray powder diffraction (XRD), infrared spectroscopy (FT-IR), micro-Raman spectroscopy (μ–RS) and thermal analysis (TGA).

- $FeCl_3$ - GIC has been prepared by heating a solid mixture of the starting products by microwave oven. The heating generate an instant expan-

sion phenomenon of the graphite. The resulting product is a magnetic expanded graphite.

- In the preliminary study, from the morphology and structural characterizations, it has been found that the time of one hour and room temperature were enough to obtain a GIC with a good intercalation degree and, therefore, good expansion property. There were not reasons to use severe condition in Time and Temperature indeed, in some cases, to use stricter conditions seemed to lead to a worse product. However, to perform the reactions under controlled temperatures, the subsequent reactions were performed at temperatures greater than room temperature. Depending on the reactivity of the oxidant, temperatures between 30 °C and 40 °C have been chosen.

- From morphology analysis, delamination and pre-expansion phenomena were observed only for nitric acid, potassium dichromate and hydrogen peroxide, while the presence of strong oxidizers ($KMnO_4$, $NaIO_4$) led to stable graphite intercalation compounds. EDS elemental analysis allowed to asses the presence of Sulfur and Oxygen characterizing the oxidation/intercalation process.

- Micro Raman spectroscopy analysis of products has shown that samples treated by $NaIO_4$ and $NaClO_3$ lead to final products with the highest intercalation degree, which is consistent with the weight loss from the TGA data. According to FT- IR data, $(-OH)$ is the only oxygen-containing group generated during the intercalation process. The SEM analysis performed on the expanded GICs showed an increase in volume and the difference in structure.

- The expanded graphite bisulphates had a worm-like shape with a lot of porous and defects. This result represent a confirmation of the obteined intercalation during the step 1. TGA analysis showed the presence of a weight loss due to the gas released for all the considered samples. The weight loss ranged from 3%, for KNO_3, up to 52% for $NaClO_3$.

- The SEM micrographs, FT-IR analysis, Micro-Raman spectroscopy, TGA thermograms and calculated weight loss (from TGA analysis), confirm that the GIC, obtained using KNO_3 as oxidizer, is the most similar to natural graphite, whereas GIC based on $NaClO_3$ seems to have a higher intercalation degree.

- The $FeCl_3$ - GIC samples prepared respond to the magnetic field. SEM images show a morphology characteristic of the expanded graphite and the presence of particles of different nature from the graphite. EDS analysis confirmed the iron content in these samples.

- LDPE coated has been prepared by dispersing the reaction product FeCl$_3$ - GIC in acetone under sonication and rubbing it up on the surface of a

low-density polyethylene film. The film obtained responds to the magnetic field (although weaker than reaction product). SEM micrograph shows the presence of white particles on the LDPE coated surface. EDS analysis confirms that the particles are formed by the element Fe, that is still present on the coated samples. This study needs more other analysis and consideration. In particular a structural investigations (X-ray diffractometry) of the samples is necessary to confirm the presence of metallic Fe.

APPENDIX A - Graphite Bisulfate Application

Polymers-Supported Graphene Preparation

A simple and effective micromechanical technique for the synthesis of graphene supported by polymeric film is proposed [1]. This method, based on the application of a combination of shear-stress and friction force to the nanographite, is able to leave single-layer graphene on a suitable flat material. Different polymer substrate can be used for graphene coating process (as PMMA substrate [2]), but very convenient substrates are the non-polar polymeric films because of their ability to give CH/π interactions, combined with the shear stress, allows the graphite nanocrystals to spread uniformly and continuously. In addition, this technique makes it possible to fabricate large area graphene layer directly on a non-electrically conducting substrate [3]. This approach can be also used to convert graphite nanoplatelets into carbon nanoscrolls using a bi-axially oriented polypropylene (BOPP) surface: the combined action of shear and friction forces causes the exfoliation of graphite nanoplatelets and the simultaneous roll-up of graphite layers [4]. In this work, large area graphene multi-layers were prepared by means of the above mentioned micromechanical technique, on a low density polyethilene (LDPE) film and on a polypropylene random co-polymer (PPR) film as substrates. The morphology of the obtained samples has been investigated. Nanographite was prepared by converting graphite flakes to graphite bisulfate (using methods explained during this work), followed by thermal expansion in a microwave oven and disaggregation in liquid phase by sonoacoustic energy. A concentrated nanographite colloid was prepared by dispersing nanographite in ethanol (Aldrich, 99.9 %) under sonication. The obtained colloid was gently rubbed up on the surface of the polymers film (by hands, using a film counterface of the same polymer) up to achieve a very uniform coating. The obtained coating of large area graphene layers on the polymeric substrate were rinsed by acetone and dried up in air at room temperature. The morphology of the achieved samples has been investigated by means of scanning electron microscopy. The adhesion property of the LDPE surface combined with the applied shear stress allows to deposit a continuous graphene multilayer coating whit a quite uniform thickness (see Figure 6.6), while using PPR substrate, the

morphology result quiet irregular and full of defects. The Figure 6.7 suggests that PPR is not a good substrate for this process.

Future Work

Different characterizations can be made on these samples: electrical, mechanical and optical properties can be investigated. These films have traditionally good electrical conductivity and transparency in the visible spectral region [1] which can be of interest for their use as transparent and conductive films alternative to metal oxides in optoelectronic devices [5].
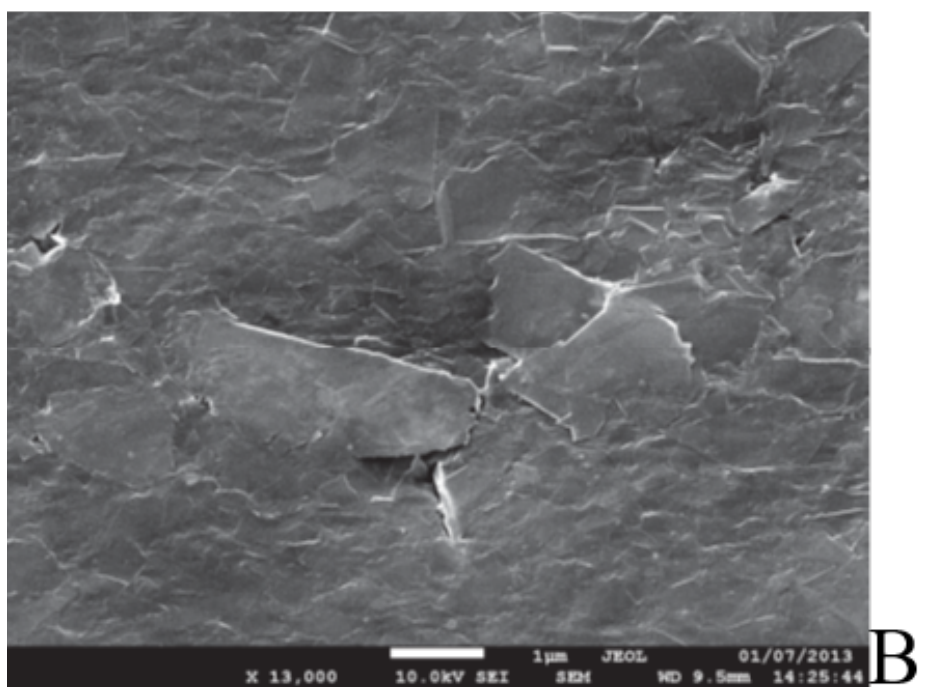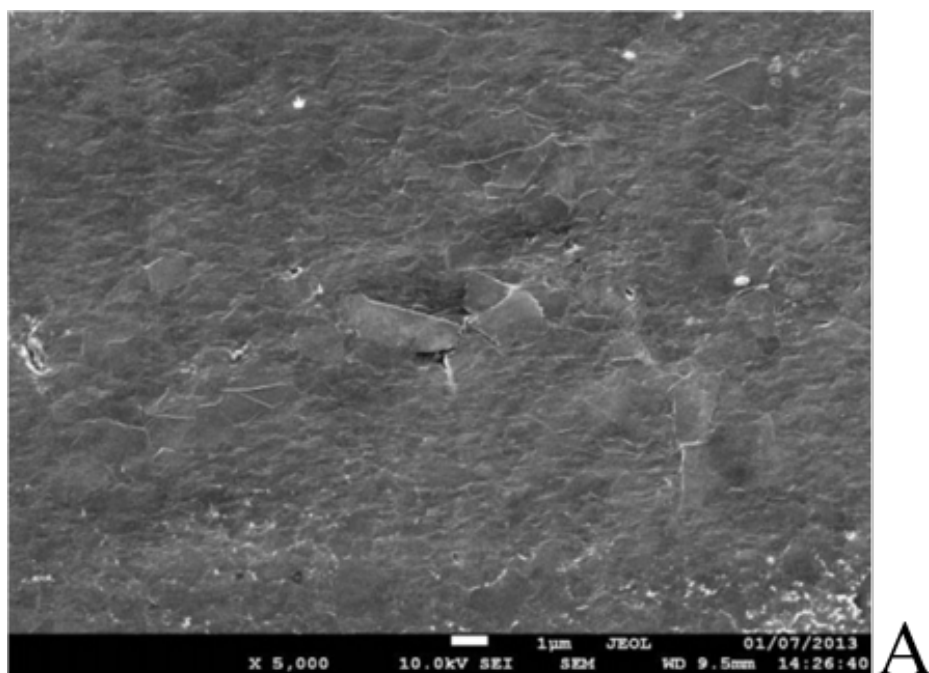
Figure 6.6: Scanning electron micrographs of the LDPE coated (magnification: A: 5000X, B: 13000X)
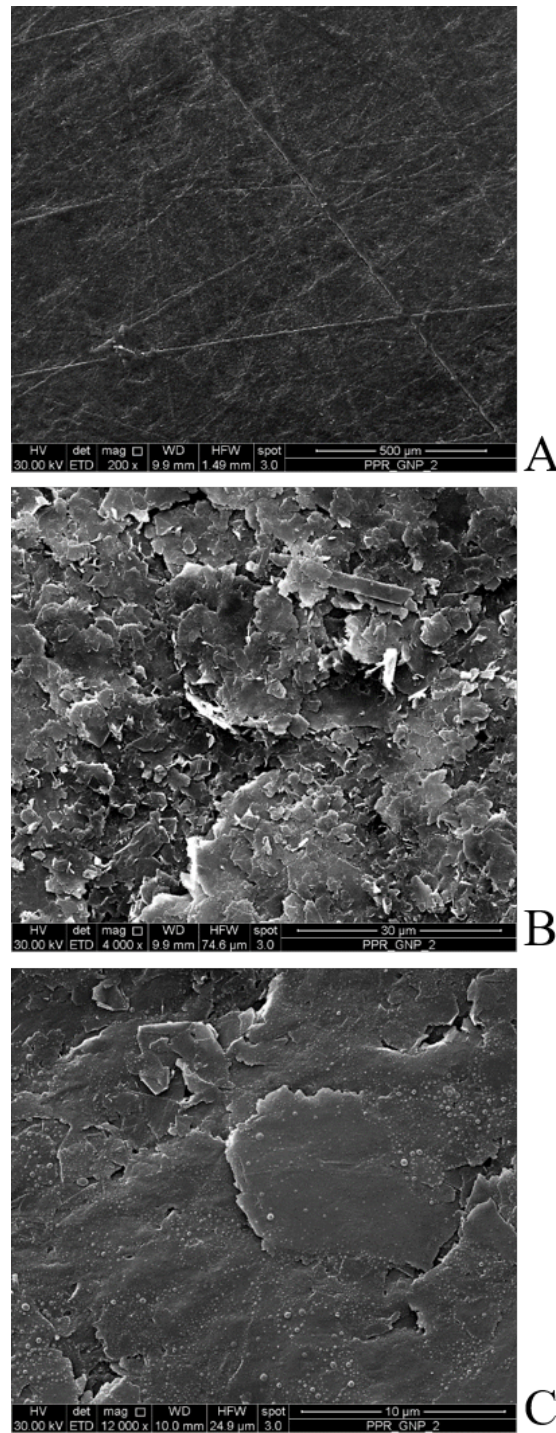
Figure 6.7: Scanning electron micrographs of the PPR coated (magnification: A: 200X, B: 4000X, C: 12000X)

References

[1] G. Carotenuto, S. De Nicola, G. Ausanio, D. Massarotti, L. Nicolais, & G.P. Pepe, *Synthesis and characterization of electrically conductive polyethylene-supported graphene films*, Nanoscale research letters, 9(1), 475, **(2014)**

[2] C. Bonavolontà, C. Aramo, M. Valentino, G. Pepe, S. De Nicola, G. Carotenuto, G. & C. Meola, *Graphene–polymer coating for the realization of strain sensors*, Beilstein Journal of Nanotechnology, 8(1), 21-27, **(2017)**

[3] M. Palomba, M. Salvatore, G. Carotenuto, U. Coscia, G. Ambrosone, & S. De Nicola, *Polymer-supported graphene obtained by a micromechanical tecnique based on shear-stress*, Nanotechnology (IEEE-NANO), 2015 IEEE 15th International Conference, 485-488, **(2015)**

[4] G. Carotenuto, A. Longo, S. De Nicola, C. Camerlingo, & L. Nicolais, *A simple mechanical technique to obtain carbon nanoscrolls from graphite nanoplatelets*, Nanoscale research letters, 8(1), 403, **(2013)**

[5] G. Carotenuto, V. Romeo, L. Schiavo, G. Ausanio, & L. Nicolais, *Preparation and characterization of optically transparent and electrically conductive polyethylene-supported graphene films*, AIP Conference Proceedings, Vol. 1599, No. 1, pp. 502-505, **(2014)**

List of Tables

List of Figures

List of Abbreviations

μ-RS   Micro-Raman Spectroscopy

CVD   Chemical Vapor Deposition

EDS   Energy Dispersive X-ray Spectroscopy

EG   Expandable Graphite

FLG   Few Layer Graphene

FTIR   Fourier Transform Infrared Spectroscopy

GIC   Graphite Intercalation Compounds

GNP   Graphite NanoPlatelets

GO   Graphene Oxide

LDPE   Low-Density Polyethylene

MW   MicroWave

PPR   PolyPropylene Random co-polymer

SEM   Scanning Electron Microscopy

TEM   Transmission Electron Microscopy

TGA   ThermoGravimetric Analysis

THF   TetraHydroFuran

WAXD   Wide Angle X-ray Diffraction

XRD   X-Ray Diffraction

Publications and Presentations

Publications related to the work

- "Synthesis and characterization of high-filled intercalated graphite bisulphate". **M. Salvatore**, *G. Carotenuto, S. De Nicola, C. Camerlingo, V. Ambrogi, C. Carfagna*, Nanoscale Research Letters, (2017) 12:167, DOI 10.1186/s11671-017-1930-2

- "Polymer – Supported Graphene Obtained by a Micromechanical Technique Based on Shear-Stress". *M. Palomba,* **M. Salvatore**, *G. Carotenuto, U. Coscia, G. Ambrosone, S. De Nicola*, International Conference "15th INTERNATIONAL CONFERENCE ON NANOTECHNOLOGY – IEEE NANO 2015" DOI: 10.1109/NANO.2015.7388644.

- "Synthesis of H2SO4-intercaleted graphite flakes based on different oxidizing agents". **M. Salvatore**, *G. Carotenuto, V. Ambrogi, C. Carfagna*, "XI Convegno nazionale Materiali Nanofasici" (2015), pp 159-160, ISBN: 978-88-8080-188-7;

Publications unrelated to the work

- "Effect of electron beam irradiation on the properties of polylactic acid / montmorillonite nanocomposites for food packaging applications". **M. Salvatore**, *A. Marra, D. Duraccio, S. Shayanfar, S. D. Pillai, S. Cimmino and C. Silvestre*, J. APPL. POLYM. SCI. 2016, DOI: 10.1002/APP.42219;

- "Effect of ionizing radiation on the properties of nanocomposites based on Polylactic Acid/Montmorillonite for food packaging applications". *S. Cimmino, D. Duraccio , A. Marra, M. Pezzuto,* **M. Salvatore** *, V. Ambrogi, D.S. Pillai , C. Silvestre*, IAEA, Report of the 2nd RCM on Application of Radiation Technology in the Development of Advanced Packaging Materials for Food Products 2014, pp 102 -106.

Presentations at national and international conferences

- "Polymer – Supported Graphene Obtained by a Micromechanical Technique Based on Shear-Stress" *M. Palomba,* **M. Salvatore***, G. Carotenuto, U. Coscia, G. Ambrosone, S. De Nicola*, International Conference "15th INTERNATIONAL CONFERENCE ON NANOTECHNOLOGY – IEEE NANO 2015", 27-30 July 2015, Rome-Italy;

- "Synthesis of graphite intercalation compounds based on different oxidizing agents for the graphene preparation" **M. Salvatore***, G. Carotenuto, V. Ambrogi, C. Carfagna*, "10th International Conference on Society & Materials, SAM 10", 9-10 May 2016, Rome-Italy;

- "Intercalation of graphite by sulphuric acid in presence of different oxidizing agents" **M. Salvatore***, G. Carotenuto, V. Ambrogi, C. Carfagna*, International conference "Bit's 2nd Annual World Congress of Smart Materials – 2016", 4-6 March 2016, Singapore;

- "Synthesis of H2SO4-intercaleted graphite flakes based on different oxidizing agents" **M. Salvatore***, G. Carotenuto, V. Ambrogi, C. Carfagna*, "XI Convegno nazionale Materiali Nanofasici", 26-28 October 2015, Rome-Italy;

- "Liquid-phase synthesis of Stage I graphite intercalation compounds for the graphene preparation" **M. Salvatore***, V. Ambrogi, G. Carotenuto, C. Carfagna*, "European Materials Research Society E-MRS, Spring meeting 2015", 11-15 May 2015, Lille-France.